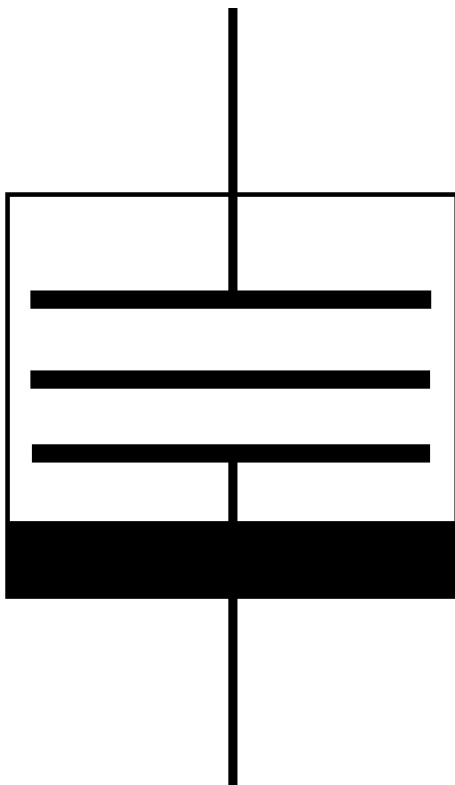# Memcapacitance in human skin

Design of a measuring system to investigate memcapacitive effects in the stratum corneum

Master thesis

Kristian Storås

Summer 2012

Acknowledgements

Firstly I would like to thank my supervisor Professor Ørjan G. Martinsen who presented me with this idea. His extensive knowledge and experience in the field of bioimpedance were indispensable for the completion of this project. The original idea came from Professor Carsten A. Lutken, who connected the new and unknown concept of memristive systems to biological systems. Christian Tronstad and the rest of the Bioimpedance Group was a great inspiration, and was the source of many clues regarding biomedical instrumentation.

Stein L. Nielsen was of great help in designing the electronics, and together with the rest of the staff at the Electronics Lab at the Physics Department deserves thanks for indispensable assistance in the PCB production.

I am grateful to Ørnulf Nordseth at IFE, who let me do unconventional measurements on very expensive equipment, and offered great help in the execution of this.

The availability of needed equipment is thanks to Torfinn Lindem, the protector of this University's small and unknown group of electronics students.

For making this year, and the previous four, into a journey full of surprising and delightful moments, I owe Kristoffer Emil Mørch Amundsen. The continued growth of my curiosity is of his doing.

At last I will thank my family and friends. Some of them for encouragement and support, some for reflective conversations, some for making me feel I can do better, some for making me feel I'm brilliant, and all for making life as good as it gets.

Oslo, August 2012
Kristian Storås

ii

Contents

List of Figures

List of Tables

Nomenclature

Amplitude	Describing the difference between the peak and mean value of a periodic signal.
Banana plug	Commonly used name for 4 mm connector.
CPE	Constant Phase Element. Electrical model with frequency independent phase angle of the impedance between $0°$ and $90°$.
DAQ card	Data acquisition card. Samples an analogue signal and converts it to digital values for signal processing on a computer. Includes sensors, signal conditioning circuitry and an analogue to digital converter.
MOS	Metal Oxide Semiconductor. Structure commonly used to make capacitors. Known for having non-linearities in the capacitance-voltage curve.
RMS	Root mean square value of a periodic signal. Equals the amplitude divided by $\sqrt{2}$ for sinusoidal signals.
SNR	Signal-to-noise ratio. Level of desired signal compared to the level of background noise, usually denoted by dB.
Stratum corneum	Outermost layer of the skin, consisting of dead cells. Acts as a barrier for the underlying tissue, in addition to a range of other known and unknown functions.
VI	Visual instrument. Program built in LabVIEW™.

Abstract

Memory capacitance, or memcapacitance, is part of the relative new concept of memristive systems. These are resistive, capacitive and inductive systems where their properties are dependent on previous dynamics. The purpose of this thesis is to investigate the presence of memcapacitive effects in human skin tissue. For this I have designed a measurement system utilizing LabVIEW™ for signal processing and data presentation. I have examined samples of the stratum corneum in vitro, and an arm segment in vivo, in an electrode setup. These measurements have been compared to measurements on a MOS capacitor, with known voltage dependent capacitance and hysteresis in the capacitance-voltage curve, and basic reference models and components. MATLAB simulations on mathematical electrical equivalents have been performed for further comparison. In addition capacitance-voltage characterization with a high end semiconductor characterization system was conducted on a sample of the stratum corneum, and a MOS capacitor for comparison. No strong evidence of voltage dependency or non-volatile memory was found. However, as there is a noticeable hysteresis in the charge-voltage curve, and it is between two outer plates in the form of the electrodes, skin do fall under the term memristive systems.

Part I

Introduction and Theory

Chapter 1

Introduction

1.1 Background

In 1971 Chua[3] suggested a 4th fundamental circuit element, next to the original three: the resistor, the capacitor and the inductor. This was the memristor, in short a resistor with memory. In 2009 Di Ventra et al.[4] extended this concept to cover capacitive and inductive elements, giving the memcapacitor and the meminductor. They refer to these elements as the 4th, 5th and 6th circuit elements, and collect them all under the generic term memristive systems.

The work of Johnsen et al.[9] shows that some of the conductive properties of human skin could be described using a memristive model. This is concerning electro-osmosis in the sweat-duct capillaries, which is the movement of water molecules due to applied electric field. It is suggested that memristive systems might help in describing other aspects of the electrical model of skin. The idea is that the memcapacitor could be a building block in the constant phase element, which describes the capacitive properties of skin and has no known passive electrical equivalent. As the main issue is the deviance from a 90° phase shift, the memcapacitor with its variable capacitance might play a part.

I expect that the electrode-skin setup will show memcapacitive properties in a similar manner as the nanopore setup theoretically described by Krems et al.[11]. The reason for this is the structure of the skin, as it consists of electrolytes separated by membranes full of pores permeable to ions located on both sides, very similar to the model in this work. The setup with skin between two electrodes creates a capacitor with the skin acting as dielectric. Since the skin contains ions with finite mobility, it is likely that it shows the same properties as the nanopore in the aforementioned work. Other mechanics might also be involved, e.g. that the cell membrane acts as a elastic memcapacitor.

If one follows the principles of Pershin et al.[15], a distinct hysteresis in the charge-voltage plot is a strong indication of memcapacitance. Then a simple measurement setup as presented in this thesis should be enough to examine a subject of this property, as suggested by Krems et al.[11]. If so, there is no need for costly high end characterization equipment, and further

research and testing could prove easy to implement.

1.2   Goals

I will investigate whether a sample of the stratum corneum of the human skin between two electrodes has memcapacitive properties. To do this I will use two methods of measuring memcapacitance.

Firstly I will construct a simple measurement system, the MemCapMeter, utilizing a collection of off-the-shelf components and equipment. With this I will conduct measurements on samples of the stratum corneum in vitro and an arm segment in vivo. I will do the same with a MOS capacitor which has a voltage dependent capacitance and hysteresis in the $C\text{-}V$ (capacitance-voltage) curve. The main area of interest is the $q\text{-}V$ (charge-voltage) curve, as this is an indication of memcapacitance. In addition I will perform measurements on selected reference models for comparison and to evaluate the performance of the constructed measurement system.

The other method is the use of a Semiconductor Characterization System to do a $C\text{-}V$ (capacitance-voltage) characterization. With this I will do measurements on samples of the stratum corneum in vitro and a MOS capacitor for reference.

In addition I will do numeric simulations in MATLAB of selected reference models to compare the measurements with.

My concern is the limitations of the equipment. I might not be able to have a stimulation signal with high enough frequency to see any memcapacitive effects. Also, the sensitivity of the measurement system might not be good enough.

Chapter 2

Basic theory

2.1 Capacitance

The capacitance of a system is its ability to store charge in an electric field. The simplest example is the basic capacitor, with two metal plates separated by an insulating medium. If you move an amount of charge from one plate to the other, they will have the same amount of charge but with opposite polarity. This will generate a static electric field between the two plates. The capacitance, C, is defined as the ratio of the charge on each plate, q, to the potential difference, V, between them:

$$C = \frac{q}{V} \tag{2.1}$$

C is the capacitance given in farads (F), q is the charge on each plate given in coulomb (C) and V is the potential difference between the plates given in volts (V). This tells us about the system´s ability to store energy.

The capacitance depends on two general attributes, the geometry of the system and the properties of the medium. In the simple example the geometry would be the area of the plates and the distance between them. The property of interest regarding the insulating medium would be its permittivity e. This tells how much electric flux is created per unit charge in that medium. It is usually denoted with the relative permittivity ε_r in reference to the permittivity of vacuum e_0. The capacitance of a plate capacitor is given by:

$$C = \varepsilon_0 \varepsilon_r \frac{A}{d} \tag{2.2}$$

ε_0 is the permittivity of vacuum ($\sim 8.85e^{-12}$ $C^2N^{-1}m^2$ or Fm^{-1}), ε_r is the unitless relative permittivity of the medium, A is the area of the plates given in square meters (m^2) and d is the distance between the plates given in meters (m). The simplest capacitor has just air ($\varepsilon_r \approx 1$) as the insulating medium, but replacing that with a material with relative permittivity greater than one will increase the capacitance. These are insulators which can be polarized by an applied electric field and are referred to as dielectrics. Examples are paper, glass, plastic and aluminium oxide. For all of these, the assumption is that over time, or if you apply a voltage to the capacitor, the capacitance stays the same, it is a fixed property of the system.

2.2   Immittance

Bioimpedance is the study of the passive electrical properties of tissue. The impedance $\mathbf{Z}$ (Ω) of a tissue segment describes the transfer function transforming an applied AC current through said segment into an AC voltage. Tissue can be regarded as both a volume conductor and dielectric[6], resulting in a complex impedance:

$$\mathbf{Z} = R + jX$$

R (Ω) is the resistance and X (Ω) the reactance given by $-j/\omega C$ for capacitive elements and $j\omega L$ for inductive elements. Being a complex value it has a phase angle θ (°), which results in corresponding phase difference between the AC current and voltage. Often the modulus Z (Ω) of the impedance is used to give a generalized description of its size, with or without θ:

$$Z = |\mathbf{Z}| = \sqrt{R^2 + X^2}$$

$$\theta = arctan(\frac{X}{R})$$

The inverse of impedance is the admittance $\mathbf{Y}$ (S), which is what transforms an applied AC potential difference into an AC current:

$$\mathbf{Y} = \frac{1}{\mathbf{Z}} = G + jB$$

G is the conductance and B is the susceptance. Similarly as with the impedance is the the modulus $|\mathbf{Y}|$ and phase ϕ given by:

$$Y = |\mathbf{Y}| = \sqrt{G^2 + B^2} = \frac{1}{\sqrt{R^2 + X^2}}$$

$$\phi = arctan(\frac{B}{G}) = arctan(\frac{-X}{R})$$

If the input to a system is voltage, and the output is current, then the transfer function of the system is admittance:

$$\mathbf{i} = \mathbf{Y} \cdot v$$

2.3 q - V plots for electrical models

A q-V curve is created by applying a periodic voltage to the subject of interest, measuring the charge sent into it, and then plotting the charge against the applied voltage. Charge is acquired by measuring the current, I, and integrating it, as charge is given by:

$$dq = I \ dt$$

q-V curves for ideal electrical models can be seen in figure 2.1 on the facing page. For a resistor the current is in phase with the voltage, making the charge lag the voltage with 90°, but with the offset shifted so the complete

signal is positive. This results in a circular q-V curve which is strictly positive charge wise. For the capacitor we see from equation 2.1 that the charge is directly proportional to, and in phase with, the voltage. This results in a diagonal q-V curve with centre in the origin. For a parallel-series RC circuit the q-V curve is a mix of these two previously described, as it possesses both resistive and capacitive properties.
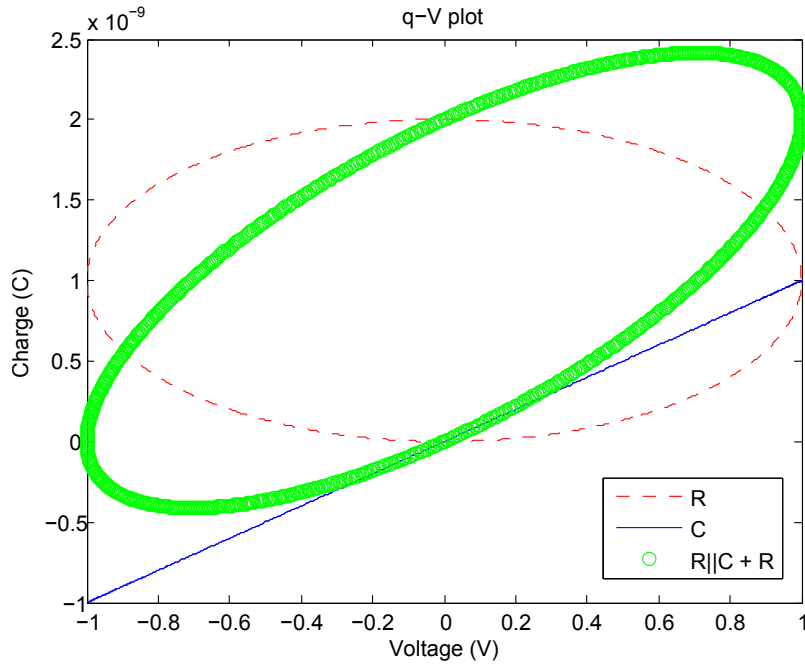
Figure 2.1: q-V plot for ideal electrical models, resistor R, capacitor C, and a parallel-series $R||C + R$ model. Signal frequency is the characteristic frequency of the $R||C$ circuit of the latter model.

Chapter 3

Bioimpedance theory

As the human tissue is mostly an electrolyte the conductivity is ionic [7]. That means that current consists of ions in motion and not electrons. The concentration of ions in a tissue segment is therefore a strong contributor to its impedance, as the concentration of free electrons is for an electronic conductor.

If one sets up a potential difference across a tissue segment it results in a electric field that make ions move and dipoles rotate. This phenomenon is referred to as relaxation. Ions and dipoles are substantially larger than electrons, and thereby has a finite mobility that is not neglectable. As the frequency of the applied potential increases, at some point the ions and dipoles are not capable of moving at the same rate, then ultimately do not move at all. This means a change in the impedance from one level to another, and this change is called a dispersion. At these levels the impedance is close to being strictly resistive, while during the dispersion it is complex (resistive and reactive). Tissue have a number of dispersions which are connected to the relaxation of its different components. The first one, the α-dispersion, is found in the Hz area and is partly caused by counter-ions moving laterally on the cell surface. The biggest one, the β-dispersion, is found in the kHz-MHz area, and is connected to the capacitance of the cell membranes. At lower frequencies the membranes block the current, but at higher frequencies they let it pass through the cells, and the total impedance decreases.

3.1 Electrical model of skin

As it is the electrical properties of skin that is of interest, electrical equivalent models are commonly used. This means representing it with a number of electrical elements, to help in understanding its function. The skin consists mainly of electrolytic intra- and extracellular spaces separated by cell membranes, giving it resistive and capacitive properties. Research has shown[6] that the capacitive component of skin does not have the usual phase change of 90° but somewhere between 0° and 90°. The solution is to use the theoretical model Constant Phase Element (CPE), which has a frequency-independent phase change somewhere in this interval. This model can not be represented by any finite number of the conventional circuit elements, but

9

can be seen as something of a mix of a resistor and a capacitor. Both these parts of the CPE are frequency-dependent, giving frequency-independent phase.
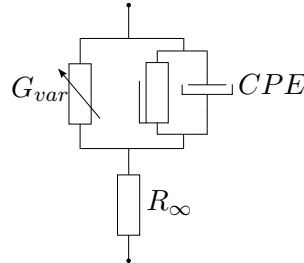
Figure 3.1: The Grimnes model of impedance for skin.

Grimnes et al.[8] have presented a model based on the traditionally used Cole model, with the improvement of being compatible with general relaxation theory. The suggested model can be seen in figure 3.1, and total impedance is given by:

$$\mathbf{Z} = R_\infty + \frac{1}{G_{var} + G_1(j\omega\tau)^\alpha}$$

Both at high (HF) and low (LF) frequencies the impedance is purely resistive, being R_∞ and $R_\infty + 1/G_{var}$ respectively. $G_1(j\omega\tau)^\alpha$ is the admittance of the CPE, and G_1 is its admittance at the characteristic angular frequency ω_m when $\omega_m\tau = 1$. τ is the average time constant for the tissue volume and varies with the independent G_{var}, which varies with frequency, thus making the model in compliance with general relaxation theory. α is connected to the phase ϕ of the CPE through $\phi = \alpha \cdot 90°$, but also to the frequency exponent in ω^α. It is an important note that this will represent one dispersion in the skin. If one wants a complete model covering the full frequency spectrum, one needs to add one of these models in series for each dispersion.

In a 2-electrode system for bioimpedance measurements, the two electrodes are used for both current carrying and signal pick-up. It is then important to remember that the electrodes affects the measurement. An electric double layer is created at the metal-skin interface, which changes the impedance of the system. The thickness of this layer will depend on the material the electrode is made of. The electrodes contribution is referred to as Electrode Polarization Impedance (EPI). A common solution is to add a Grimnes model in series with the existing model to illustrate the EPI, ergo it adds a dispersion. In addition the deeper layer tissue contribute to the measured impedance. This can also be covered by adding another Grimnes model in series. At lower frequencies (<1 kHz) the skin impedance with influence from EPI is dominating, while at higher frequencies (>100 kHz) the deeper tissue impedance is the most prominent[7].

Bioimpedance measurements are usually presented in Bode and Wessel[1] diagrams. Bode diagrams are used to present the modulus of the impedance

---

[1]Caspar Wessel (1745-1818), Norwegian surveyor, first person to describe complex numbers in the complex plane, 9 years before Argand.
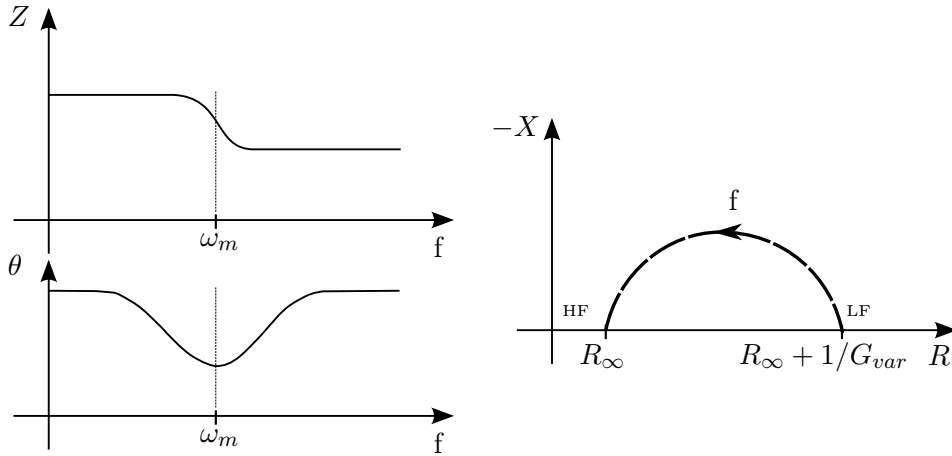
Figure 3.2: Bode (left) and Wessel (right) diagrams for the Grimnes model. Notice the downwards shifted half circle locus in the Wessel plot, moving the centre of the circle below the x-axis. This is caused by the CPE's deviance from $90°$ phase shift.

or admittance, and its phase as a function of frequency. This illustrates clearly the nature of the dispersions. In Wessel diagrams, the imaginary part of $\mathbf{Z}$ or $\mathbf{Y}$ is plotted against the real part. For impedance that means plotting the reactance against the resistance, and for admittance the susceptance against the conductance. Bode and Wessel diagrams for the model shown in figure 3.1 on the facing page can be seen in figure 3.2. The diagrams gives insight into the nature of the resistive and capacitive parts of the measurand.

Chapter 4

Memcapacitance

4.1 Memory systems

4.1.1 General description

Memory as we usually see it consists of three phases: encoding information, storing it, and retrieving it. A system having memory will then have to be capable of performing all these tasks. Another interpretation is that a system having memory means that its current state depends on the past dynamics. External perturbations can change its properties, which would be a new state for the system. It will ideally stay in this state until it gets told otherwise, and this will be the stored information. One will then sense the properties to retrieve the information. Preferable, this last action will not change the stored information, but this is not always the case.

An example is computer flash memory which is used in numerous applications. The memory cells are floating gate transistors, which has a normal control gate and a floating gate protected by an insulating oxide layer. If one applies an above-threshold voltage, a channel is created and electrons are injected onto the floating gate. This changes the conductivity of the transistor. One has changed the state of the system, and encoded information. Because the gate is surrounded by an insulating layer, electrons will be trapped there, and the information is stored. To retrieve the information, one applies a sub-threshold voltage and sense the conductivity.

Another example is the ion conductivity of biological cell membranes, which I will present a simplified model of. In nerve cells, potassium (K^+) and sodium (Na^+) ions are used as signal carriers. The cell membrane is semi-permeable, and has certain conductivity for these ions when it is in its resting state. If the potential difference between the intracellular and extracellular space decreases enough because of some stimulation, sodium ions will flow into the cell. This will increase the conductivity of the sodium channels, which in turn increases the inward flow of sodium ions and so on. This is the start of an action potential that "fires" the nerve and travels as a signal down the nervous system. This is not in the traditional sense of a read/write memory, but the change of the ion conductivity as a response to the ion transport makes this a memory system and one of many examples of memory effects in biology.

13

As seen in both these examples, one could say that memory is created by electrons or ions changing their state in a material under external perturbations. It is then natural to expect that any nanoscale system exhibits memory properties as the change of state for electrons and ions is not instantaneous and generally depends on past dynamics[15].

4.1.2   System equations

The easiest model of a system would be:

$$y(t) = g(t) \cdot u(t)$$

Where y is the output, g the transfer function, or response, of the system, and u the input. A scalar offset is commonly added, but disregarded in this review. The transfer function might be fixed, or it might depend on many variables, including the input and output. If we introduce a vector x of state variables that the transfer function depends on, we get:

$$y(t) = g(x, u, t) \cdot u(t) \tag{4.1}$$

$$\dot{x} = f(x, u, t)$$

Where x is the n-dimensional vector of state variables, which has its own equation of motion $\dot{x}$, given by the continuous n-dimensional vector function f. $\dot{x}$ describes how the state vector will change, and can depend on x itself, the input u and time t.

4.2   Memcapacitive systems and the memcapacitor

The notion of a memory system can be applied to a capacitive system. That a system is memory capacitive, or memcapacitive for short, means that its capacitance at a given moment is dependent on its history. If we apply equation (4.1) to the definition of capacitance in equation (2.1) and set the voltage as input and charge as output, we get a **voltage-controlled memcapacitive system** (as contrary to charge-controlled, where the input is charge and output is voltage) where the transfer function is the capacitance:

$$q(t) = C(x, V, t) \cdot V(t) \tag{4.2}$$

$$\dot{x} = f(x, V, t)$$

If we simplify by saying the capacitance is only dependent on the history of the applied voltage:

$$C(t) = C\left(\int_{-\infty}^{t} V(\tau) \, d\tau\right)$$

This gives an **ideal memcapacitor**, hereby referred to as the memcapacitor, described by:

$$q(t) = C\left(\int_{-\infty}^{t} V(\tau) \, d\tau\right) \cdot V(t)$$

It is worth noting that as with all ideal components, the ideal memcapacitor does not exist in reality, but it's still an approximation of practical use. Time will always be a factor to some extent, as might temperature, electromagnetic fields, mechanical vibrations etc. These will be the state variables in x. An electrical equivalent of the memcapacitor cannot be made by any finite number of traditional circuit elements, but this can be done with some memcapacitive systems.

An important requirement of the memcapacitive system is that the whole of the system must be confined within two "plates" connected to the external circuit. Thus taking the same form as a traditional capacitor.

One of the main trademarks of memcapacitance is a hysteresis in the q-V (charge-voltage) curve when subject to a periodic stimulus[15]. From equation (4.2) we see that as long as $C \neq 0$ and $C \neq \pm\infty$, $q(t)$ will be zero when $V(t)$ is zero, which gives a pinched curve going through the origin. This curve can be self-crossing, or non-self-crossing as seen in figure 4.1. The memcapacitor will have the pinched curve, while with the different memcapacitive systems the curve can be a number of shapes, depending on the nature of the system. As we see later, in some cases of memcapacitive systems the capacitance can get negative and/or diverge, which will mean that $q(t)$ doesn´t have to be zero when $V(t) = 0$ and vice versa. In any case, the current can be zero when $q(t) \neq 0$ and vice versa, ergo the system can store information.
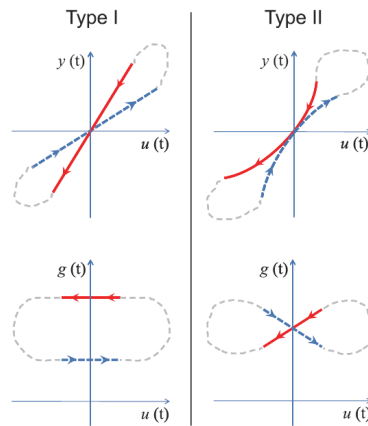
Figure 4.1: Upper: Pinched hysteresis q-V curves[15]. Type I is self-crossing, and Type II is non-self-crossing. Lower: Associated C-V curves.

A memcapacitive system could be both passive and active. In a passive system, the control parameter itself changes the capacitance. In an active system, parameters that control the equation of motion ($\dot{x}$) is needed to change the capacitance (e.g. elastic energy or a power source that apply a polarization field to the system). A passive system can be non-dissipative, where the amount of added energy equals amount of removed energy, and dissipative, where removed energy is greater than added energy. The latter is likely to always be the case, as dissipative effects will be involved when you change properties of the system. With an active system, the total amount

of added energy is greater than the amount of removed energy. This thesis
will focus exclusively on passive systems.

Frequency will always be a strong factor regarding memory effects, just
as with regular capacitance. As previously mentioned, memory stems from
rearranging of electrons and ions, and the nature of these dynamics are
dependent on the frequency of the external perturbations. This means that
memcapacitive properties of systems will be frequency dependent, and might
only show in certain frequency regions.

4.3   Memory mechanisms

There is a number of known mechanisms that do or are likely to contribute
to memory effects in a system. If we utilize the traditional capacitor model
and look at equation (2.2) we can divide them into two groups, those related
to the geometry of the system (A/d), and those related to the permittivity
of the system (ε_r).

4.4   Geometry related memory

Geometry related mechanisms would be about the change of the area or
distance between the plates. It can also be redox reactions or charging that
changes the properties of the plates, but this will not be discussed.

4.4.1   Distance changing

Elastic membrane[15]

This could for example be a capacitor with one plate fixed and the other
elastically suspended. When charge is added to the plates they will attract
each other because of the opposite charging, and the distance will decrease.
This will again change the capacitance, as we see from equation (2.2). The
q-V curve will typically be a Type II pinched hysteresis curve.

This is also an effect appearing in the lipid bilayer, a major component of
the biological membrane, where applied electric field will result in a physical
stress which will change the thickness of the membrane. This in turn affects
both the resistance and capacitive properties of the membrane. The same
apply to the electric double layer at the electrode-skin interface[14].

4.5   Permittivity related memory

Permittivity-related mechanisms can be divided into three subcategories:
delayed response, permittivity switching, and spontaneously polarized
medium.

4.5.1   Delayed response

Delayed response describes systems where dynamics in the dielectric
permittivity are not instantaneous, but involves a time delay. The changes

are caused by tunnelling or ionic transfer in the medium.

Superlattice - Tunnelling[13]

This is a capacitor embedded with a multilayer structure of metallic layers separated by an insulator. No charge is transported between the outer plates (negligible) but non-linear electronic transport between the internal layers occurs by tunnelling. The result of this is a change in the permittivity of the system. This can give a trapezoidal hysteresis q-V curve and diverging and possible negative C-V curve.

Ionic - Ionic transfer[11]

This could be a nanopore in an ionic solution, with electrodes submerged in the solution on either side of the nanopore. The memory effects are from slow polarizability of the ionic solution caused by the finite mobility of ions in water, and transport of ions through the nanopore. These mechanisms appear at different frequencies. The q-V curve will typically be a tilted circle, with a star shaped C-V curve with diverging and possible negative capacitance.

Biological tissue, with extra- and intracellular electrolytes separated by a cell membrane would most likely possess these properties.

4.5.2 Permittivity switching

With permittivity switching mechanisms the permittivity changes under external input without time delay. This would be caused by ionic doping or phase transitions.

Polymer based - Ionic doping[12]

A field-configurable ion-doped polymer can have programmable capacitance. This can be realized by integrating a layer of polymer with a layer of ionic conductor between electrodes in a multilayer structure. This can also be inserted into a metal-oxide-semiconductor (MOS) capacitor. The memory effect stems from modulation of the ionic concentration in the polymer layer. Applying voltage pulses will change the ionic concentration, which in turn induce non-volatile changes in the polymer dielectric property.

An example is MEH-PPV polymer with a layer of $RbAg_4I_5$ ionic conductor in an $Al/Ti/RbAg_4I_5/MEH$-PPV/Pt multilayer structure. Ag cations with high concentration and mobility in the ionic conductor diffuse over to the polymer to reach a quasi-equilibrium profile. I anions will chemically bond with the polymer, and need a large external electrical force to drift. With large negative voltage pulses applied, the I anions will drift into the polymer layer and bond with the Ag cations to form ionic dipoles, which in turn increase the polymer permittivity and thereby the device capacitance. An applied positive voltage pulse will then be able to reverse this change.

Metal Insulator Transition - Phase transition[5]

Memory metamaterials can be fabricated by the use of Metal Insulator Transitions (MIT). For example temperature can be used to progress the MIT, which in turn changes both the resistance and dielectric properties of the medium. An example of this is the deposition of a split-ring resonator array on a vanadium-dioxide (VO_2) thin film between two electrodes. Both external heating, and internal heating caused by applying voltage pulses, will induce the before mentioned changes, showing a change in the resonance frequency of the construction.

4.5.3   Spontaneously polarized medium

Spontaneously-polarized mediums are ferroelectric materials which has non-zero average electrical polarization. This shows hysteresis as a function of electric field, revealing well-defined polarization states.

Ferroelectric - Non-zero polarization[2]

Capacitors where the dielectric material is replaced by a ferroelectric material are realized a long time ago, and are used for example in Ferroelectric RAM. One commonly used material is PZT. A newer application is the coupling of ferroelectric material and high performance semiconductors, which would have numerous uses in electronic and optoelectronic applications. An example is a PZT-ZnO heterostructure between Pt electrodes.

4.5.4   Other

MOS capacitors with nanocrystals - Charge capture[10]

Non-linearity in the C-V curve is common in MOS capacitors. Embedding nanocrystals have shown to give the possibility of controlling the displacement of the C-V curve. The amount of charge deposited on the nanocrystals is the controlling factor, and acts as the state-variable controlling the capacitance of the structure. It is worth mentioning that this device would include resistive properties, since the charge transfer to the nanocrystals involves dissipation processes. An example is Ge nanocrystals inserted into SiO2 film, in a SiO2/nc-Ge/SiO2/Si system. The discharge phenomenon is mainly caused by tunnelling.

Part II

Equipment & Method

Chapter 5

MemCapMeter

5.1 Measurement principle

The general principle of the MemCapMeter, short for memory capacitance meter, is fairly simple. In short, a small signal AC voltage is applied to a pair of electrodes placed on the measurement subject. Both the voltage potential over the electrode setup and the current going through them is measured and the current is integrated to acquire the charge. The main result is the resulting q-V curve, but a range of other plots and values are calculated from the data to examine the subject's properties.

The AC signal is generated by a function generator. Analogue to digital conversion is performed with a data acquisition (DAQ) card. The voltage and current sensing and the interfacing between the function generator, electrodes and the DAQ card is performed by a self manufactured Front End. Integration of current and all other signal processing in addition to data presentation is done in software using LabVIEW™ from National Instruments. Additional data presentation is performed with Microsoft Excel. Details about the setup is described in the following sections.
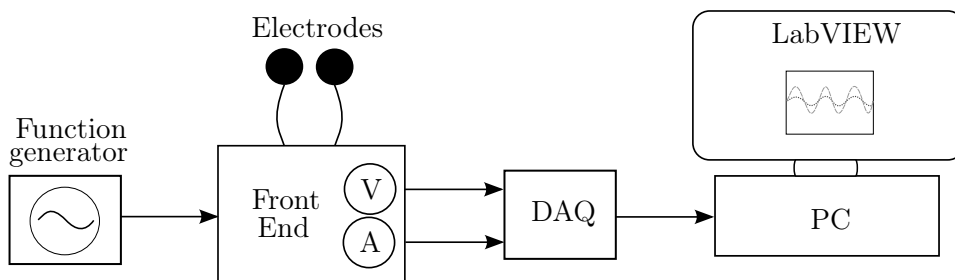
Figure 5.1: Block diagram of MemCapMeter.

A 2-electrode system was used for two reasons. The first is the intrinsic simplicity of this measurement principle. The other is that this will cover all the elements of the typical bioimpedance measurement, the electrodes, the skin and deeper tissue. As mentioned in section 4.4.1 the double layer at the electrode-skin interface might also introduce memory properties, which would also be of interest. I leave it to future work to determine the exact

21

location of any memcapacitive contributions.

Since a voltage was applied and the current sensed, it was actually admittance that was measured. As impedance is more commonly used to present bioimpedance measurements, and since it is a more easily perceived quantity, the results were presented from a impedance perspective.

5.2   Hardware

5.2.1   Front End

This is a self made Front End for interfacing and current sensing. Current sensing is performed using a operational amplifier set up as a transimpedance amplifier with adjustable gain. This is to cater to different subject impedances which results in different currents. The resulting output voltage from the transimpedance amplifier have been kept in the same range as the applied AC voltage. The schematic can be seen in figure 5.2 on the next page. A picture of the Front End can be seen in figure 5.3 on page 24.

A BNC contact was used to connect with the external function generator with a 50 Ω coax cable. This was followed by a 100 μF capacitor acting as a DC-block, which could be bypassed with a jumper. For all measurements this was bypassed. A 1 kΩ resistor was inserted to limit current if electrodes were short circuited. This will in most cases introduce a negligible contribution as the impedances measured were mostly far greater than this. Next in the signal pathway were the electrode outputs, where test pins with 4 mm connectors were fitted. At last a TL071C operational amplifier wired as a transimpedance amplifier, thereby giving out a voltage proportional to the current, hereby referred to as current sense voltage. This had a jumper selectable resistor in negative feedback, to choose amplifier gain. The choices were 100 Ω, 1 kΩ, 10 kΩ and 100 kΩ, supplying the same gain as resistance value. Test pin outputs for differential connection with the DAQ card were supplied at the electrode outputs to monitor voltage applied, hereby referred to as electrode voltage, and between transimpedance amplifier output and common to monitor current sense voltage. The first was connected to input channel 0 and the latter to input channel 1 on the DAQ card. Power was ± 9 V, supplied by two 9 V batteries to minimize power supply noise. The design included two resistors and a potentiometer for balance adjustment of the operational amplifier, but this was regarded as not needed, and the components were not mounted.

The TL01 operational amplifier was chosen based on its good all-round properties, high input impedance (JFET) and high slew rate (13V/µs).

The card was designed in CADSTAR$^{\copyright}$ version 13.0 by Zuken Ltd. Complete PCB production was performed at the Electronics Lab at the Department of Physics.
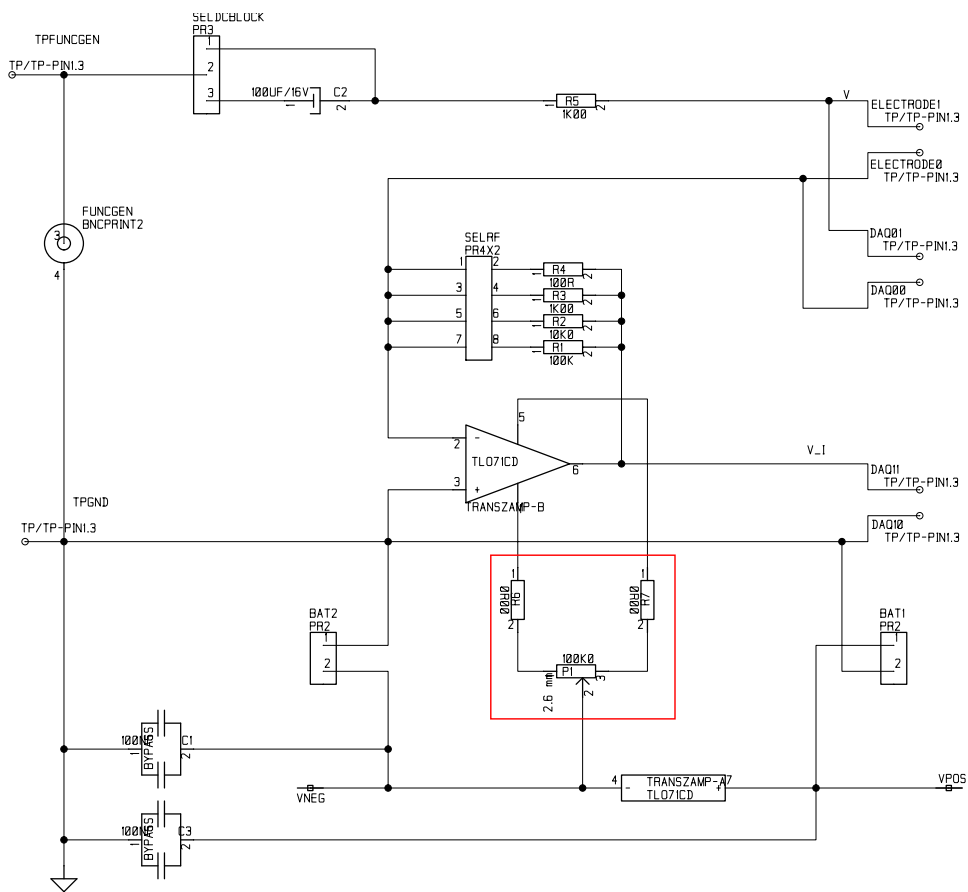
Figure 5.2: Front End schematic. Purpose was current sensing and to be an interface between function generator, electrodes and DAQ. Components marked with red were not mounted on PCB. Schematic and PCB design was conducted in CADSTAR$^{©}$ 13.0.
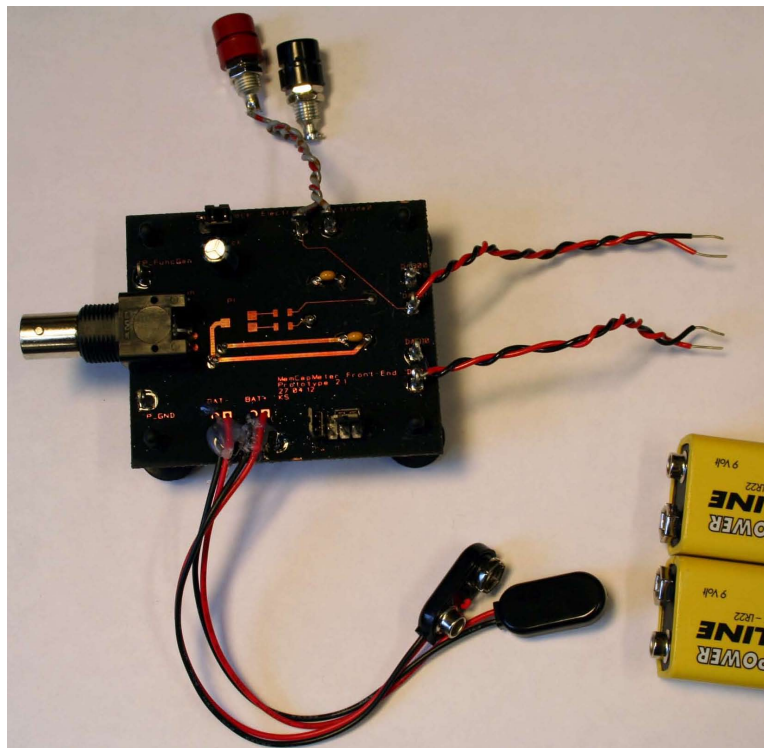
Figure 5.3: Front End setup with the battery power source. Left is BNC connector for connection of function generator. Upper is banana plug outlets for connection of electrodes. Right is wires for connection with DAQ.

Figure 5.4: The DAQ car used, a NI9223 Analogue Input Module and a 1-slot NI CompactDAQ chassis with USB connection. Left is connection panel for inputs. To the right is USB plug for PC connection and wire for ground connection.

5.2.2   DAQ

For analogue to digital conversion a measurement bundle from National Instruments was used. This consisted of a NI9223 Analogue Input Module and a 1-slot NI CompactDAQ chassis with USB connection. The Input Module supplied four 16-bits, 1 MS/s, differential analogue input channels with 1 GΩ input impedance. A picture of the DAQ can be seen in figure 5.4. This simplified the interfacing between the Front End and the software used.

The inputs had a maximum voltage rating of ±10 V, with an accuracy of 3 mV. With 16-bits resolution this gave voltage resolution of 0.3 mV. This was adequate as measurements were in the range ±50 mV.

5.2.3   Function generator

I used a TG550 Function Generator from Thurlby Thandar Instruments, a precision 5 MHz generator.

5.2.4   Electrodes

I used three different types of electrodes, to observe their contribution to the results. All are Ag/AgCl, but with different electrode skin interface principle.

- Ambu$^{®}$ Blue Sensor N **wet gel** electrodes

- Kendall™ KITTYCAT™ **dry gel** electrodes

- Quickels QN 500 **dry button** electrodes

The mentioned gel is a contact electrolyte gel, commonly used in skin surface electrodes to enhance electric contact. As the Blue Sensor and the QN 500 electrodes both had 4 mm connectors (commonly referred to as banana plug), test leads with banana plugs were used to connect it to the Front End. The KITTYCAT™ electrodes were used with the model dock described in section 5.4. As the whole surface of the latter was covered in conductive dry gel, they where cut to an area smaller than the measurement subject to avoid short circuit. When using the QN 500 electrodes, they were held together with the use of a 200 g weight inside a Plexiglas cylinder for stability. Both the gel type electrodes were adhesive and required no other means to be kept together. The electrode setups can be seen in figures 5.5 and 5.6. The electrodes will from now on be referred to as wet gel (Blue Sensor), dry gel (KITTYCAT™) and dry button (QN 500) electrodes.
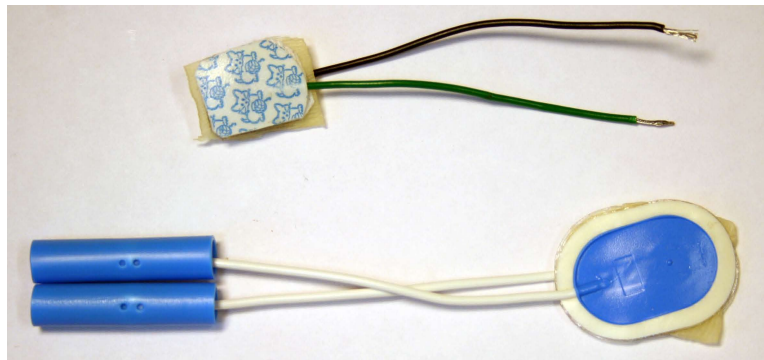
Figure 5.5: KITTYCAT™(upper) and Blue Sensor (lower) electrodes setups with skin sample. The KITTYCAT™electrodes were pre-cut to fit the skin sample.
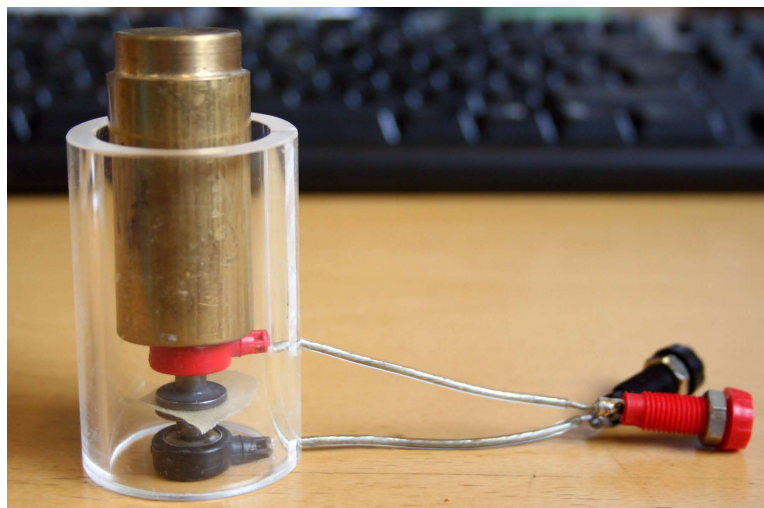
Figure 5.6: QN 500 electrode setup with skin sample in between. Mechanical stability was achieved by the use of a 200 g weight inside a Plexiglas cylinder.

5.3 Software

5.3.1 LabVIEW™

For signal processing I have used LabVIEW™ 2011 from National Instruments. This is a system design platform utilizing the visual data flow programming language G. In this environment one can create programs, also referred to as visual instruments (VI), which can be built into one another. When a VI is used in another VI, it is referred to as a subVI. They consist of a Front Panel, used to control and indicate; a Block Diagram, where the program is built; and a Connector Panel, which defines inputs and outputs when included as a subroutine in another program. The reason for using LabVIEW™ is the plug and play compatibility with the Measurement Bundle, the built in signal processing functions and the data presentation capabilities.

I have created the VI *MemCapMeter.vi* to process, present and store the desired data. Further description of this follows in the next section.

5.3.2 MemCapMeter.vi

The *MemCapMeter.vi* is as mentioned a program made in LabVIEW™, to perform the signal processing, presentation and storing of data collected by the DAQ card.

A picture of the Front Panel, which is the user interface, can be seen in figure 5.7 on page 29. Description of controls can be seen in table 5.1, graphs in 5.2 and indicators in table 5.3. Vch refers to input channel 0 of the DAQ card, which measures electrode voltage and V_Ich refers to input channel 1, which measures current sense voltage.

Table 5.1: Controls on MemCapMeter.vi Front Panel.

Name	Description
Number of samples	Number of samples that the DAQ card should read.
Sample rate (Hz)	Sample rate (f_s) for the DAQ card.
Curr Gain Res. Rf	Value of chosen feedback resistor (gain) for the transimpedance amplifier on Front End.
1 Period plotting	If the plots DAQ Raw Signal; V,I,Q (Normalized); Charge vs Voltage; and Capacitance vs Voltage will present only one period.
Remove DC-offset	If the calculated mean of the signal will be subtracted from the signal.
Read from:	Select source to read from: DAQ or Measurement file.
Write to file	If the sampled data will be written to a measurement file (.lvm).
Write to report	If calculated values will be written to a report file (.txt).
Measurement file name	Name of measurement file (.lvm) to write to/read from.
Report file name	Name of report file (.txt) to write calculated values to.
Measurement subject	Description of measurement subject, will be written to report file if enabled.

Table 5.2: Graphs on MemCapMeter.vi Front Panel.

Name	Description
DAQ Raw Signal - All Channels	Raw signals read from the DAQ card. Shows only one signal period if '1 Period plotting' is enabled.
Full Sample Plot of Charge	Charge sent to the electrodes over the full sample period.
V,I,Q (Normalized)	Normalized plot of electrode voltage, current and charge. Shows only one signal period of '1 Period plotting' is enabled..
Charge vs Voltage	Charge sent to electrodes plotted against applied voltage.
Capacitance vs Voltage	Capacitance of measurement subject versus applied voltage.
Phase difference in reference to voltage	Phase difference in degrees for charge and current in reference to applied voltage.
Frequency spectrum	Frequency analysis of raw signals. Upper graph shows full analysis (1->$f_s/2$), centre is zoomed in on signal frequency, bottom shows low frequency.
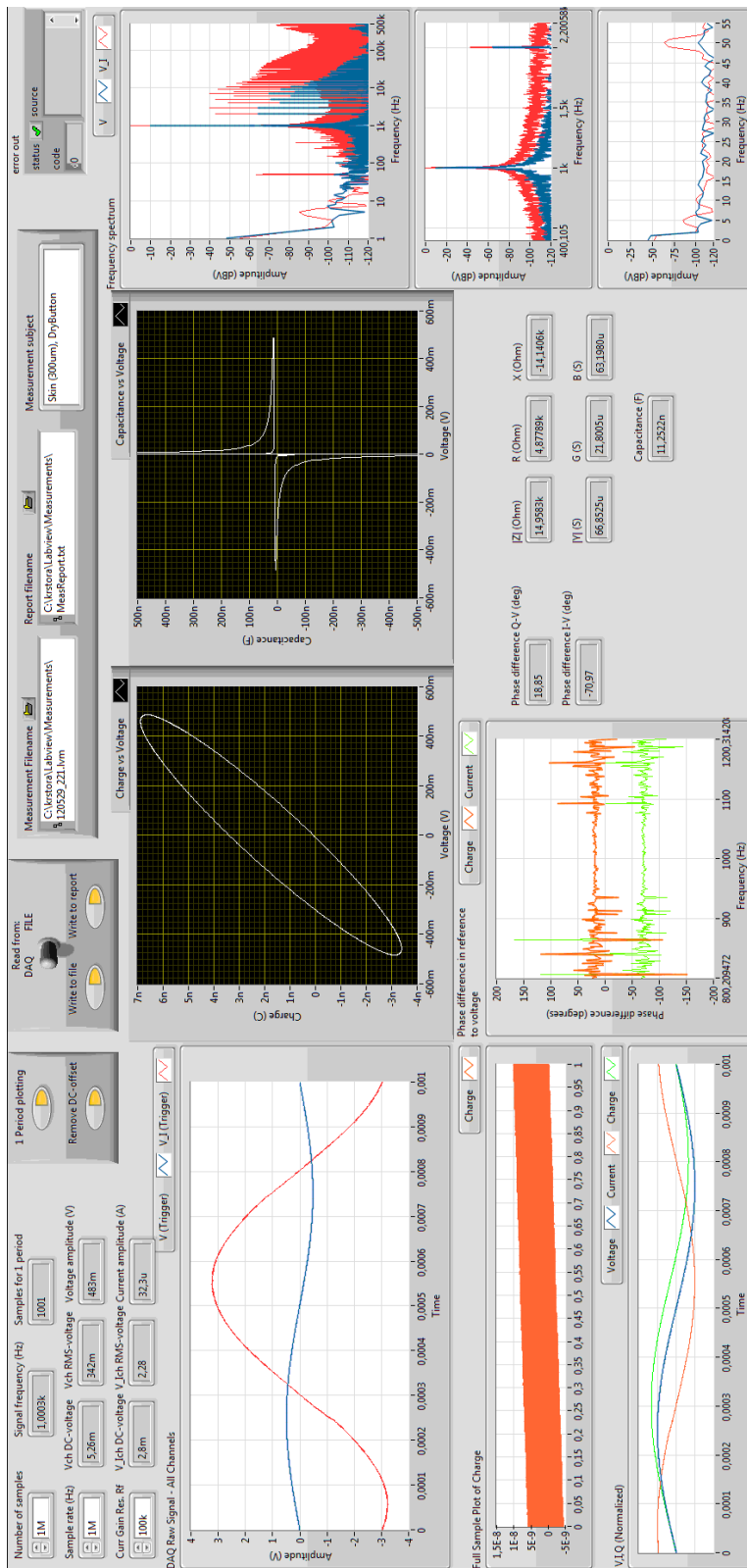
Figure 5.7: MemCapMeter.vi Front Panel.

Table 5.3: Indicators on MemCapMeter.vi Front Panel.

Name	Description
Signal frequency (Hz)	Frequency of main tone.
Samples for 1 period	Number of samples covering one period of main tone.
Vch DC-voltage	DC-voltage (mean) for electrode voltage from Front End.
V_Ich DC-voltage	Same as previous for current sense voltage from Front End.
Vch RMS-voltage	Root mean square voltage for electrode voltage.
V_Ich RMS-voltage	Root mean square voltage for current sense voltage.
Voltage amplitude	Amplitude of electrode voltage.
Current amplitude	Amplitude of current through the electrodes.
Phase difference Q-V (deg)	The phase difference between charge sent to the electrodes and applied voltage.
Phase difference I-V (deg)	The phase difference between current through the electrodes and applied voltage.
|Z| (Ohm)	Impedance modulus of measurement subject.
R (Ohm)	Resistance of subject.
X (Ohm)	Reactance of subject.
|Y| (S)	Admittance modulus of subject.
G (S)	Conductance of subject.
B (S)	Susceptance of subject.
Capacitance (F)	Capacitance of subject.
Error out	Status of VI, and describes any occurred errors. Error codes can be entered in the "Explain error" function under the Help tab to get further details.

The Block Diagram is the structure of the program, and can be seen in figure A.1 on page 96 in Appendix A. Short descriptions of the functions and VI's used follows.

Controls from Front Panel can be seen at the far left. The DAQass.vi controls and reads the data from the DAQ card. Sample length and sample frequency are as mentioned selected on Front Panel. The sampled raw data is stored to a .lvm measurement file for later reference, if this is enabled on Front Panel. Two pathways follows, the main path which uses the full sample length for calculation of different values, and the plotting path which is used for creating a range of graphs. The latter path can be set to extract samples covering one period of the main tone for the mentioned plotting, triggering when the voltage crosses 0 V upwards.

In the main pathway a FFT analysis is performed, and three plots are created with different x-axis range to highlight different parts of the spectrums. The RMS and DC voltage for both channels are calculated, and the DC value (mean) can be removed from both channels if enabled on Front Panel. Current is calculated from the current sense voltage by dividing on the given value given in Curr Gain Res. Rf, which is the value of the amplifier feedback resistor on the Front End setting the current amplification. The frequency and amplitude of the main tone of the electrode voltage is calculated, and the amplitude for the current. From the frequency of the voltage the sample length for one signal period is calculated, which is used in the extraction of one period in the plotting pathway. The current is integrated to acquire the charge. The phase differences for current and charge in reference to the voltage are calculated and plotted. The charge is plotted for the full sample. A range of values are calculated by *MathVI1.vi*. These together with other calculated and set values are written to a report file by *writeReportTXT.vi*, if this is enabled. A *.txt* report file have been used, in which the values have been added for each run. This could then easily be imported to other programs for further signal processing or data presentation.

In the plotting pathway the DC values is also subtracted if enabled. The current and charge are calculated as in the main pathway. The continuous capacitance is calculated by dividing the charge on the voltage signal. In the end are the plotting of raw signals; charge vs. voltage; normalized voltage, current and charge; and capacitance vs. voltage.

MathVI1.vi and *writeReportTXT.vi* are self-designed VI's building on existing functions, and can be seen in figure A.2 on page 97 and A.3 on page 98 in Appendix A. In the former figure is also the other instances of the case structures. All other subVI's are built-in functions and express functions saved as instances with properties set.

Table 5.4: List of software used for various purposes.

Program	Manufacturer	Description of use
LTspice 4.15	Linear Technology	Simulation of components and Front End performance
PSPICE 9.1	Cadence	Same as over
TINA-TI V9	DesignSoft/Texas Instruments	Same as over
Texniccenter 1.0	ToolsCenter	Editing thesis
Excel 14.0	Microsoft	Plotting results
Inkscape 0.48	Free Software Foundation	Editing figures

5.3.3   Other software

I have used a range of other software during the work on this thesis. A list of these and a short description on what I have used them for can be seen in table 5.4.

5.4   Measurement subjects

A range of subjects were examined. Primarily on in vitro samples of the outermost layer of the human skin, the stratum corneum, but also on other subjects to use as reference.

The skin samples have all been from a 27 year old male, removed from heel with an Aesculap$^{®}$ Acculan$^{®}$ Dermatome model GA5643 from B. Braun Melsungen AG. The skin was mildly abraded with sand paper before removal. All samples have been 300 μm thick, and had an approximate area of 2x2 cm. These measurements were performed with the electrodes mentioned in section 5.2.4. Measurements on an arm segment in vivo have also been performed. This have been on lower arm of 27 year old male, with a separation of electrodes of approximately 5 cm. These measurements were performed with the wet gel electrodes. Measurements with the dry button electrodes was also performed on a piece of paper tissue to evaluate potential hysteresis effects contribution from the electrodes. A skin sample and the paper tissue sample can be seen in figure 5.8 on the next page.

As reference subject with hysteresis properties a MOS capacitor wafer was used. This can be seen in figure 5.8 on the facing page. The MOS capacitor wafer was chosen based on a known hysteresis in the capacitance-voltage plot. This was a p-type silicon substrate with deposited aluminium monoxide (AlO). The wafer had one common bottom electrode and several top electrodes constituting individual capacitors. The bottom of the wafer also had a layer of AlO, which was penetrated and silver adhesive was added to ensure sufficient electrical contact with the bottom electrode. Connection between this and the Front End was performed with a test lead and a crocodile clip. For the top electrode a banana plug with a simple wire secured at the electrode with the use of a wooden clothes pin. Measurements with
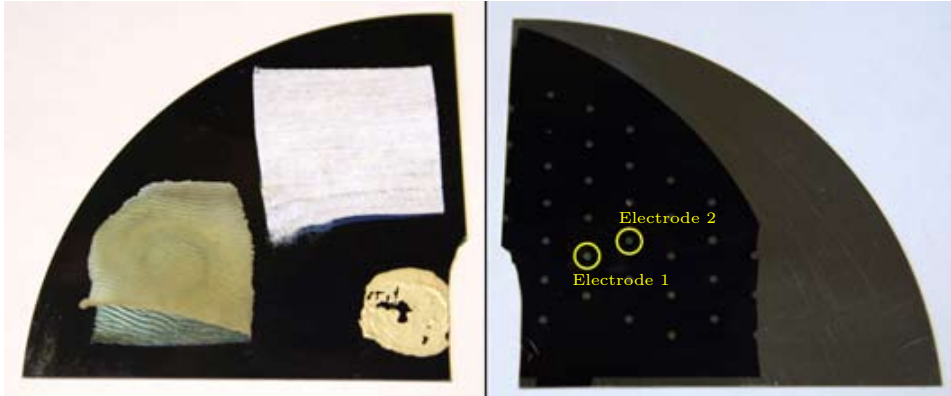
Figure 5.8: Left: An example skin sample and the paper sample on the bottom of the MOS capacitor wafer. The blue layer is AlO. In the bottom right corner the AlO layer is removed and silver adhesive is added. Right: Top of MOS capacitor wafer. The small metal circles are electrodes giving individual capacitors. The electrodes circled with yellow were studied.

Figure 5.9: Model dock constructed of cardboard and two banana plug connectors. Ceramic capacitor mounted for measurement.

the MemCapMeter was done on Electrode 1.

Additional reference subjects were a few simplified electrical models to see how this compares to the skin measurements. The models were:

- $R_p||C + R_s$

- C (1 nF)

- R

Component values were: $R_p = 747$ kΩ, $C = 10$ nF, $R_s = 999$ Ω for the parallel-series model, $C = 1$ nF for the single capacitor model and $R = 99.3$ kΩ for the single resistor model. Component values of the $R_p||C + R_s$ model were chosen to approximate the properties of the measurement on skin with dry button electrodes. To perform these measurements a constructed Model dock was utilized. This had 4 mm connectors so it could be used with the same test leads as with the electrodes. A picture of the Model dock can be seen in figure 5.9.

Chapter 6

Reference work

6.1 MATLAB simulations

Simple simulations in MATLAB of measurements on selected subjects was performed. The models used were:

- $R_p||C + R_s$

- $R_p||CPE + R_s$

- $R_p||C_{mem} + R_s$

- C

Component values were selected to the same values as the reference models measured with the MemCapMeter, as described in section 5.4. The $R_p||C_{mem} + R_s$ implemented a voltage dependent capacitive component, where the capacitance was given by:

$$C_{mem} = 10 \text{ nF} \cdot (1 + V) \tag{6.1}$$

The results were the same values and plots as acquired with the MemCap-Meter, and they were calculated in the same manner. This was compared to the measurement results to examine how they related to suggested theories.

Additional simulations were performed to show some different effects on measurements:

- 50 Hz noise and DC offset effect on q-V curves

- Current limit resistor effect on C-V curves

- Calculation of capacitance for $R_p||C + R_s$ model

MATLAB code can be seen in Appendix C.

6.2   C-V characterization

This was a different measurement technique than the one used with the MemCapMeter. This was a *C-V* characterization performed with a high end semiconductor characterization system. In short, a DC potential was applied over the measurement subject, then a small signal AC-voltage was applied to calculate the properties of the subject. The DC bias varied from a minimum value to a maximum value and back. The resulting data was the capacitance of the subject for each DC bias voltage step, from which *C-V* plots were built.

The setup used was a Keithley SCS-4200 system with 4210-CVU measurement unit for C-V-measurements and a Signatone (Model S-1060R-6XG-D3-220V) probe station. A 4-electrode setup was used, with one pair for voltage application and measurement, and one pair for current measurement. However, the electrode pairs were attached to the same locations, resulting in a 2-electrode measurement. These measurements were performed at the Solar Cell Laboratory at Institute for Energy Technology (IFE) with the help of Ørnulf Nordseth.

Skin

Measurements were taken on one skin sample, 300 μm thick, approximately 2 x 2 cm. This acquired as described in section 5.4 ten minutes before the measurements. One pair of wet gel electrodes were used, connected to the probe station with banana plug test leads, thereby bypassing the built-in electrodes. Two measurement runs were performed, with AC signal frequency 10 kHz and 100 kHz, both with DC bias varying between +10 V and -10 V.

MOS capacitors

Measurements were taken on the MOS capacitor wafer described in section 5.4. The built-in electrodes of the probe station were used for these. Electrode 1 and 2 were examined, constituting two separate capacitors. Both measurement runs were performed with AC frequency 10 kHz, and with DC bias varying between +5 V and -5 V.

6.3   SPICE modelling of memcapacitor

Biolek et al.[1] have presented a SPICE model of a memcapacitor. An effort was made replicating this work, but this however was not successful. As it was not connected to any of the primary goals of this thesis, it was discontinued.

Part III

Results

Chapter 7

MemCapMeter

Results from measurements with the MemCapMeter are presented in this chapter. Measurements were performed as described in chapter 5.

For each subject, three figures are presented. Firstly the q-V curves for a selected range of frequencies. Secondly the raw signal curves (electrode voltage and current sense voltage) at a selected frequency. Thirdly the C-V curve for the same frequency.

Bode diagrams and capacitance plots for all measurements can be found in Appendix B.

As results from measurements on an arm segment in vivo were so similar in nature as the measurements on the skin sample in vitro, they are not presented.

Results from measurements with the dry button electrodes on a piece of paper tissue are not presented either. Caused by too high impedance in the electrode-paper setup, the SNR was too poor to produce any good results.

General remarks

A comment to the q-V curves is that one can see the charge amplitude decrease as the frequency increases. This is natural, as the charge is the time integral of current, and increased frequency results in decreased time period. At 1 Hz the plotting of the q-V curves were not started at zero phase for the voltage, which resulted in an unknown vertical offset of the curve.

For raw signal and C-V plots for the measurements, 1 kHz was chosen. This because it was the frequency where the reactive part in overall was the most prominent. For the MOS capacitor 5 kHz was chosen, as this was the frequency where the memory effects were most visible in the plot.

In some high frequency measurements the electrode voltage is noticeable less than than the applied voltage. This is because the electrode-skin impedance at this frequency is not far greater than the 1 kΩ current limitation resistor on the Front End. This however causes a negligible contribution to the q-V and raw signal curves, as electrode voltage and current are affected equally, making phase and signal shape unchanged. It is however expected to affect the C-V curves to some degree, as shown in section 8.6.

A comment to the raw signal curves is that the amplitude of the current sense voltage can vary. This is to be disregarded, as this is in part a result of selected amplification at the Front End. Distortion of the sinusoidal curve is what is to be evaluated in these figures. Note that the V_I signal is the current sense voltage which are 180° phase shifted from the current by the inverting transimpedance amplifier.

In all measurements at 100 kHz the phase difference between measured current and calculated charge is noticeable smaller than 90°. This might suggest that the number of samples per period is too small for usable calculations. This is also the case in some measurements at 1 Hz, probably because the calculations were based on only one signal period.

7.1   Skin in vitro

7.1.1   Wet gel electrodes

Skin sample measured with wet gel electrodes. Measurements were performed within 1 hour after skin removal and electrode attachment. Applied voltage amplitude was 100 mV.

Figure 7.1: q-V curves for measurements on skin sample with wet gel electrodes. Applied signal frequency is indicated in the plots. The curves appear strictly resistive at low frequency, with an increasing capacitive component with increasing frequency. All the curves are ellipses indicating sinusoidal q and V motions.
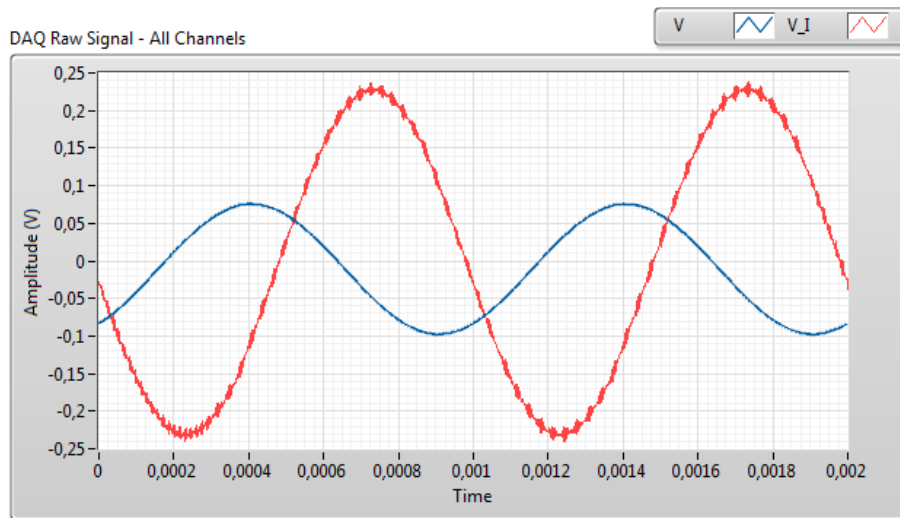
Figure 7.2: Both signal curves for skin sample with wet gel electrodes at
1 kHz, two periods plotted. Blue = electrode voltage, red = current sense
voltage. No noticeable harmonic distortion of current sense voltage.

Figure 7.3: C-V curve for skin sample with wet gel electrodes at 1 kHz. Left:
the full plot. Note the diverging positive and negative capacitance around 0
V. Right: Zoomed in across the calculated capacitance (47.3 nF). The curve
is antisymmetric around the diagonal.

Old skin sample

Old skin sample measured with wet gel electrodes. Measurements were performed 27 days after skin removal and electrode attachment. Applied voltage amplitude was 500 mV.

Figure 7.4: *q-V curves for measurements on old skin sample with wet gel electrodes. Applied signal frequency is indicated in the plots. The curves appear strictly resistive at low frequency, with an increasing capacitive component with increasing frequency, then approaching resistive again. All the curves are ellipses indicating sinusoidal q and V motions.*
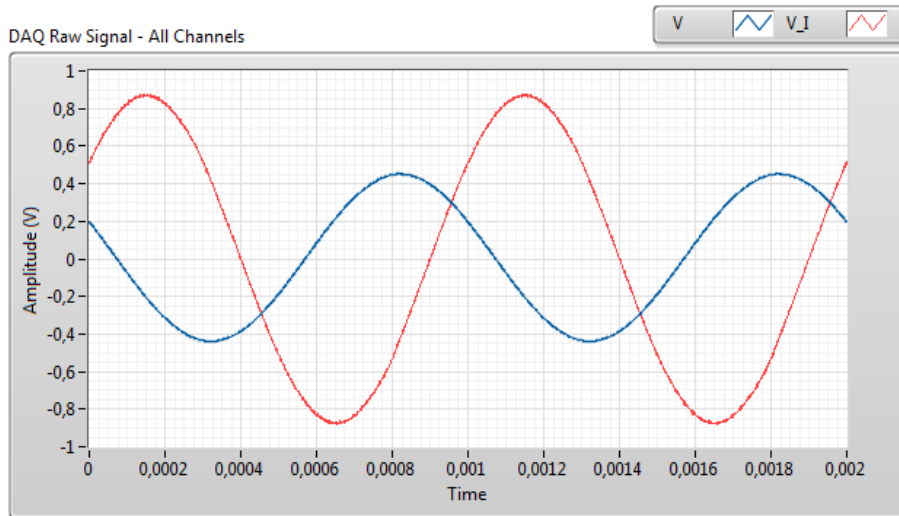
Figure 7.5: Both signal curves for old skin sample with wet gel electrodes at 1 kHz, two periods plotted. Blue = electrode voltage, red = current sense voltage. No noticeable harmonic distortion of current sense voltage.

Figure 7.6: C-V curve for old skin sample with wet gel electrodes at 1 kHz. Left: the full plot. Note the diverging positive and negative capacitance around 0 V. Right: Zoomed in around the calculated capacitance (35.6 nF). The curve is antisymmetric across the diagonal.

Remarks

The q-V curves show an earlier capacitive influence for the old skin sample than the previous measurements in regards to frequency. Impedance and phase shift calculations suggests a decrease in characteristic frequency and increase in resistive properties, which are in accordance. Reactive properties is found to be larger, which is in accordance with decreased calculated capacitance.

7.1.2 Dry gel electrodes

Skin sample measured with dry gel electrodes.   Measurements were
performed within 1 hour after skin removal and electrode attachment.
Applied voltage amplitude was 100 mV.
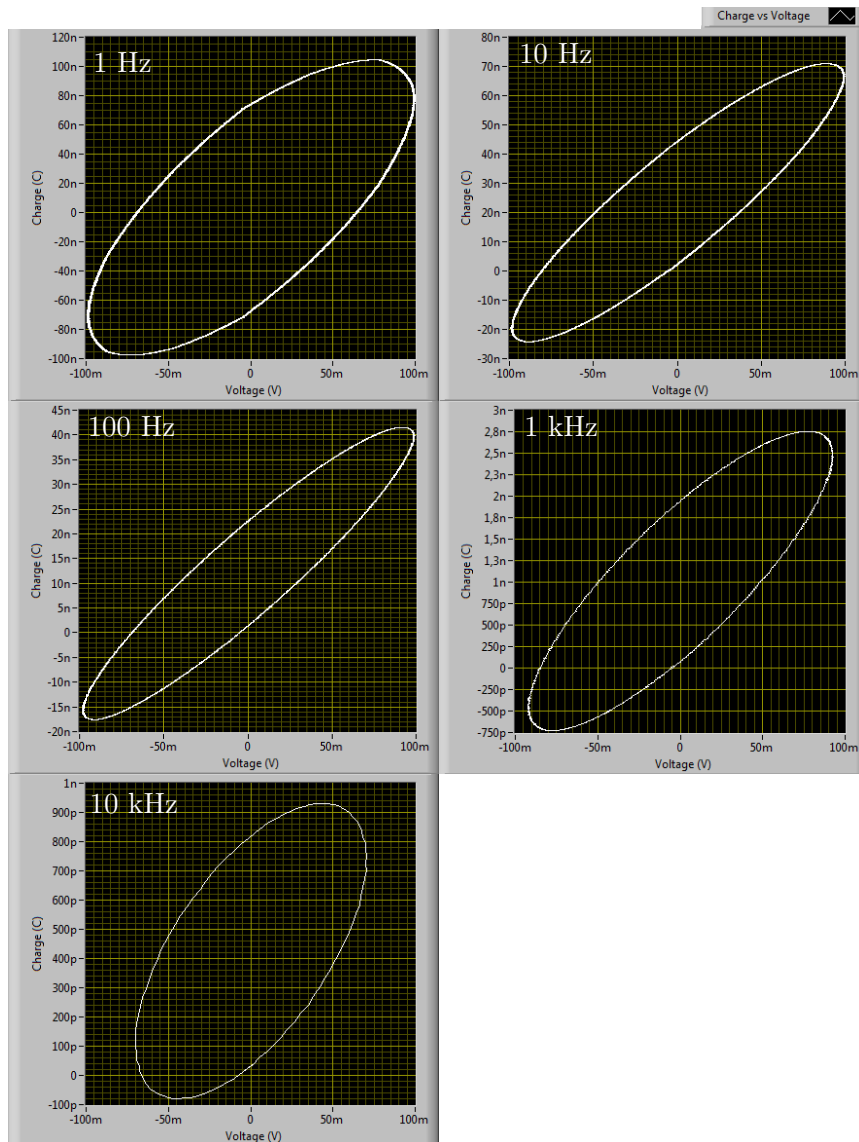
Figure 7.7: q-V curves for measurements on skin sample with dry gel
electrodes. Applied signal frequency is indicated in the plots. The curves
appear strictly resistive at low frequency, with an increasing capacitive
component with increasing frequency, then approaching resistive again. All
the curves are ellipses indicating sinusoidal q and V motions.

Figure 7.8: *Both signal curves for skin sample with dry gel electrodes at 1 kHz, two periods plotted. Blue = electrode voltage, red = current sense voltage. No noticeable harmonic distortion of current sense voltage.*
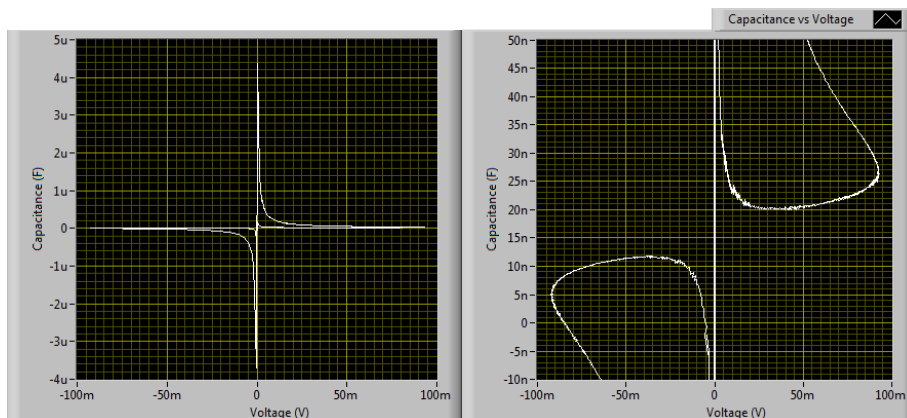
Figure 7.9: *C-V curve for skin sample with dry gel electrodes at 1 kHz. Left: the full plot. Note the diverging positive and negative capacitance around 0 V. Right: Zoomed in around the calculated capacitance (22.5 nF). The curve is antisymmetric across the diagonal.*

Remarks

The *q-V* curves show earlier capacitive properties than with wet gel electrodes with regards to frequency. Impedance and phase difference calculations shows both smaller characteristic frequency and larger resistive which are in accordance. This is most likely caused by the dry gel not penetrating the skin as much as the wet gel, resulting in a higher resistive contribution. Reactive properties are larger, in accordance with smaller calculated capacitance.

Old skin sample

Old skin sample measured with dry gel electrodes. Measurements were performed 7 days after skin removal and electrode attachment. Applied voltage amplitude was 500 mV.
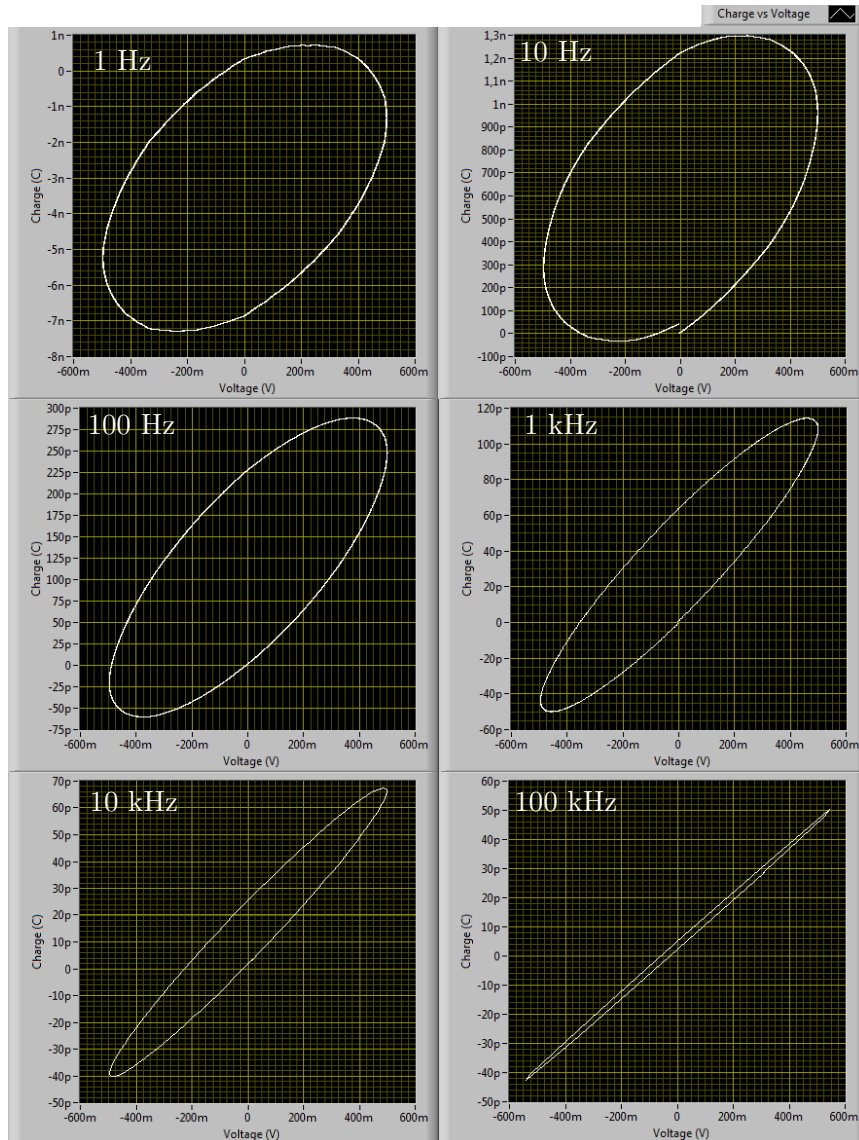
Figure 7.10: q-V curves for measurements on old skin sample with dry gel electrodes. Applied signal frequency is indicated in the plots. The curves appear strictly resistive at low frequency, with an increasing capacitive component with increasing frequency. All the curves are ellipses indicating sinusoidal q and V motions.
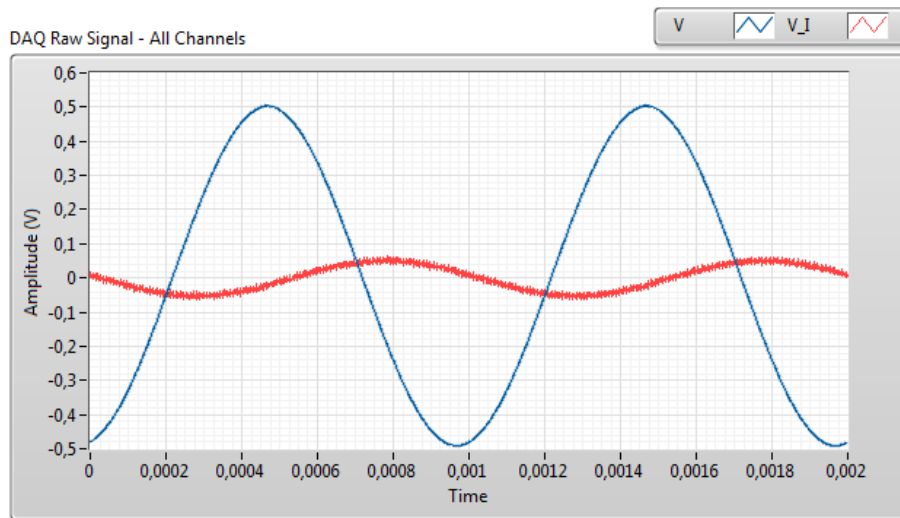
Figure 7.11: *Both signal curves for old skin sample with dry gel electrodes at 1 kHz, two periods plotted. Blue = electrode voltage, red = current sense voltage. No noticeable harmonic distortion of current sense voltage.*

Figure 7.12: *C-V curve for old skin sample with dry gel electrodes at 1 kHz. Left: the full plot. Note the diverging positive and negative capacitance around 0 V. Right: Zoomed in around the calculated capacitance (179 pF). The curve is antisymmetric across the diagonal.*

Remarks

The q-V curves show less capacitive properties than the earlier measurements at low frequency. Impedance and phase shift calculations suggests a large increase in characteristic frequency and increase in resistive properties, which are in accordance. Reactive properties is found to be larger, which is in accordance with decreased calculated capacitance. At very high frequency (100 kHz) the q-V curve suggest an almost strictly reactive impedance.

7.1.3   Dry button electrodes

Skin sample measured with dry button electrodes. Measurements were performed within 1 hour after skin removal and electrode attachment. Applied voltage amplitude was 500 mV.
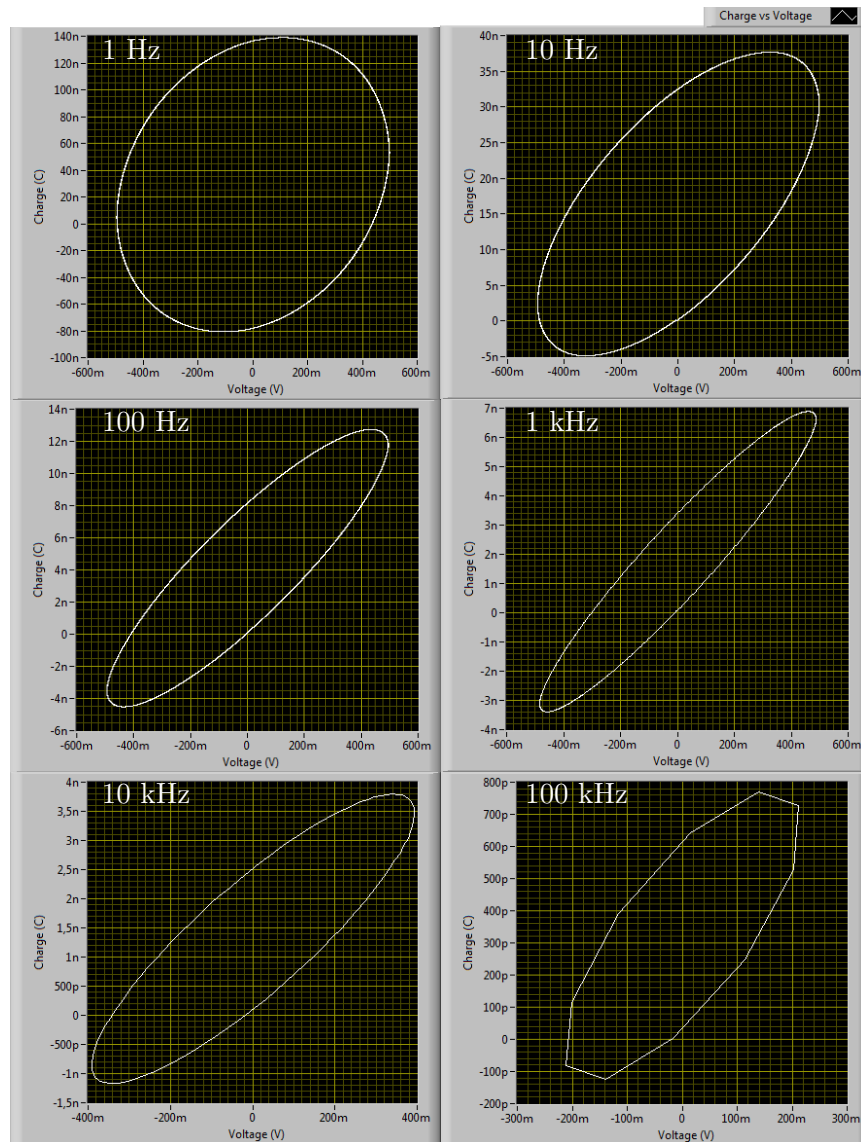
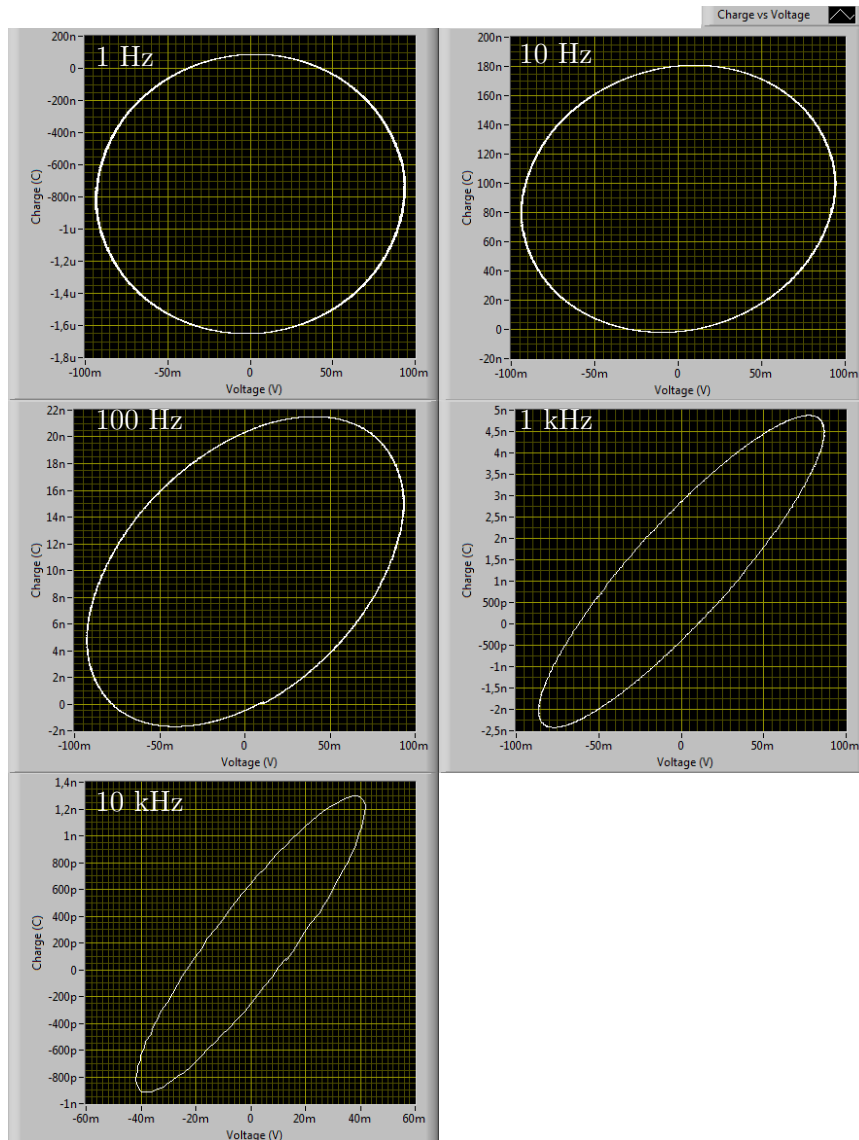Figure 7.13: q-V curves for measurements on skin sample with dry button electrodes. Applied signal frequency is indicated in the plots. The curves appear strictly resistive at low frequency, with an increasing capacitive component with increasing frequency, then approaching resistive again. All the curves are ellipses indicating sinusoidal q and V motions.

Figure 7.14: Both signal curves for skin sample with dry button electrodes at 1 kHz, two periods plotted. Blue = electrode voltage, red = current sense voltage. No noticeable harmonic distortion of current sense voltage.
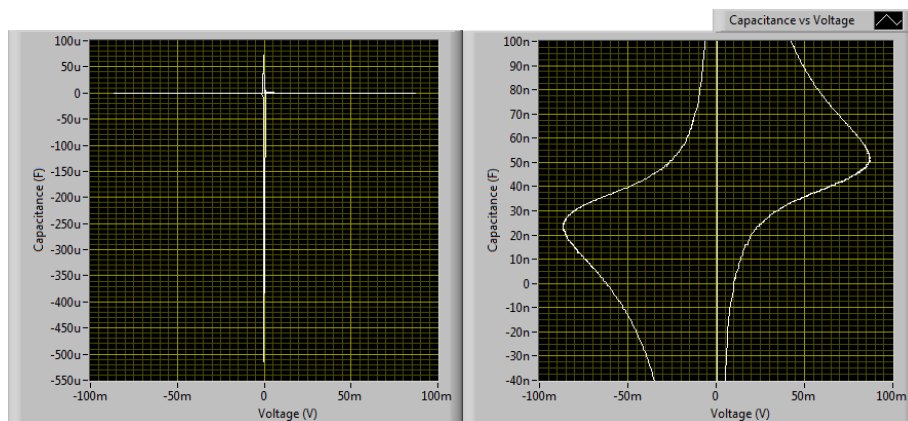

Figure 7.15: C-V curve for skin sample with dry button electrodes at 1 kHz. Left: the full plot. Note the diverging positive and negative capacitance around 0 V. Right: Zoomed in around the calculated capacitance (8.83 nF). The curve is antisymmetric across the diagonal.

Remarks

Calculations show higher impedance than the wet gel electrodes, but lower than the dry gel electrodes.

Old skin sample

Old skin sample measured with dry button electrodes. Measurements were performed 4 hours after skin removal and electrode attachment. Applied voltage amplitude was 500 mV.
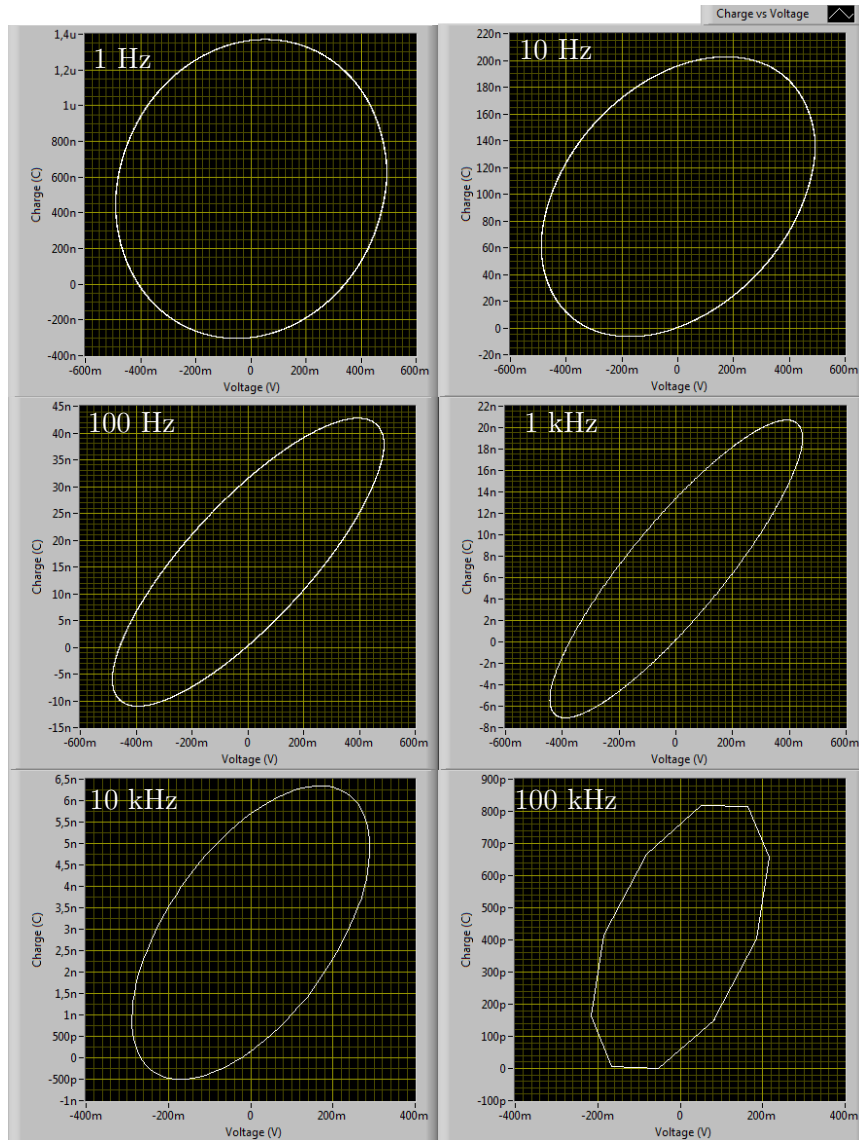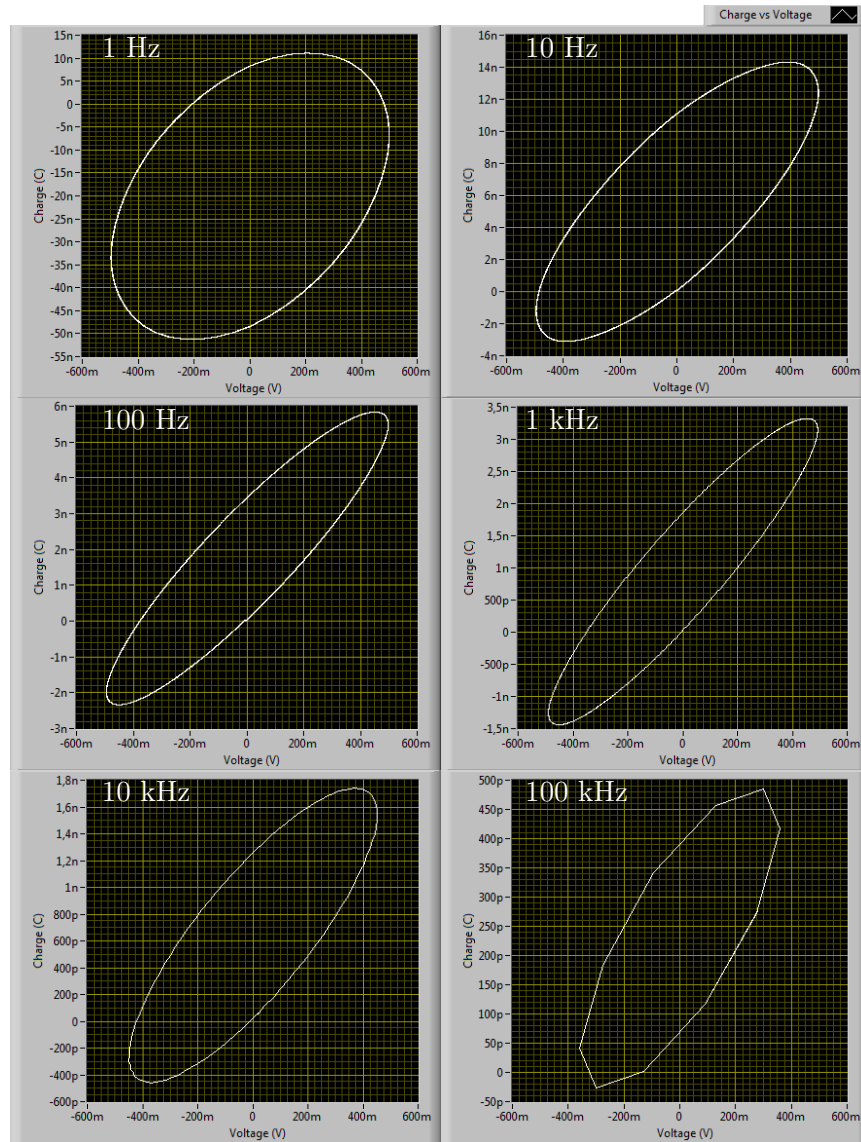

Figure 7.16: q-V curves for measurements on old skin sample with dry button electrodes. Applied signal frequency is indicated in the plots. The curves appear strictly resistive at low frequency, with an increasing capacitive component with increasing frequency, then approaching resistive again. All the curves are ellipses indicating sinusoidal q and V motions.

Figure 7.17: *Both signal curves for old skin sample with dry button electrodes at 1 kHz, two periods plotted. Blue = electrode voltage, red = current sense voltage. No noticeable harmonic distortion of current sense voltage.*
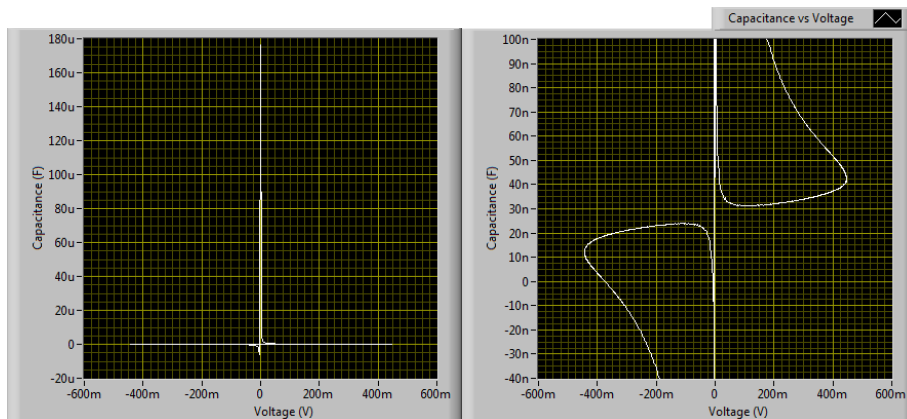

Figure 7.18: *C-V curve for old skin sample with dry button electrodes at 1 kHz. Left: the full plot. Note the diverging positive and negative capacitance around 0 V. Right: Zoomed in around the calculated capacitance (5.29 nF). The curve is antisymmetric across the diagonal.*

Remarks

The q-V curves show more capacitive properties than the earlier measurements at low frequency. Impedance and phase shift calculations suggests a decrease in characteristic frequency and increase in resistive properties, which are in accordance. Reactive properties is found to be larger, which is in accordance with decreased calculated capacitance.

7.2   MOS capacitor

Electrode 1 on MOS capacitor wafer. Applied voltage amplitude was 500 mV.
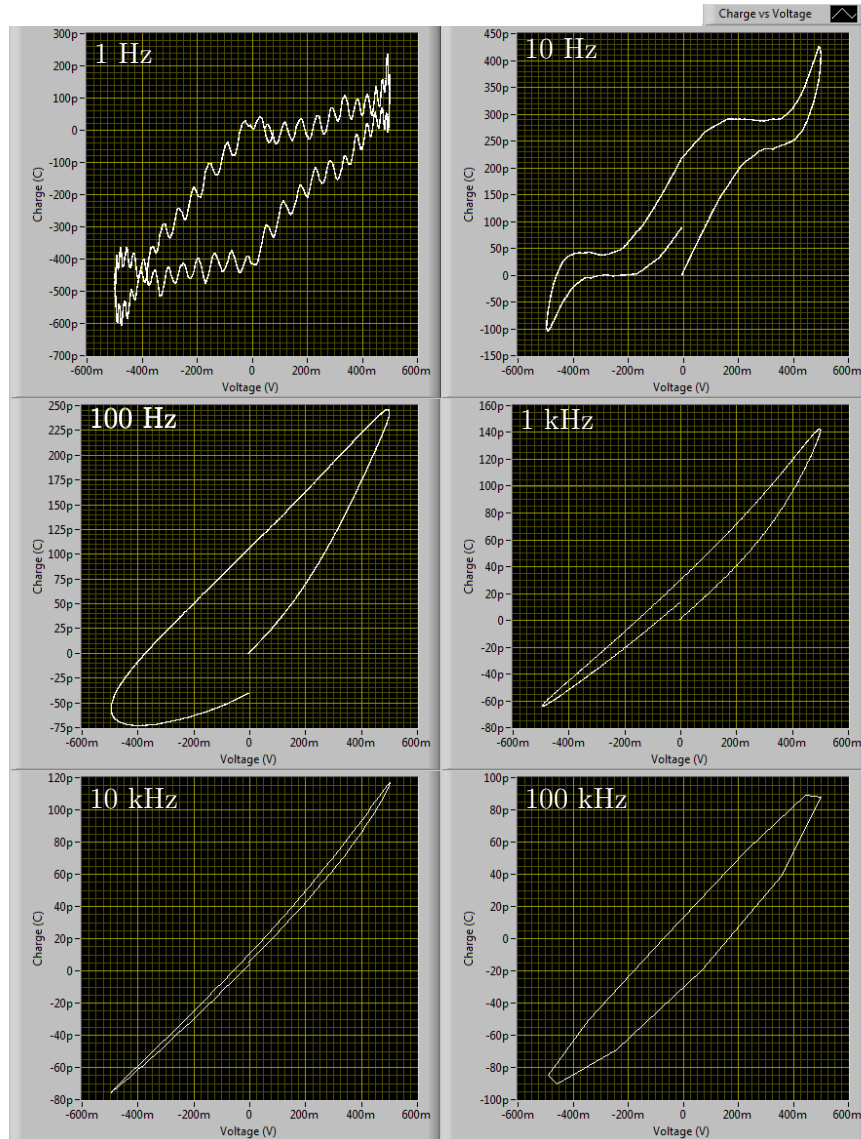
Figure 7.19: q-V curves for MOS capacitor. Applied signal frequency is indicated in the plots. At low frequencies (1 and 10 Hz) the curves appear strongly influenced by noise. At the other frequencies the curves show a banana shaped hysteresis, suggesting a change in capacitance with applied voltage.
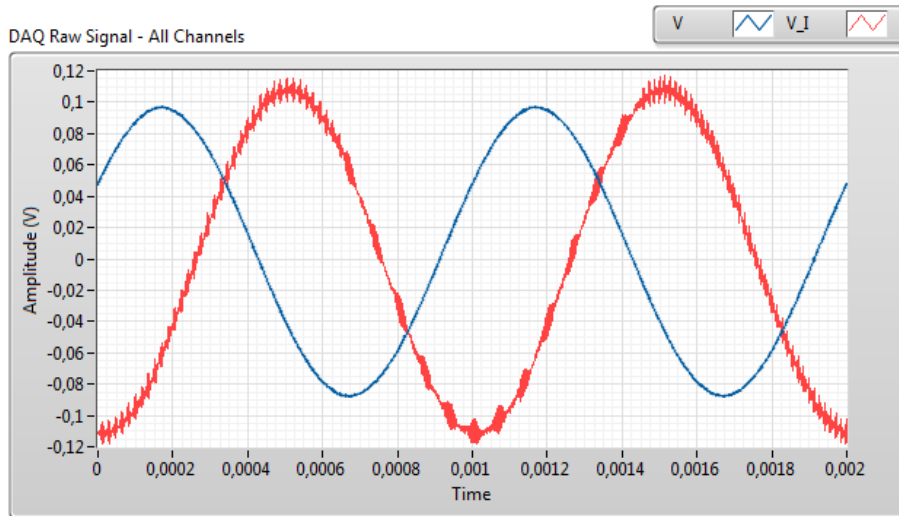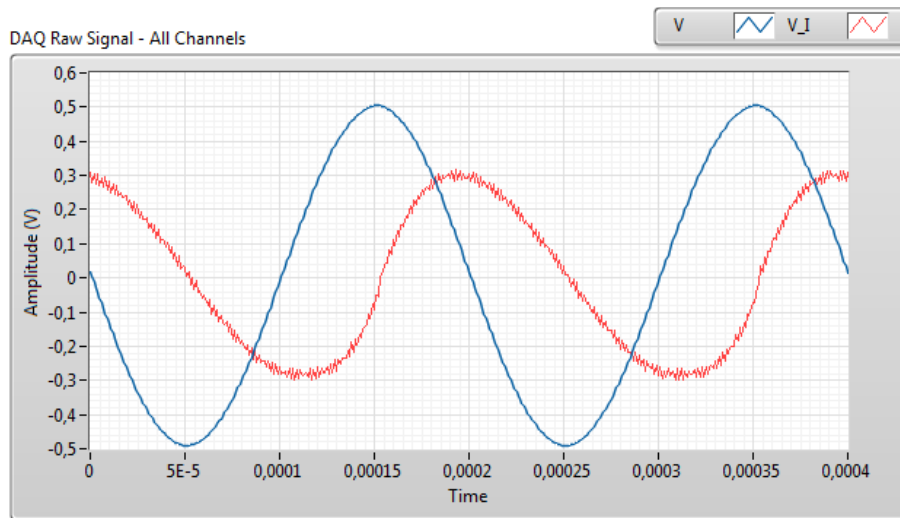
Figure 7.20: Both signal curves for MOS capacitor at 5 kHz, two periods plotted. Blue = electrode voltage, red = current sense voltage. The current sense voltage clearly contains harmonic distortion. This suggests that the properties of the MOS capacitor changes with applied voltage.
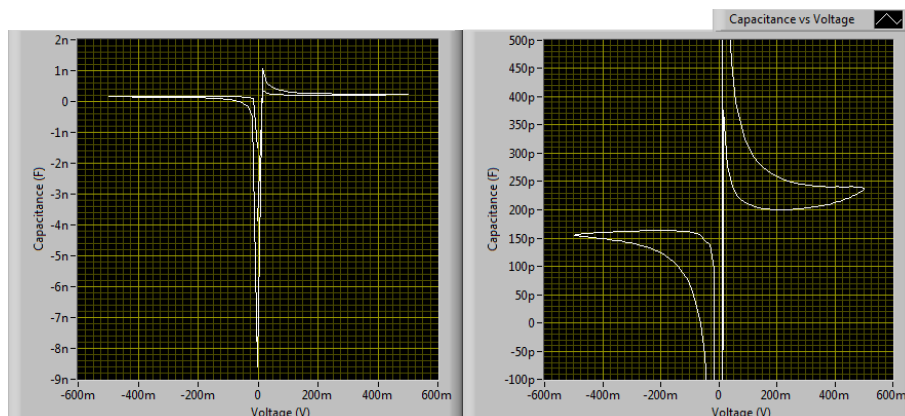
Figure 7.21: C-V curve for MOS capacitor at 5 kHz. Left: the full plot. Note the diverging positive and negative capacitance around 0 V. Right: Zoomed in around the calculated capacitance (192 pF). The curve is not antisymmetric across the diagonal, and shows an upwards shift at maximum positive voltage.

Remarks

The offset in charge from start to end of the q-V curve for 100 Hz and 1 kHz could suggest a hysteresis in the C-V relation. It might also be caused by a DC offset contribution, as illustrated in 8.13 on page 72. The low capacitance of the MOS capacitor results in a very high impedance and thereby low current at low frequency. This gives a poor SNR, probably causing the fluctuations and hysteresis effects in the low frequency q-V curves.

7.3   Reference models

7.3.1   Rp||C + Rs

A basic $R_p||C + R_s$ model. $R_p = 747k\Omega$, $C = 10nF$, $R_s = 999\Omega$. Applied
voltage amplitude was 500 mV.
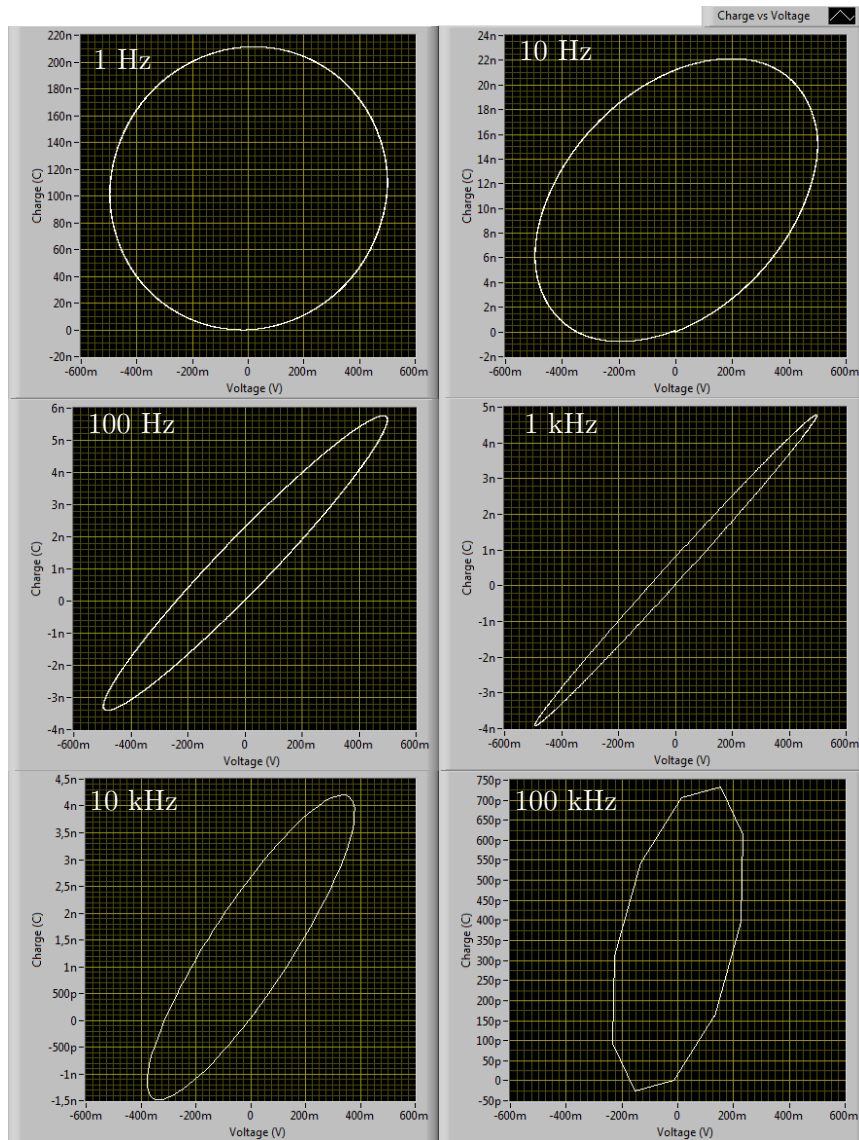
Figure 7.22: q-V curves for $R_p||C + R_s$ model. Applied signal frequency is
indicated in the plots. The curves appear strictly resistive at low frequency,
with an increasing capacitive component with increasing frequency, then
approaching resistive again. All the curves are ellipses indicating sinusoidal
q and V motions.
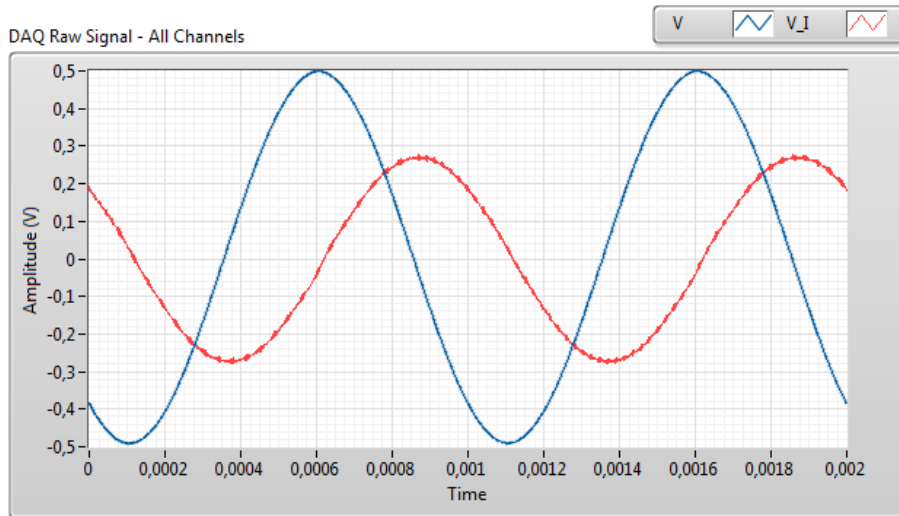
Figure 7.23: Both signal curves for $R_p || C + R_s$ model at 1 kHz, two periods plotted. Blue = electrode voltage, red = current sense voltage. No noticeable harmonic distortion of current sense voltage.
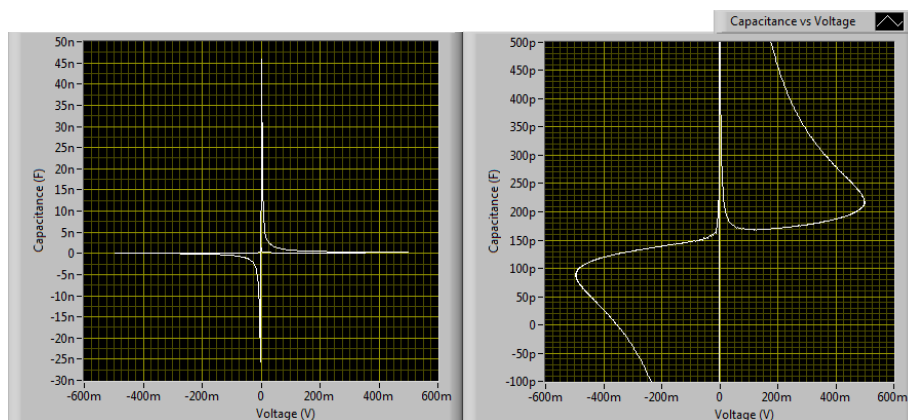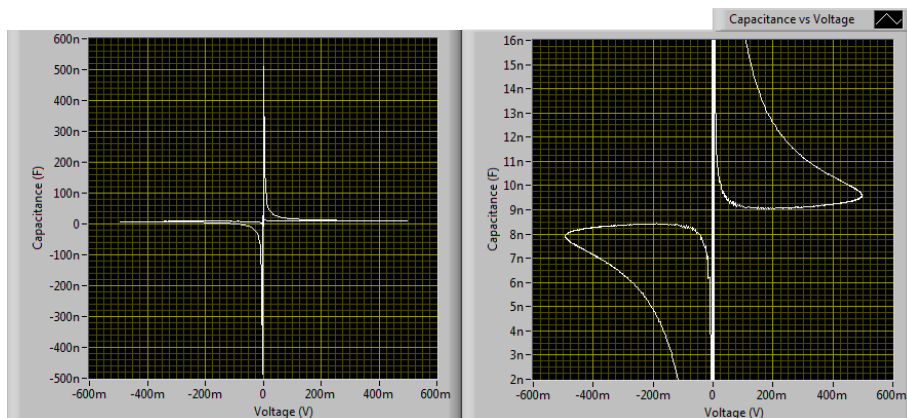

Figure 7.24: C-V curve for $R_p || C + R_s$ model at 1 kHz. Left: the full plot. Note the diverging positive and negative capacitance around 0 V. Right: Zoomed in around the calculated capacitance (8.83 nF). The curve is antisymmetric across the diagonal.

Remarks

The curves show expected behaviour, as does the impedance and phase calculations. Calculated capacitance are close to marked value.

7.3.2   Ceramic capacitor

Ceramic capacitor, 1 nF. Applied voltage amplitude was 500 mV.
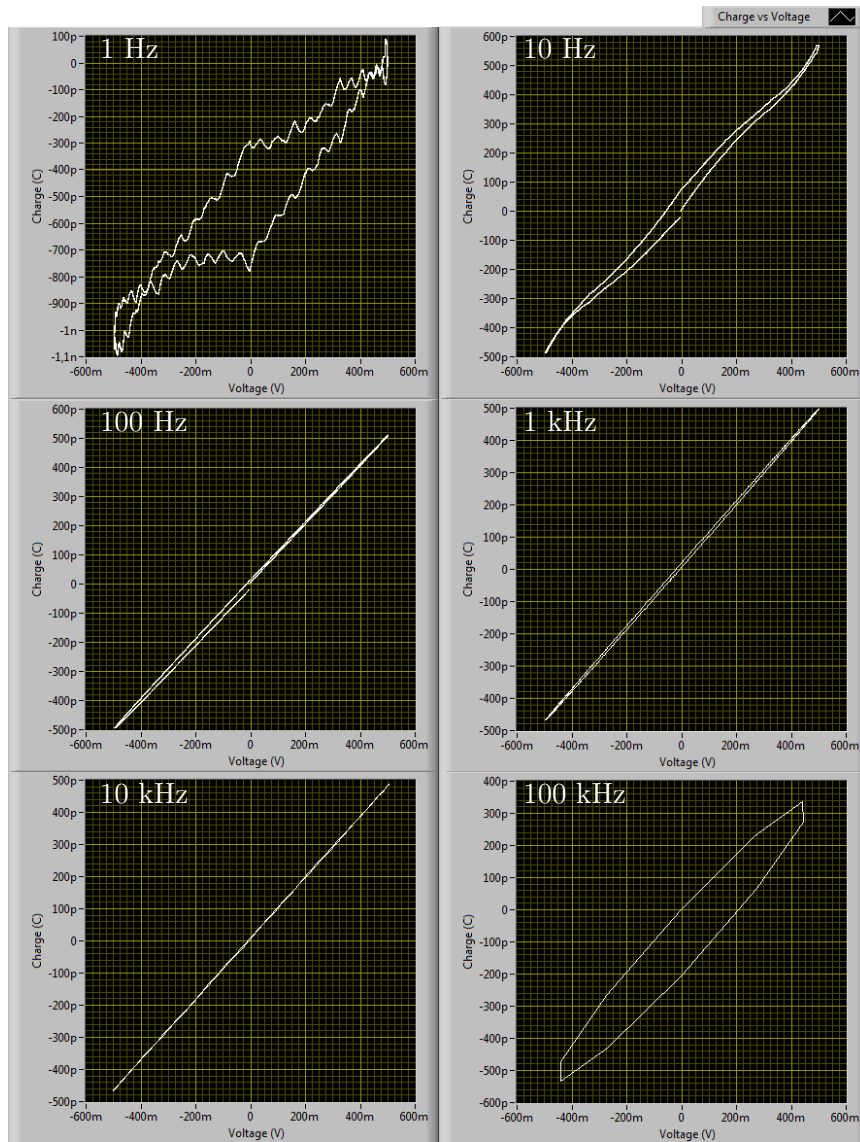
Figure 7.25: q-V curves for capacitor. Applied signal frequency is indicated in the plots. At low frequencies (1 and 10 Hz) the curves appear strongly influenced by noise. At 100 kHz there is a hysteresis, possible caused by calculation error.
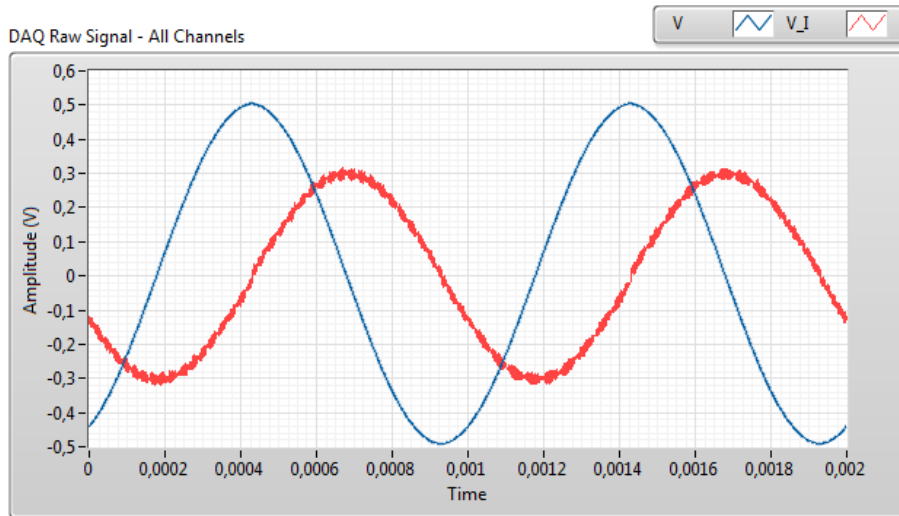
Figure 7.26: Both signal curves for capacitor at 1 kHz, two periods plotted. Blue = electrode voltage, red = current sense voltage. No noticeable harmonic distortion of current sense voltage.
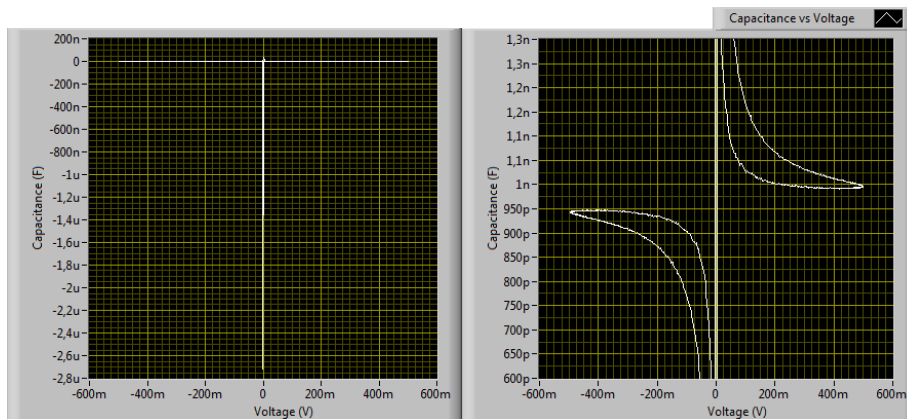
Figure 7.27: C-V curve for capacitor at 1 kHz. Left: the full plot. Note the diverging positive and negative capacitance around 0 V. Right: Zoomed in around the calculated capacitance (970 pF). The curve is antisymmetric across the diagonal.

Remarks

The offset in charge through the q-V curve for 100 Hz might be caused by a DC offset contribution, as illustrated in 8.13 on page 72. The hysteresis in the q-V curve for 100 kHz might related to the before mentioned phase error between measured current and calculated charge.

7.3.3   Resistor

Resistor, 99.3 kΩ. Applied voltage amplitude was 500 mV.
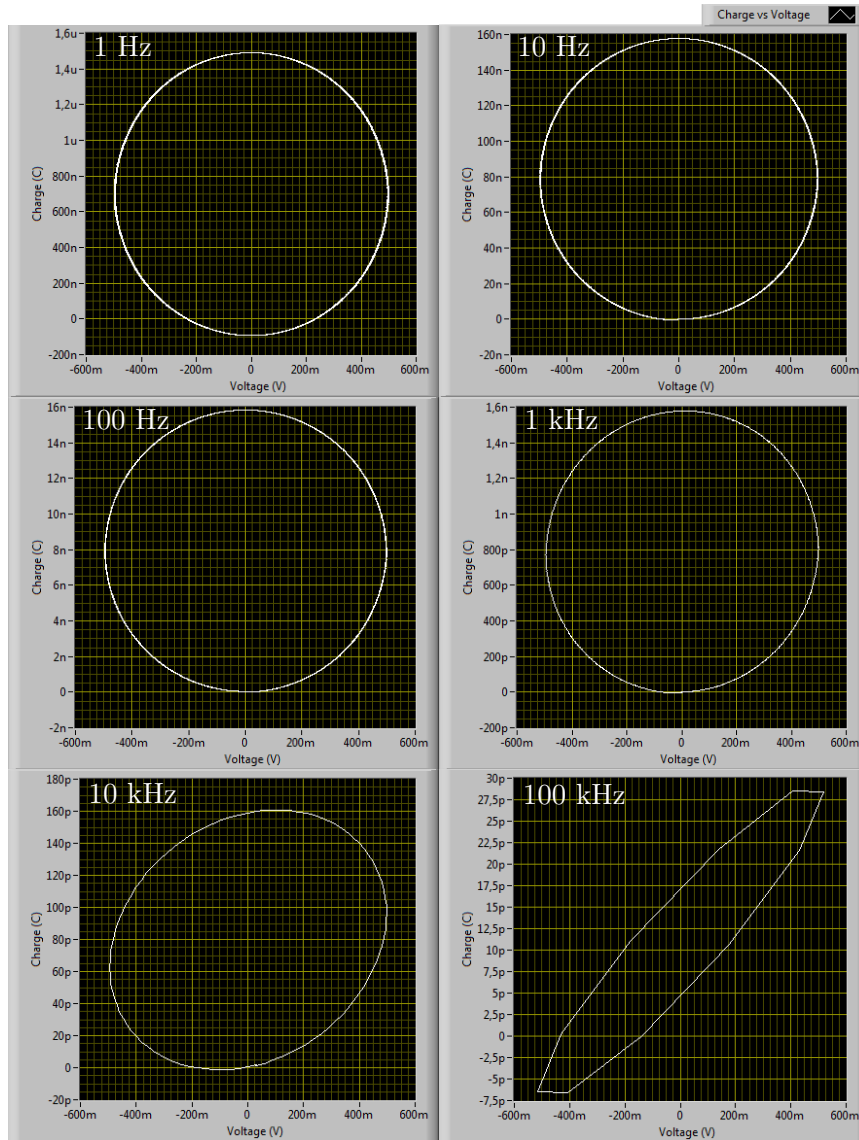
Figure 7.28: q-V curves for resistor. Applied signal frequency is indicated in the plots. The curve appears fully resistive at low and medium frequencies, but start to show apparent capacitive properties at 10 kHz, and strongly at 100 kHz.
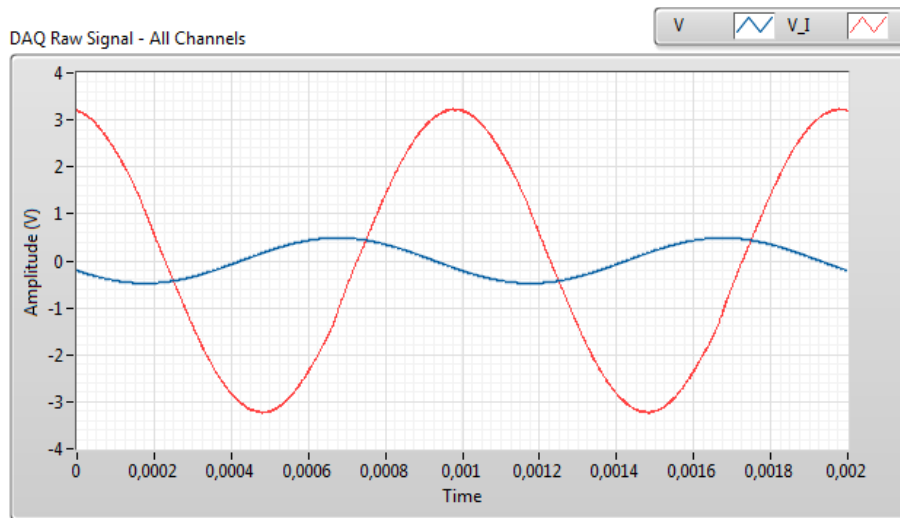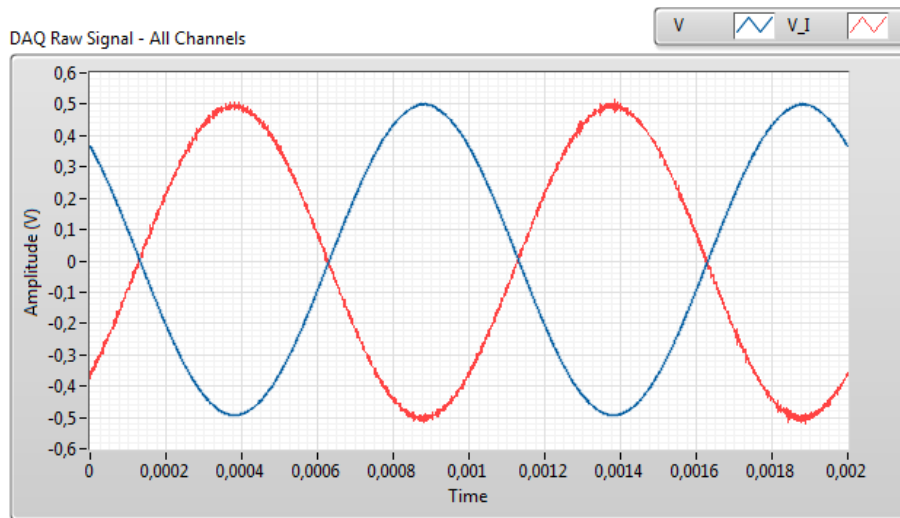
Figure 7.29: Both signal curves for resistor at 1 kHz, two periods plotted. Blue = electrode voltage, red = current sense voltage. No noticeable harmonic distortion of current sense voltage.
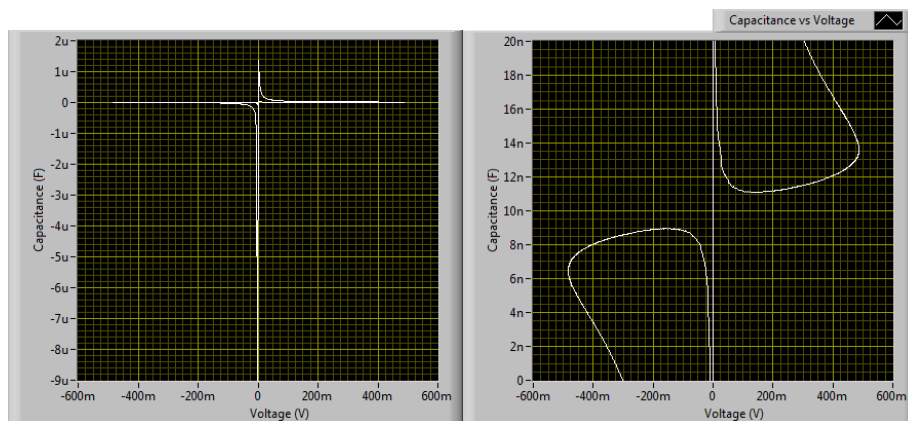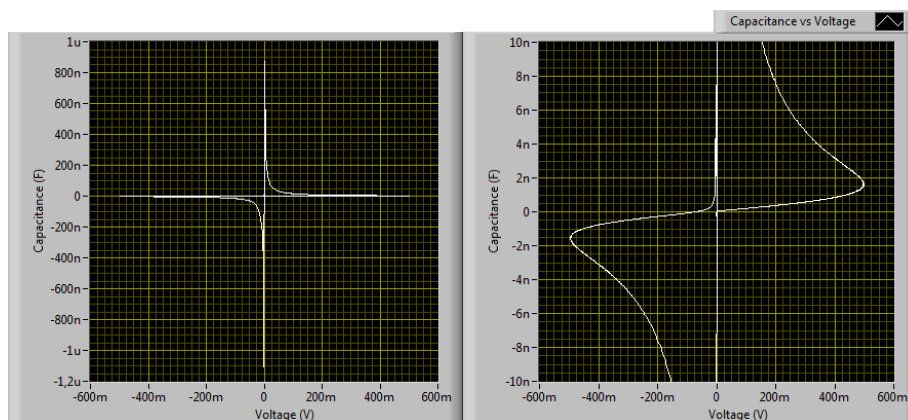

Figure 7.30: C-V curve for resistor at 1 kHz. Left: the full plot. Note the diverging positive and negative capacitance around 0 V. Right: Zoomed in around the x-axis. The curve is antisymmetric across the diagonal.

Remarks

q-V for 10 kHz and 100 kHz shows apparent capacitive properties in the resistor. The current measurement should be without phase distortion according to the ideal properties of the operational amplifier used, but this is not the case.

Chapter 8

MATLAB simulations

The following pages contain the results from the MATLAB simulations described in section 6.1.

For each model three figures are presented. Firstly the q-V curves for a selected range of frequencies. Secondly the raw signal curves (electrode voltage and current sense voltage) at a selected frequency. Thirdly the C-V curve for the same frequency.

8.1   Rp||C + Rs

A basic $R_p || C + R_s$ model. $R_p = 747k\Omega$, $C = 10nF$, $R_s = 999\Omega$. Applied voltage amplitude was 500 mV.
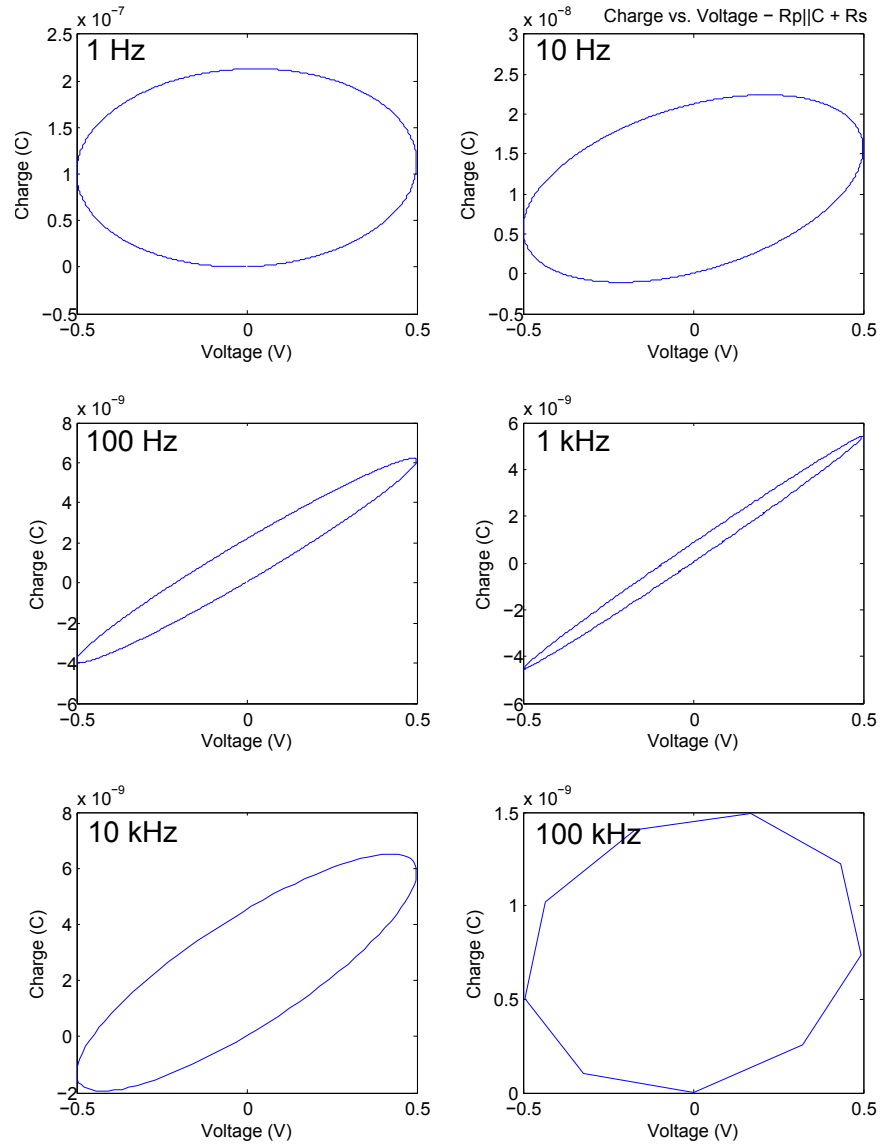
Figure 8.1: q-V curves for simulated $R_p || C + R_s$ model. Applied signal frequency is indicated in the plots. The curves appear strictly resistive at low frequency, with an increasing capacitive component with increasing frequency, then approaching resistive again. All the curves are ellipses indicating sinusoidal q and V motions.
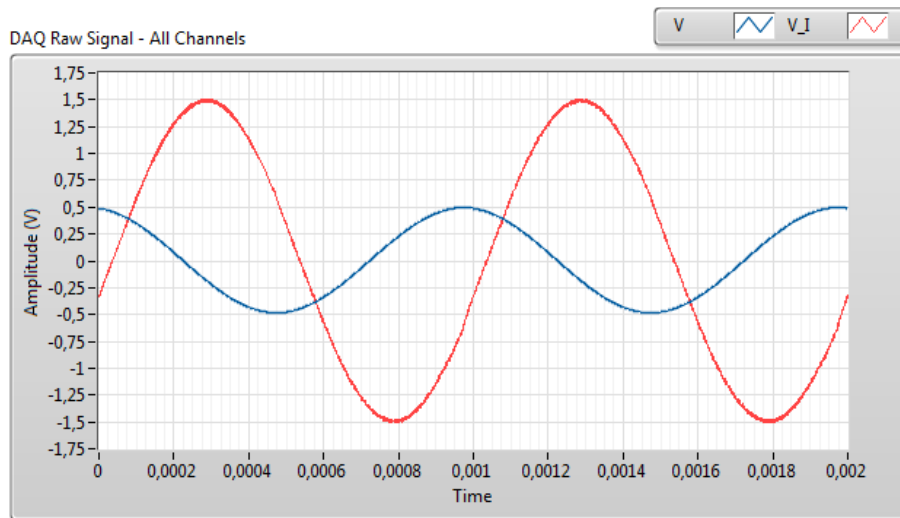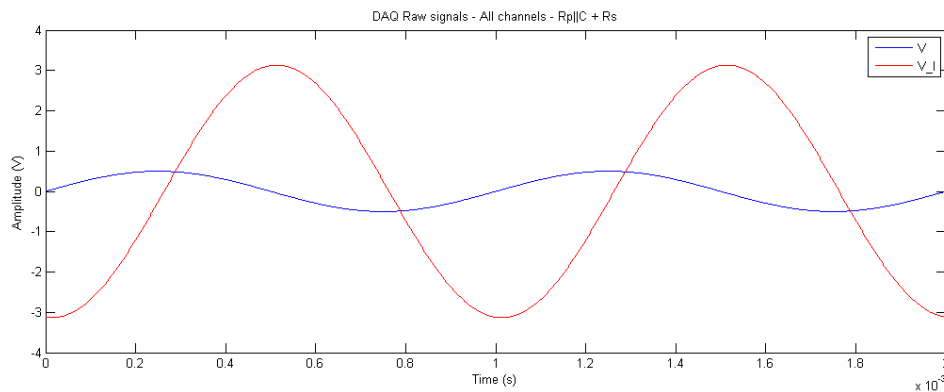
Figure 8.2: Both signal curves for simulated $R_p||C + R_s$ model at 1 kHz, two periods plotted. Blue = electrode voltage, red = current sense voltage. No noticeable harmonic distortion of current sense voltage.
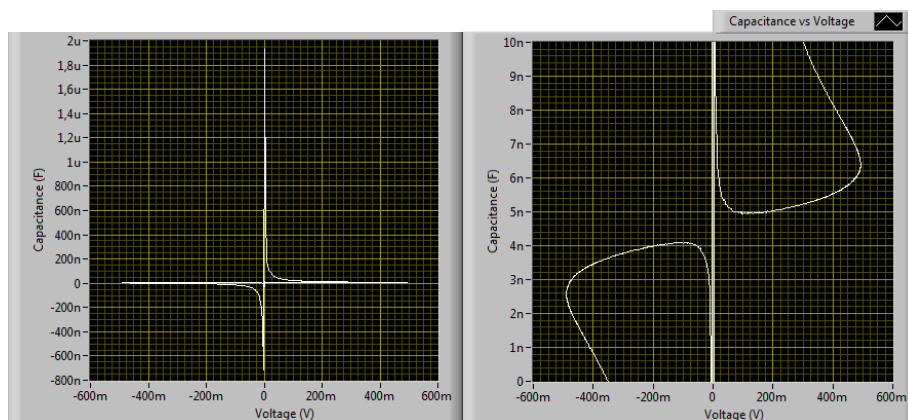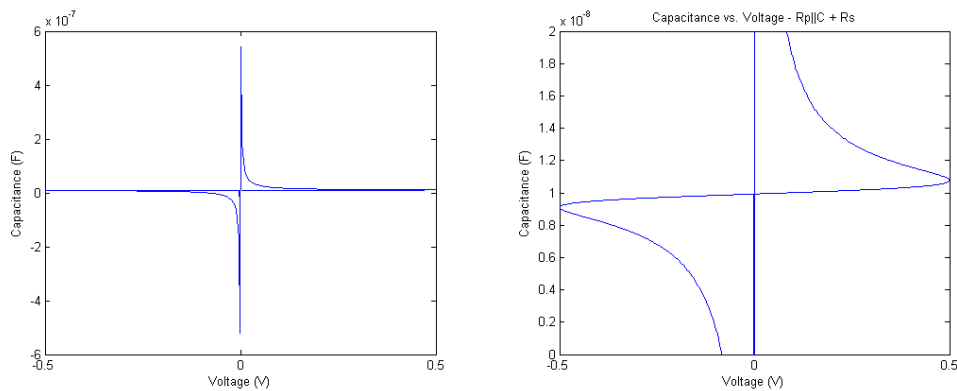

Figure 8.3: C-V curve for simulated $R_p||C + R_s$ model at 1 kHz. Left: the full plot. Note the diverging positive and negative capacitance around 0 V. Right: Zoomed in around the calculated capacitance (10.0 nF). The curve is antisymmetric across the diagonal.

Remarks

All the curves show the same features as the results from measurements with the MemCapMeter on the same model in section 7.3.1.

8.2   Rp||CPE + Rs

A $R_p||CPE + R_s$ model where the capacitive component has an impedance with phase $70°$ in stead of $90°$. $R_p = 747k\Omega$, $CPE = 10nF$, $R_s = 999\Omega$. Applied voltage amplitude was 500 mV.
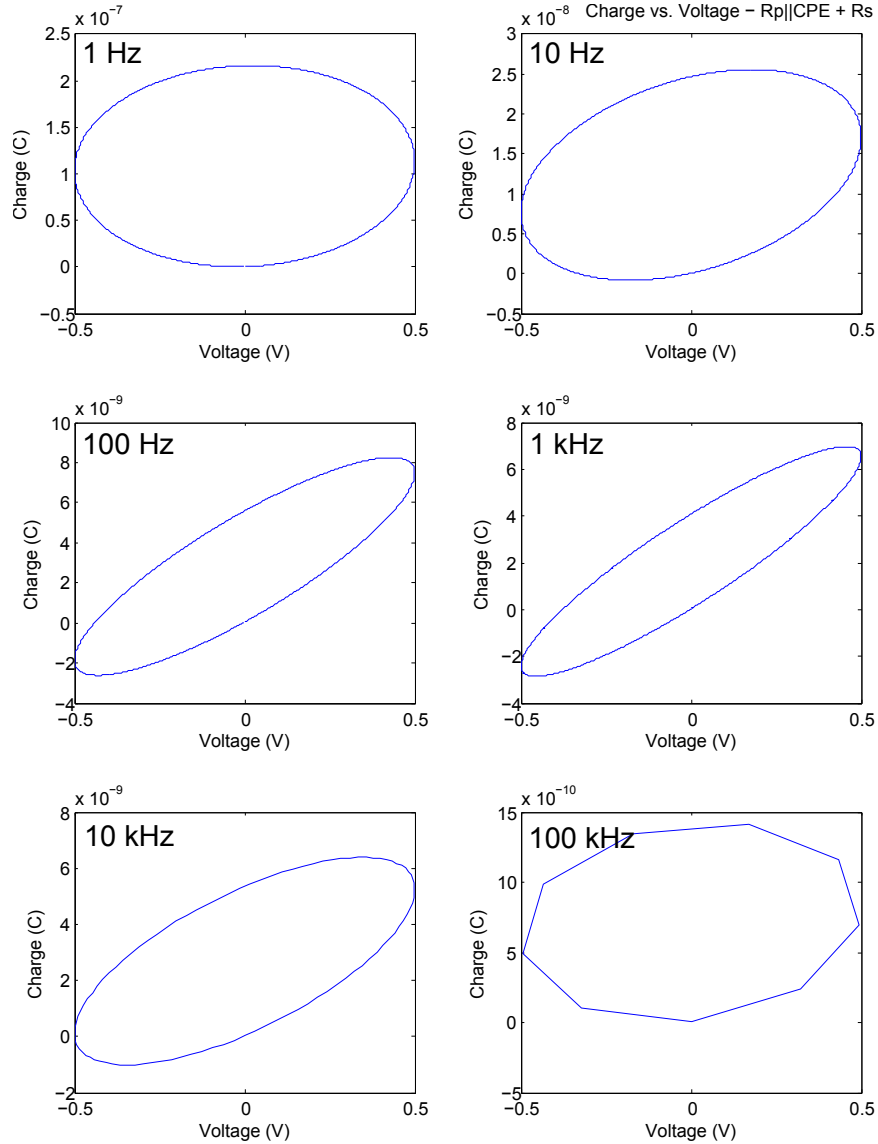
Figure 8.4: q-V curves for simulated $R_p||CPE + R_s$ model. Applied signal frequency is indicated in the plots. The curves appear strictly resistive at low frequency, with an increasing capacitive component with increasing frequency, then approaching resistive again. All the curves are ellipses indicating sinusoidal q and V motions.
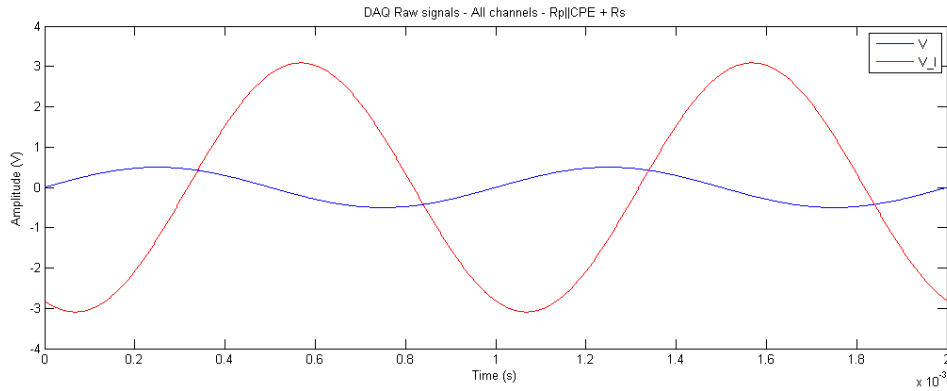
Figure 8.5: Both signal curves for simulated $R_p||CPE + R_s$ model at 1 kHz, two periods plotted. Blue = electrode voltage, red = current sense voltage. No noticeable harmonic distortion of current sense voltage.
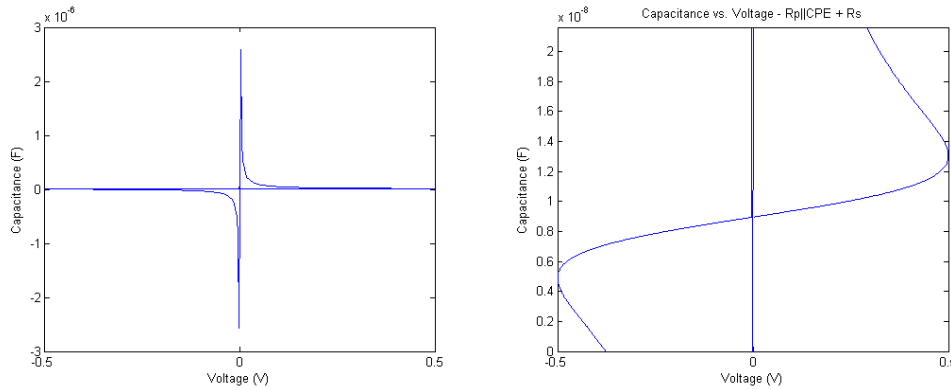
Figure 8.6: C-V curve for simulated $R_p||CPE + R_s$ model at 1 kHz. Left: the full plot. Note the diverging positive and negative capacitance around 0 V. Right: Zoomed in around the calculated capacitance (10.8 nF). The curve is antisymmetric across the diagonal.

Remarks

The q-V curves show a smaller hysteresis than the $R_p||C + R_s$ at 100 Hz and 1 kHz. The C-V curve shows a greater deviance from true capacitance value when $V \neq 0$.

8.3   Rp||Cmem + Rs

A $R_p||C_{mem} + R_s$ model where the capacitive component has voltage dependent capacitance. $R_p = 747k\Omega$, $C_{mem} = 10$ nF $\cdot (1 + V)$, $R_s = 999\Omega$. Applied voltage amplitude was 500 mV.
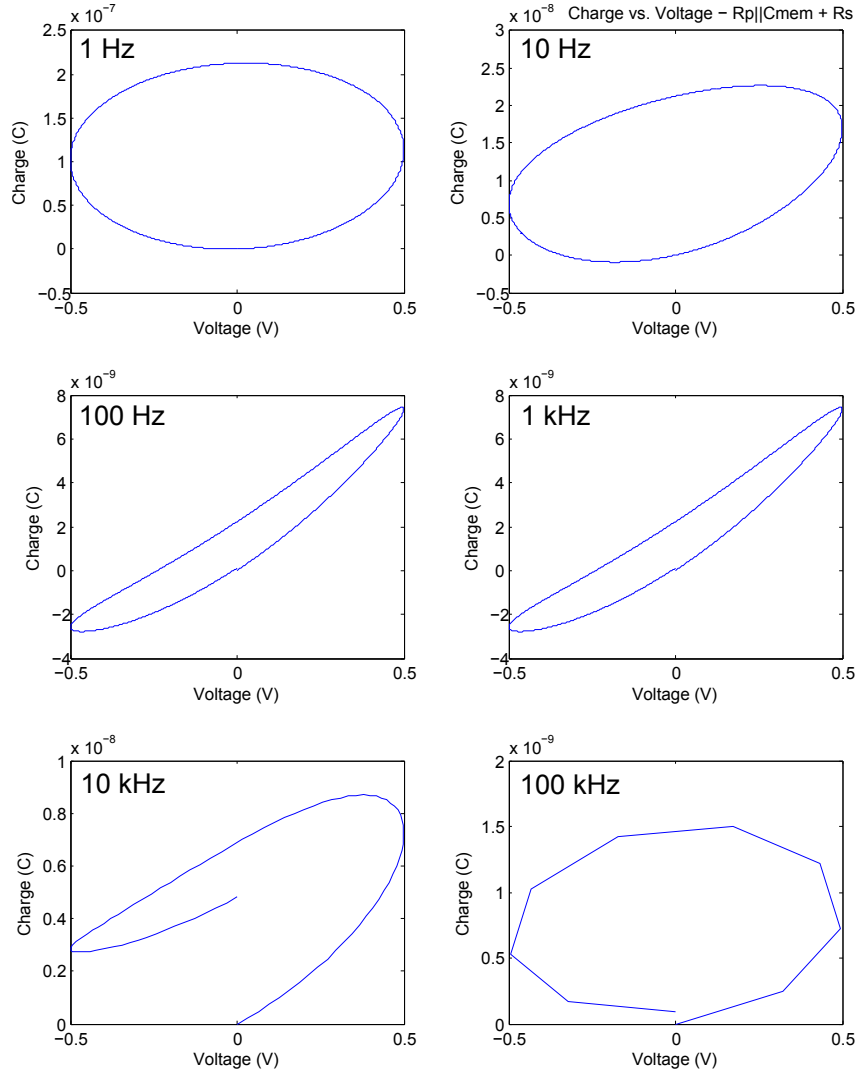
Figure 8.7: q-V curves for simulated $R_p||C_{mem} + R_s$ model. Applied signal frequency is indicated in the plots. The strictly resistive at low frequency, with an increasing capacitive component with increasing frequency, then approaching resistive again. Starting at 10 Hz and increasing with frequency the hysteresis takes on a banana shape, suggesting a change in capacitance with applied voltage. At 10 kHz a strong positive shift in charge occurs through the curve.
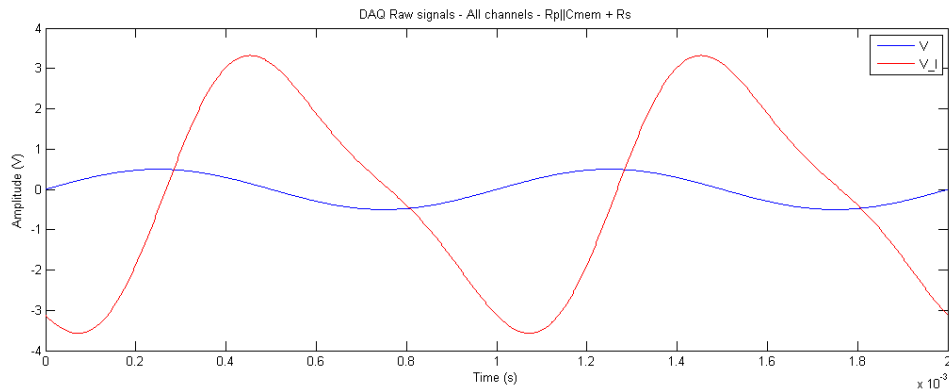
Figure 8.8: Both signal curves for simulated $R_p||C_{mem} + R_s$ model at 1 kHz, two periods plotted. Blue = electrode voltage, red = current sense voltage. There is a clear harmonic distortion of the current sense voltage, suggesting that the capacitive properties changes with the voltage.
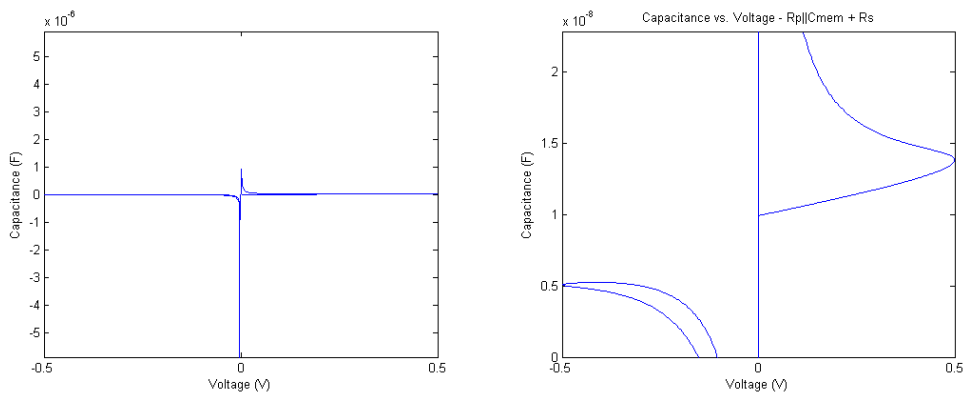
Figure 8.9: C-V curve for simulated $R_p||C_{mem} + R_s$ model at 1 kHz. Left: the full plot. Note the diverging positive and negative capacitance around 0 V. Right: Zoomed in around the calculated capacitance (10.8 nF). There is a clear difference in the curve with positive and negative voltage, showing a much greater hysteresis at the former.

Remarks

The q-V curves show at 10 kHz a strong positive shift in charge through the curve, which might suggest some kind of resonance has occurred.

8.4   C

A basic ideal capacitor model. $C = 1nF$. Applied voltage amplitude was 500 mV.
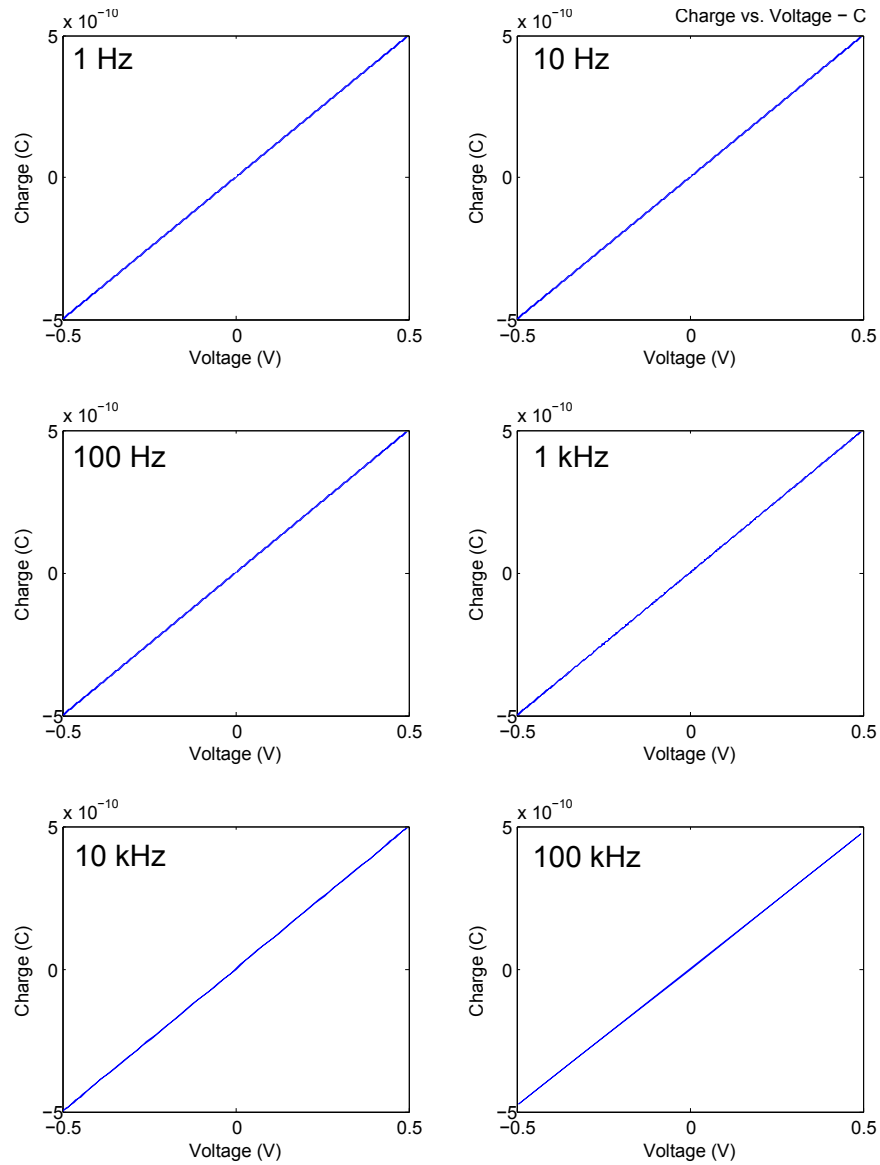
Figure 8.10: q-V curves for simulated C model. Applied signal frequency is indicated in the plots. All the curves show the ideal diagonal curve with centre in the origin.
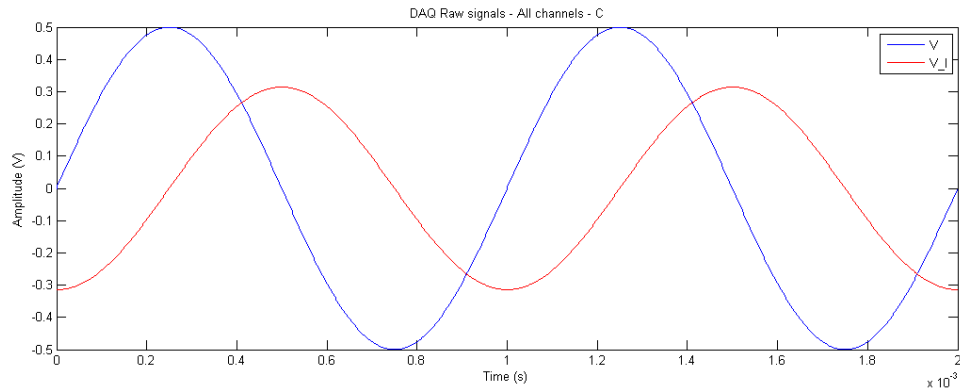
Figure 8.11: Both signal curves for simulated C model at 1 kHz, two periods plotted. Blue = electrode voltage, red = current sense voltage. No noticeable harmonic distortion of current sense voltage.
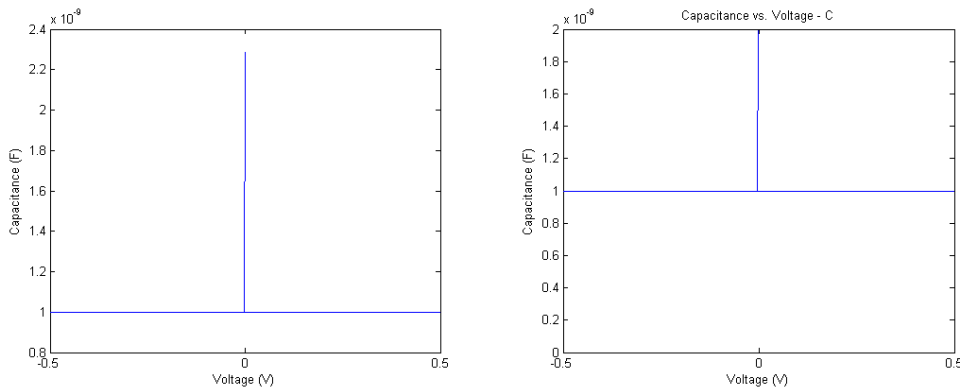

Figure 8.12: C-V curve for simulated C model at 1 kHz. Left: the full plot. Note the diverging positive capacitance at 0 V, caused by a mathematical 0/0 situation. Otherwise the capacitance is independent of voltage. Right: Zoomed in around the calculated capacitance (1.00 nF).

8.5   Noise effects

Two different noise signals are added to the applied voltage for a $R_p||C + R_s$ model. Figure 8.13 shows how the q-V curves are affected.
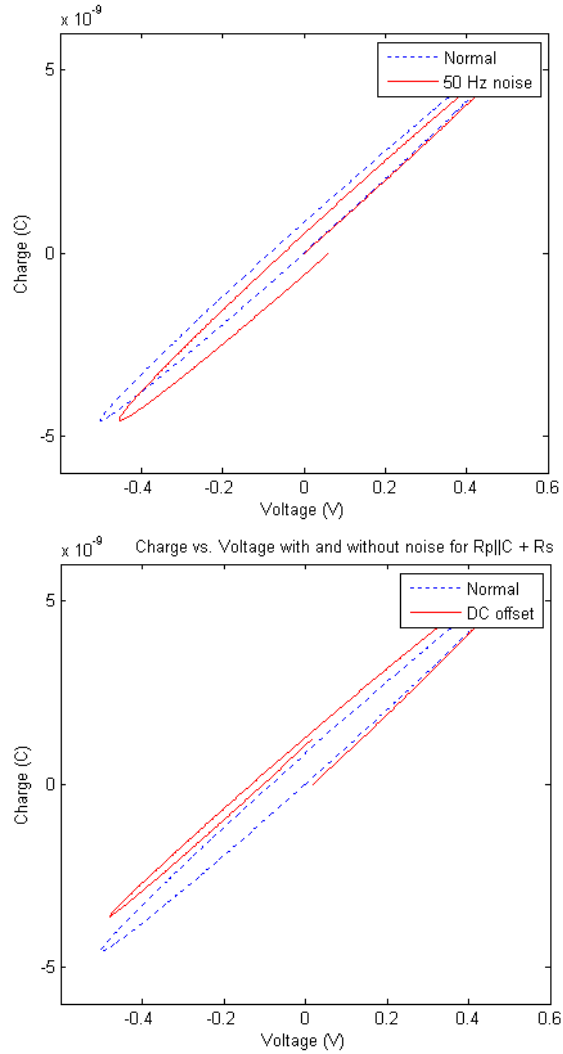

Figure 8.13: q-V curves for simulated $R_p||C + R_s$ model with two noise effects. Applied voltage amplitude was 500 mV with frequency 1 kHz. Upper: blue = normal q-V curve, red = voltage has 50 Hz signal noise at amplitude 40 % of main signal frequency. Lower: blue = normal q-V curve, red = voltage has an DC offset of 4 % of signal amplitude.

Remarks

From the left plot in figure 8.13 one can see that the curve has a positive shift in voltage at the end, caused by the 50 Hz noise. From the right plot in figure 8.13 one can see that the curve has a positive shift in charge at the end, caused by the DC offset in the voltage.

8.6   Current limit resistor

Simulation of how the current limit resistor R_{cl} affects the C-V curve for a $R_p||C + R_s$ model. $R_p = 747$ kΩ, $C = 10$ nF, $R_s = 999$ Ω, $R_{cl} = 1$ kΩ.
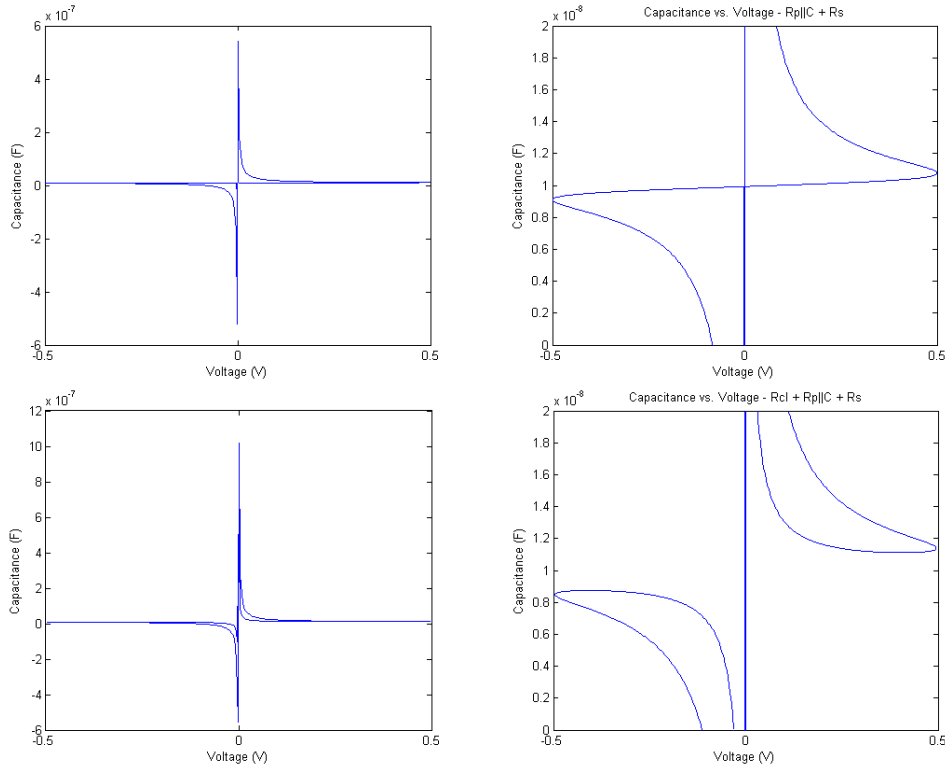
Figure 8.14: C-V curve showing the effect of current limit resistor R_{cl} on simulated $R_p||C + R_s$ model at 1 kHz. Upper: C-V curve for original $R_p||C + R_s$ model. Lower: C-V curve for $R_{cl} + R_p||C + R_s$ model. The hysteresis of the positive and negative parts of the curve are clearly changed, and the values at maximum and minimum voltage also altered slightly. The mean capacitance value of the curve and the calculated capacitance however is unchanged.

8.7   Calculating capacitance

Simulation of phase and capacitance response for frequency $R_p || C + R_s$ model. $R_p = 747$ kΩ, $C = 10$ nF, $R_s = 999$ Ω.
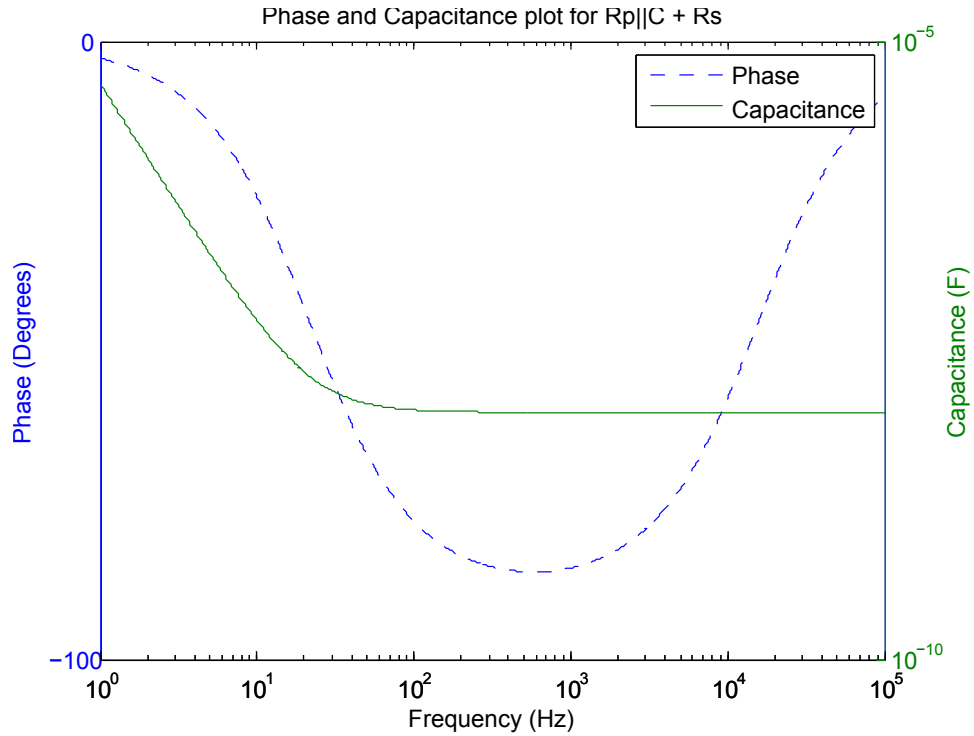
Figure 8.15: Calculated phase and capacitance plot for simulated $R_p || C + R_s$ model, 1 Hz to 100 kHz. The calculated capacitance converge to the true value of the capacitive component with increasing frequency.

Remarks

It is clear that the calculated capacitance converge to the true value of C with increasing frequency. Here it is close to the true value at the characteristic frequency, but this depends on the component values of the model, and can happen at lower or higher frequency. The inability to calculate correct capacitance at low frequency is because the impedance of the parallel resistor is much smaller than that of the capacitor, resulting in the capacitor being "invisible" in the model.

Chapter 9

C-V characterization

C-V characterization curves for the skin sample can be seen in figures 9.1 and 9.2 on the next page. *C-V* characterization curves for the MOS capacitor wafer can be seen in figure 9.3 on page 77. They are all collected in figure 9.4 on page 77, with a logarithmic y-axis.

Skin

In both measurements there is a clear variation of the capacitance as a function of the applied DC bias. There is also a clear hysteresis, in a similar shape as a Type II hysteresis curve as seen in figure 4.1 on page 15. On the other hand, the actual change in capacitance is very small. This is also seen in figure 9.4, where the change is negligible compared to that of the MOS capacitors. The relative changes in capacitance for the two measurements are $\sim 3\%$ (10 kHz) and $\sim 2\%$ (100 kHz).

MOS capacitors

In both capacitors there is a clear change of capacitance from negative to positive DC bias. There is also a clear hysteresis in this transition. The change is not negligible as it is also very clear in figure 9.4 on page 77. This is supported by the relative changes in capacitance which for the two measurements are $\sim 115\%$ (10 kHz) and $\sim 113\%$ (100 kHz). In other words, the differences in maximum and minimum capacitances are larger than the mean capacitance.
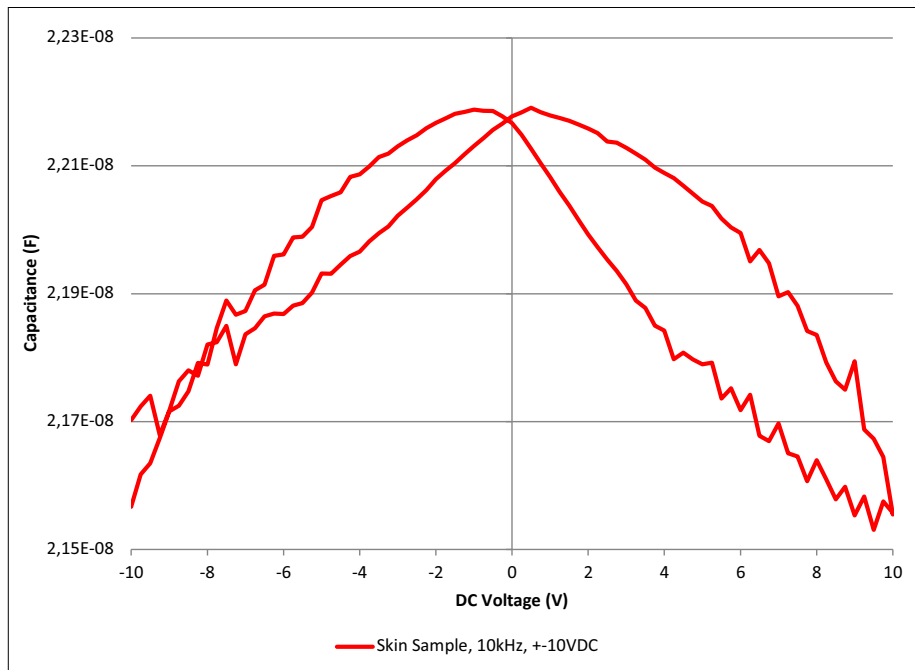
Figure 9.1: C-V curve for skin sample at 10 kHz, ±10 VDC. The curve has a bow tie shaped hysteresis, but the relative change in capacitance is small.
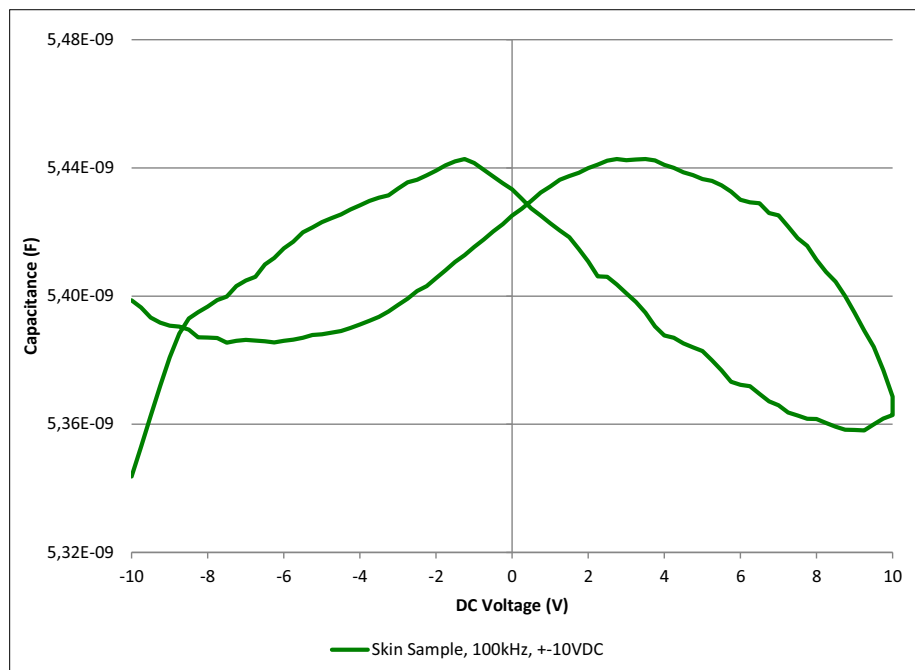
Figure 9.2: C-V curve for skin sample at 100 kHz, ±10 VDC. The curve has a bow tie shaped hysteresis, but the relative change in capacitance is small.
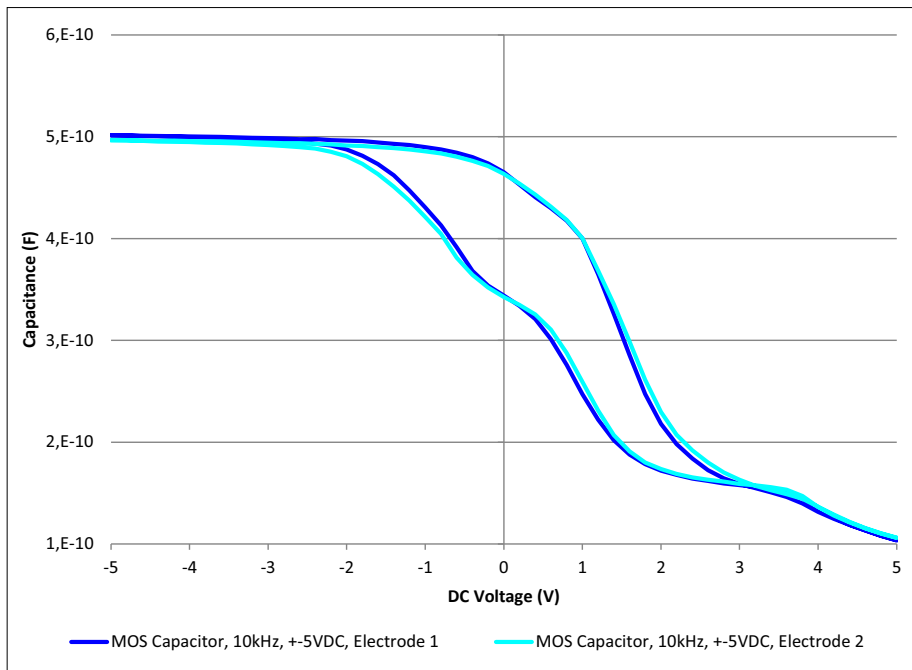
Figure 9.3: C-V curves for MOS capacitor, electrode 1 and 2 at 10 kHz, ±5 VDC. The curve shows a clear shift in capacitance from negative to positive DC bias, with a not negligible hysteresis in the transition.
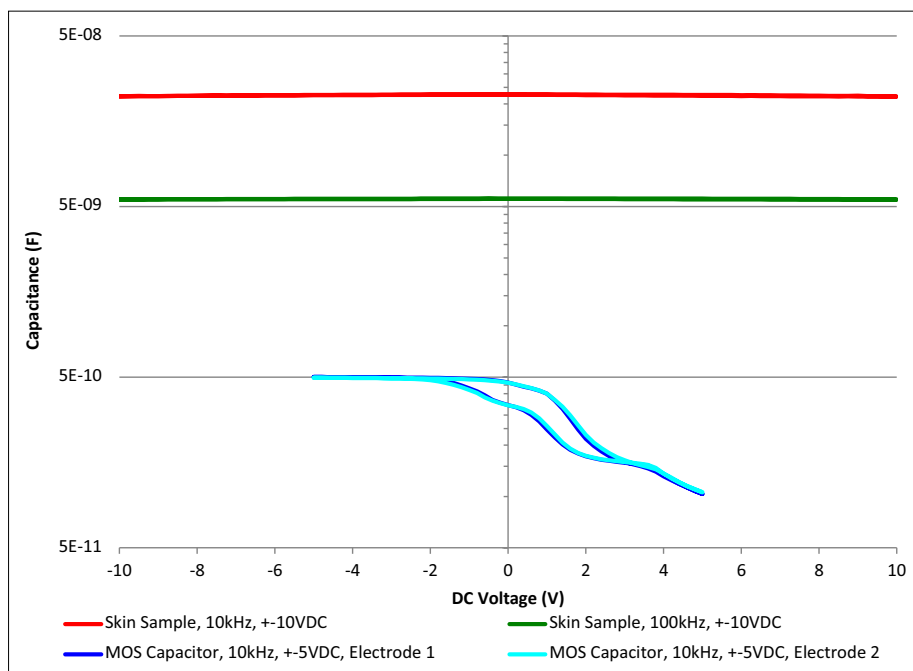
Figure 9.4: C-V curves for skin sample and MOS capacitor. Mind the logarithmic y-axis. The relative change in capacitance is clear for the MOS capacitor, but not visible for the skin samples.

Part IV

Discussion

Chapter 10

Memcapacitance

MemCapMeter

The q-V plots in section 7.1 for the different electrode-skin setups are all similar in nature. They all appear similar as for the $Rp||C + R_s$ and $Rp||CPE + R_s$ models shown in 2.1 on page 7. They start out close to a resistive model in the beginning, approaching a capacitive model with increasing frequency, and in some of the cases, starts on the return back to a resistive model at high frequency. Throughout they keep an elliptic shape. This transition is caused by a dispersion in the electrode-skin setup. If one compare these plots to the MATLAB simulations of the $R_p||C + R_s$ and $R_p||CPE + R_s$ models in chapter 8, one can see that they are very similar, differing only in the magnitude of the impedance properties. In other words, the mere appearance of hysteresis in the q-V curves do not suggest a change in capacitance more than for a basic $R_p||C + R_s$ circuit. The q-V plots for the MOS capacitor show a banana shaped curve, even with a slight hysteresis. The same is seen for the simulated $R_p||C_{mem} + R_s$ model, where the capacitive component is a voltage dependant memcapacitor. This is features not visible in the results from skin measurements.

The raw signal plots from the electrode-skin measurements, the $R_p||C + R_s$ model and the ceramic capacitor all show the same. The current sense voltage do not have any noticeable harmonic distortion apart from noise, suggesting static properties in reference to voltage. The MOS capacitor and the simulated $R_p||C_{mem} + R_s$ model however, show a strong difference in the current sense voltage curve shape with positive and negative electrode voltage. This is caused by a variation in the impedance and thereby a strong indication of variation in the capacitance with applied voltage.

With regards to the C-V curves, they all appear star-shaped with hysteresis, with diverging positive and negative capacitance around 0 V. This is natural as the voltage and charge are both sinusoidal curves that are slightly out of phase, causing mathematical 0/0 situations. This is also the case in the MATLAB simulations, and the C-V curves of these models are very similar to the ones from the electrode-skin measurements. The C-V curve for both the MOS capacitor and ceramic capacitor measurements have the star shape as for the skin measurements, but do have a substantial smaller hysteresis. There is small differences between these two curves,

which suggests that a hysteresis in the C-V is not necessarily an indication of variable or memory capacitance. The lack of antisymmetry around the diagonal means that the capacitance value are different with positive and negative voltage. Still, it does not imply any further memory properties beyond that.

C-V characterization

From the C-V characterization, we have both variation and hysteresis in the C-V curves of skin. But as mentioned in chapter 9, they are very small. Especially when they are compared to the results from the MOS capacitors. These curves show a strong variation of the capacitance from positive to negative voltage. Most importantly they also show a hysteresis in the transition from positive to negative voltage and reverse. One can not rule out that the variations seen for skin are introduced by the measurement setup.

Chapter 11

Evaluation of methods

11.1 MemCapMeter

The MemCapMeter measurement principle seems suitable to examine memcapacitive properties. The total system cost is fairly reasonable, and if Labview™ and a suitable DAQ are available by other means, it is a very reasonable system. Labview™ offers a wide range of functionality, both with included functions and the possibility of combining them, and building new ones. It is also possible to include C-code if that is of interest. A great deal of plots and values are calculated in *MemCapMeter.vi*, giving a great deal of information about the measurement subject.

One problem with measuring the capacitance of the skin-electrode setup is that we know that the capacitance varies with frequency according to the Grimnes model. As pointed out in section 8.7 one cannot measure the capacitance of a $R_p || C + R_s$ model accurately without a high enough applied signal frequency, depending on the values of the component. This makes it hard to get the full picture of the capacitance behaviour.

The current measurements were mostly held in the frequency range without phase distortion by the operational amplifier, according to its ideal properties. Only the measurements with the dry button electrodes on skin and paper, and on the ceramic capacitor was slightly outside. On the other hand, section 7.3.3 shows that phase distortion did occurred to some degree at 10 kHz and strongly at 100 kHz. This means that the operational amplifier did phase shift the signal, or parasitic capacitances in the system was to blame. The measured capacitance curve was not converging at the highest measured frequency, meaning no value could be determined. The measurements were not corrected with this in mind, and should be evaluated accordingly. This means that measurement subjects were probably more resistive in nature at the high frequencies than originally observed in the q-V plots. This does not affect the memory evaluation though, as it affects the tilt of the curve and not its elliptic shape.

At low frequencies there was poor SNR of current sense voltage, caused by high subject impedance. This affected especially the q-V curves of the MOS and ceramic capacitor measurements, and the dry button electrode measurements on paper in full.

In addition, at low and high frequencies, the measurement sample length was not optimal. At low frequency (1 HZ) only one period were sampled, and at high frequency (10 kHz) there was only 10 samples per period. Both cases resulted in poor calculation of phase especially, which propagated into consequent calculations.

The influence of the current limit resistor on the *C-V* curves are not negligible, as seen in section 8.6. The function generator also contribute a 50 Ω series resistance, which will also affect the *C-V* curves in the same manner. In other words, series resistance influence from measurement equipment is not fully avoidable, but should be limited.

More time and effort should have been put into characterization of the accuracy and precision of the MemCapMeter. The only action taken towards an accuracy evaluation was with the reference measurements, noting that the measured values were within a 10 % margin compared to actual component values. As no reference measurement equipment was used with the skin measurements, an accuracy evaluation of those measurements were not taken. The reason for this not being prioritized was the fact that it was not the absolute model values that was of interest, but its relative behaviour. This was considered as not strongly influenced by the accuracy of the system. Precision evaluation consisted of performing three repetitions of each measurement, and comparing them. No quantititive evaluation was performed, but considered as sufficient.

11.2   MATLAB simulations

It is an important remark that the simulations performed in MATLAB were with ideal components and models that are simplified electrical equivalents of the electrode-skin setup. It was not an attempt to recreate the results from the measurements, but to be used to compare the measured curves to ideal ones from these simplified models.

11.3   C-V characterization

The equipment used in these measurements can be said to be very competent in capacitance measurements. And the method used is suitable for measuring capacitance as a function of DC voltage applied, and thereby the deposited charge on the capacitor plates. One drawback is that it lacks the possibility of monitoring the the *q-V* curve within the signal period of the applied periodic signal. Another drawback is the price, as this is a high end characterization system.

Part V

Summary

Chapter 12

Conclusions

Memcapacitance in skin

Can the properties that the electrode-skin setup shows be called memcapacitance, or is it just that it is a subject with both resistive and capacitive properties? The electrode-skin setup can in some ways be described as just a leaky capacitor, because the skin is not an insulator but a conductor with capacitive properties. The q-V curves are far from pinched, so it is not an ideal memcapacitor. If one follows Pershin et al.[15] it can be called a memcapacitive system, as long as it is encapsulated by two plates which are its connection to the outside circuitry. It can then be referred to as an ionic memcapacitive system, as the one presented by Krems et al.[11]. This is far from an ideal memcapacitor and can be represented by a combination of series and parallel RC circuits.

Even though it was not shown with these measurements, the skin most likely has voltage dependent capacitance to some degree, as the cell membranes act as elastic capacitors as previously mentioned.

In any case, the memory cannot be said to be non-volatile, as the change in capacitance disappears as the applied voltage is removed. The state of the system is dependent on external influence not to return to its steady state.

With this said, there is no evidence that there is not other mechanisms outside these measurement's sensitivity or frequency range, that are close to the ideal memcapacitor and/or holds non-volatile memory.

MemCapMeter and C-V Characterization

The MemCapMeter can not be said to be a high precision measurement system. Especially when it comes to measuring absolute values. To measure memory effects however it should have some validity. The semiconductor characterization system explored seems more capable of performing a high precision capacitance measurement. On the other hand, one lacks the q-V curves that the MemCapMeter produces. The customizability of the MemCapMeter is its main advantage, making it possible to investigate a wider range of properties of the measurement subject.

Chapter 13

The road from here

Further study to investigate the memory properties of skin are needed to get the full picture. Improving on the basic MemCapMeter design utilized in this thesis could be a way to. Performing measurements on other systems with known or potential memory properties, as the elastic memcapacitor, would be good both to evaluate the measuring equipment and to compare with results from skin. Other tissues should also be investigated, as it is highly likely that the numerous biological processes causes memcapacitive effects.

Memcapacitance is a concept that is far from well-defined in theory. It needs far more study both in theoretical and practical work. Pershin and Di Ventra [15] have made a solid contribution to structuring this mildly confusing field of study, but more strict definitions could be an improvement. Memory effects are a big part of biological systems, and defining these within the frames of memristive, memcapacitive and meminductive systems could be a good approach to induce further understanding of these effects. Bioimpedance research with this in mind should therefore be conducted. In addition, practical work with emphasis on the memory effects as a resource in stead of a problem would be a profitable way to go, as such functionality has usefulness in a range of disciplines.

Possible applications for memcapacitance are:

- Data storage, analogue and potentially loss free

- Adaptive learning circuits, building towards artificial intelligence

- Modelling biological tissue properties, to understand and sense its condition

- Modelling biological processes, e.g. function of neurons

Bibliography

[1]   D. Biolek, Z. Biolek and V. Biolkova. 'SPICE modelling of memca-
       pacitor'. In: *Electronics Letters* 46.7 (Jan. 2010), pp. 520–522. DOI:
       10.1049/el.2010.0358.

[2]   E. Cagin et al. 'Hysteretic metal-ferroelectric-semiconductor capacitors
       based on PZT/ZnO heterostructures'. In: *J. Phys. D, Appl. Phys.* 40
       (2007), pp. 2430–2434. DOI: 10.1088/0022-3727/40/8/003.

[3]   L. Chua. 'Memristor-The missing circuit element'. In: *Circuit Theory,
       IEEE Transactions on* 18.5 (1971), pp. 507 –519. DOI: 10.1109/TCT.
       1971.1083337.

[4]   M. Di Ventra, Y.V. Pershin and L.O. Chua. 'Circuit Elements
       With Memory: Memristors, Memcapacitors, and Meminductors'. In:
       Proceedings of the IEEE 97.10 (2009), pp. 1717 –1724. DOI: 10.1109/
       JPROC.2009.2021077.

[5]   T. Driscoll et al. 'Memory Metamaterials'. In: *Science* 325.5947 (2009),
       pp. 1518–1521. DOI: 10.1126/science.1176580.

[6]   S. Grimnes and Ø.G. Martinsen. *Bioimpedance and Bioelectricity
       Basics, Second Edition*. Academic Press, 2008. ISBN: 0123740045. URL:
       http://www.elsevier.com/wps/find/bookdescription.cws_home/714113/
       description.

[7]   S. Grimnes and Ø.G. Martinsen. 'Bioimpedance'. In: *Wiley Encyclo-
       pedia of Biomedical Engineering*. John Wiley & Sons, Inc., 2006. DOI:
       10.1002/9780471740360.ebs0128.

[8]   S. Grimnes and Ø.G. Martinsen. 'Cole electrical impedance Model-
       a critique and an alternative'. In: *Biomedical Engineering, IEEE
       Transactions on* 52.1 (2005), pp. 132 –135. DOI: 10.1109/TBME.2004.
       836499.

[9]   G.K. Johnsen et al. 'Memristive model of electro-osmosis in skin'. In:
       Phys. Rev. E 83 (3 2011), p. 031916. DOI: 10.1103/PhysRevE.83.031916.

[10]   M. Kanoun et al. 'Electronic properties of Ge nanocrystals for non
       volatile memory applications'. In: *Solid-State Electronics* 50 (2006),
       pp. 1310–1314. DOI: 10.1016/j.sse.2006.07.006.

[11]   M. Krems, Y.V. Pershin and M. Di Ventra. 'Ionic Memcapacitive
       Effects in Nanopores'. In: *Nano Lett.* 10 (2010), pp. 2674–2678. DOI:
       0.1021/nl1014734.

[12]   Q. Lai et al. 'Analog memory capacitor based on field-configurable ion-doped polymers'. In: *Appl. Phys. Lett.* 95 (2009), p. 213503. DOI: 10.1063/1.3268433.

[13]   J. Martinez-Rincon, M. Di Ventra and Y.V. Pershin. 'Solid-state memcapacitive system with negative and diverging capacitance'. In: *Phys. Rev. B* 81.19 (2010), p. 195430. DOI: 10.1103/PhysRevB.81.195430.

[14]   M.B. Partenskii and P.C. Jordan. 'Electroelastic Instabilities in Double Layers and Membranes'. In: *Liquid Interfaces In Chemical, Biological And Pharmaceutical Applications*. CRC Press, 2001. Chap. 3. ISBN: 978-0-8247-0457-5. DOI: doi:10.1201/9780203908754.ch3.

[15]   Y.V. Pershin and M. Di Ventra. 'Memory effects in complex materials and nanoscale systems'. In: *Advances in Physics* 60.2 (2011), pp. 145–227. DOI: 10.1080/00018732.2010.544961.

Part VI

Appendices

Appendix A

MemCapMeter.vi
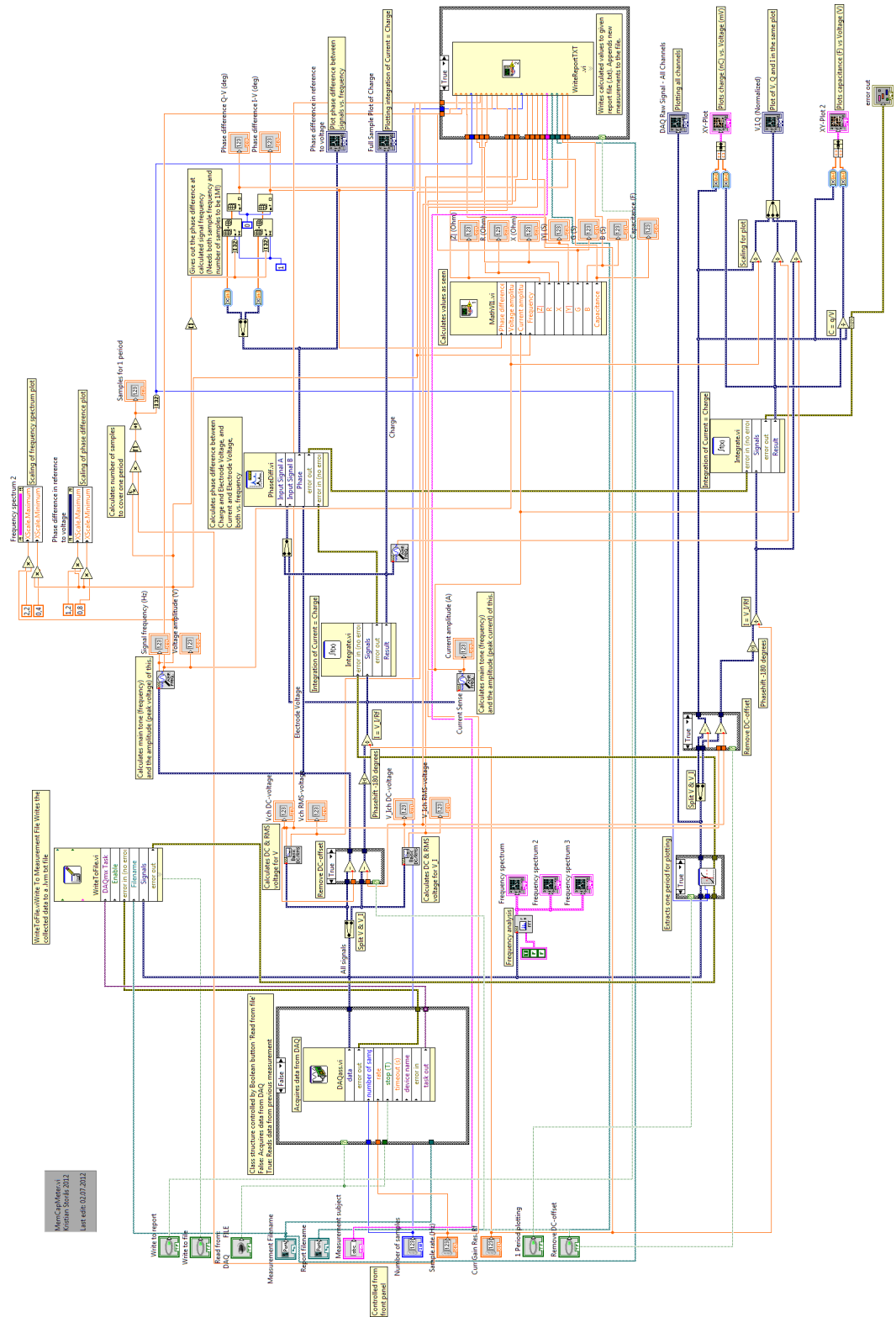
Figure A.1: MemCapMeter.vi Block Diagram.

Other instances of case structures
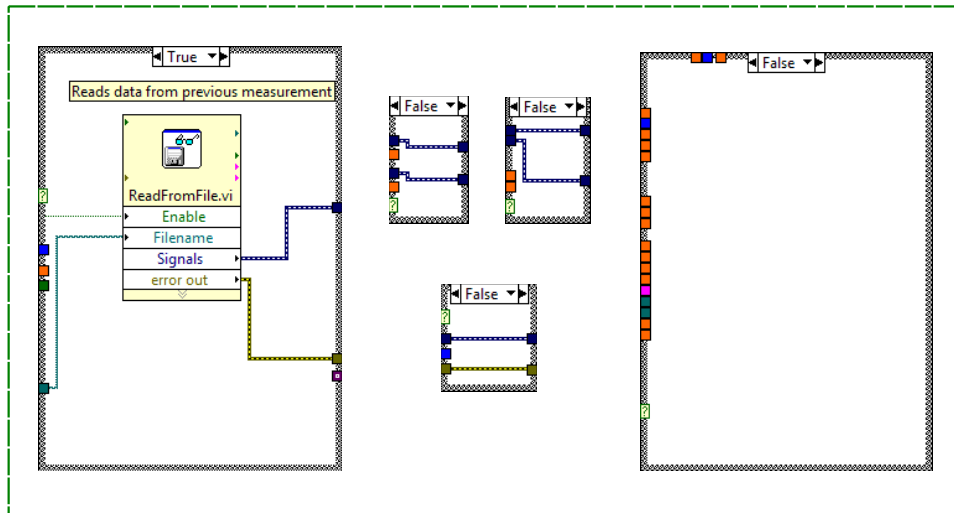
MathVI1.vi
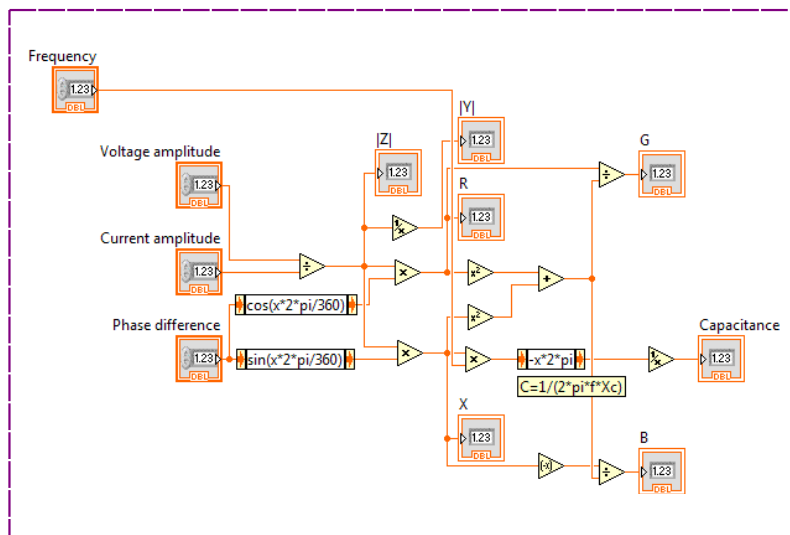
Figure A.2: MemCapMeter.vi case structures and subVI MathVI1.vi. Upper: Other instances of case structures in MemCapMeter.vi, not shown in figure A.1. Lower: MathVI1.vi, subVI used to calculate a range of values.
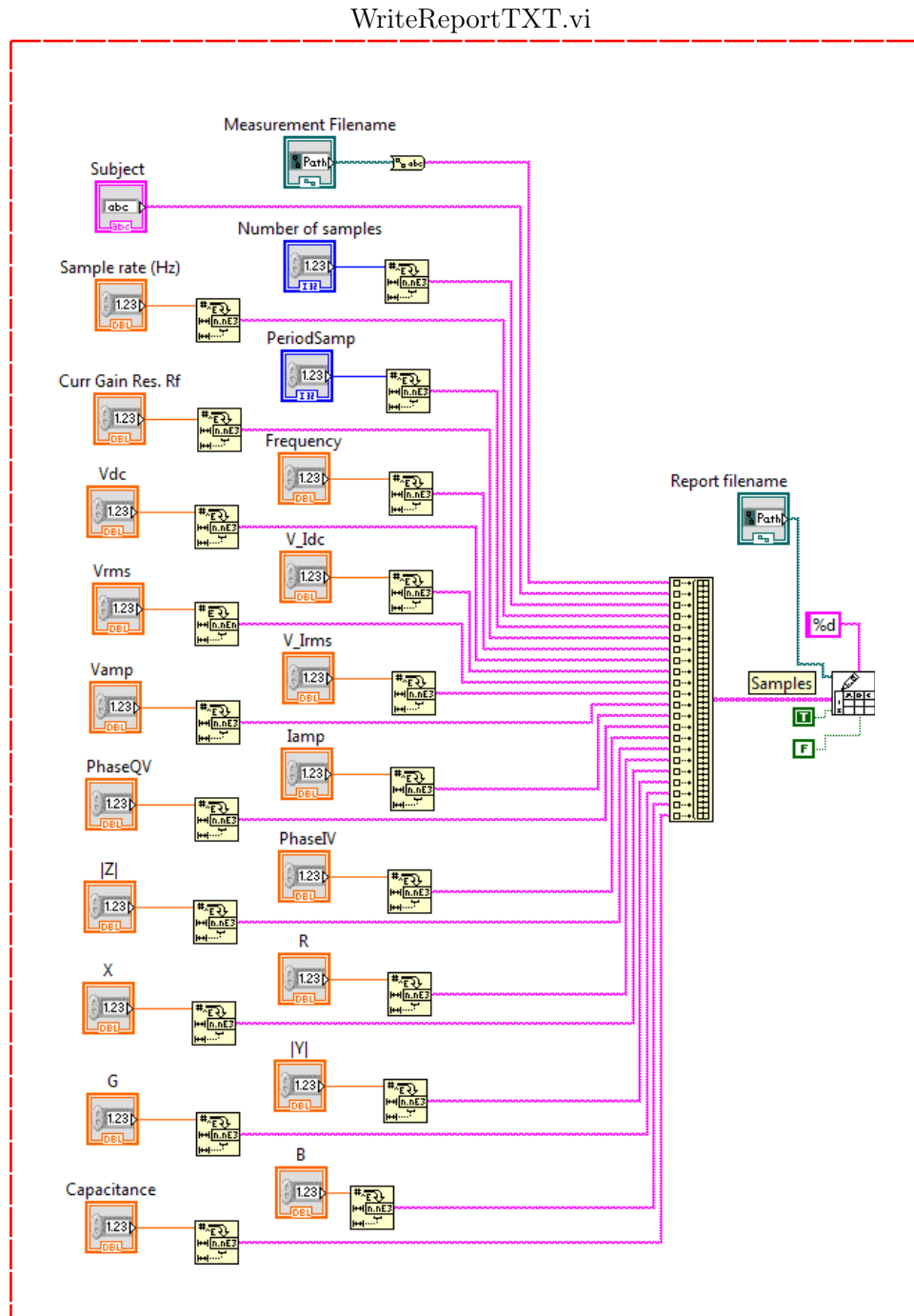
WriteReportTXT.vi

Figure A.3: MemCapMeter.vi subVI writeReportTXT.vi, used to write values to a .txt report file.

Appendix B

Excel plots
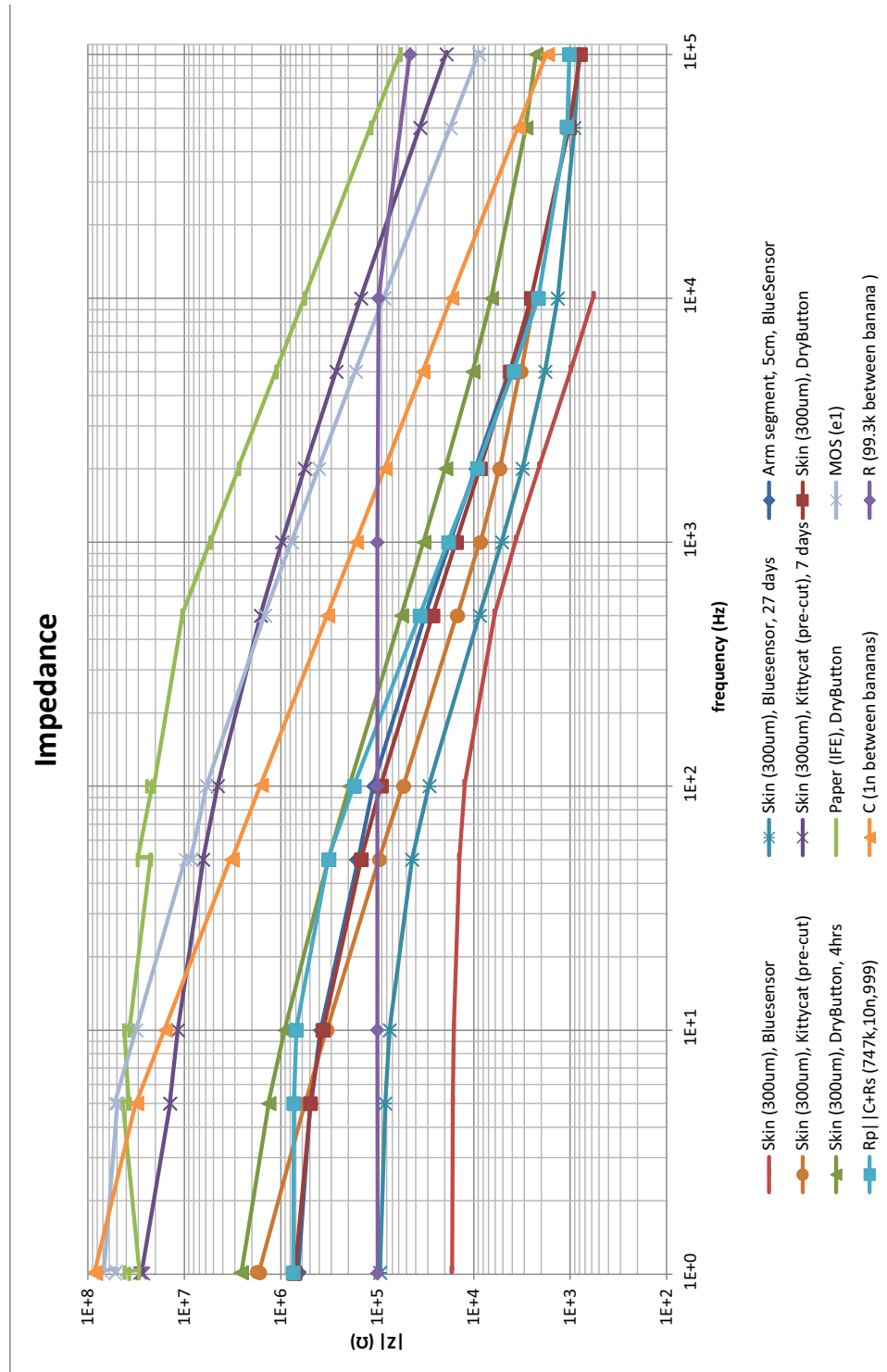
Figure B.1: Impedance part of Bode diagram for measurements performed with MemCapMeter.
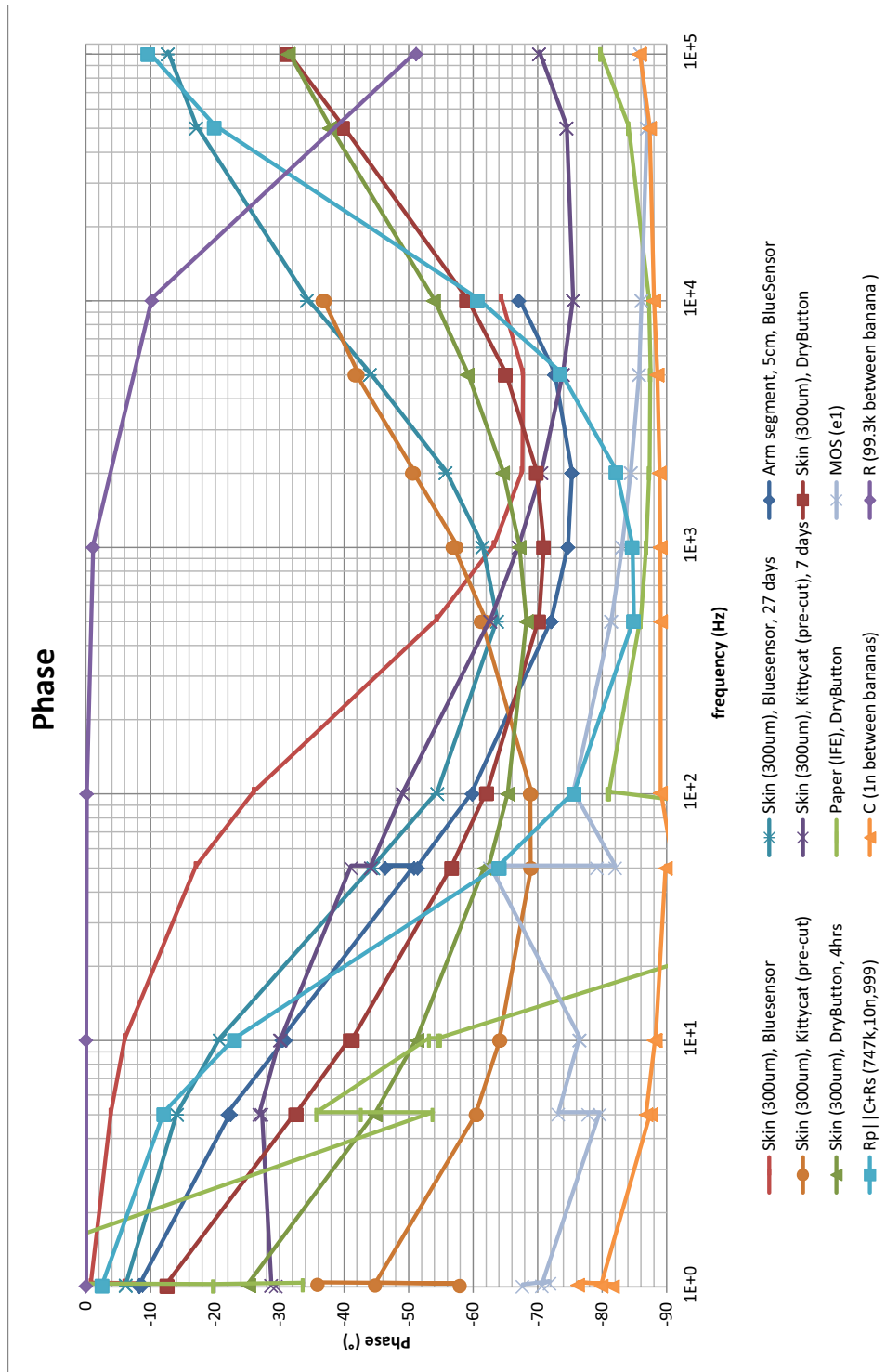
Figure B.2: Phase part of Bode diagram for measurements performed with MemCapMeter.
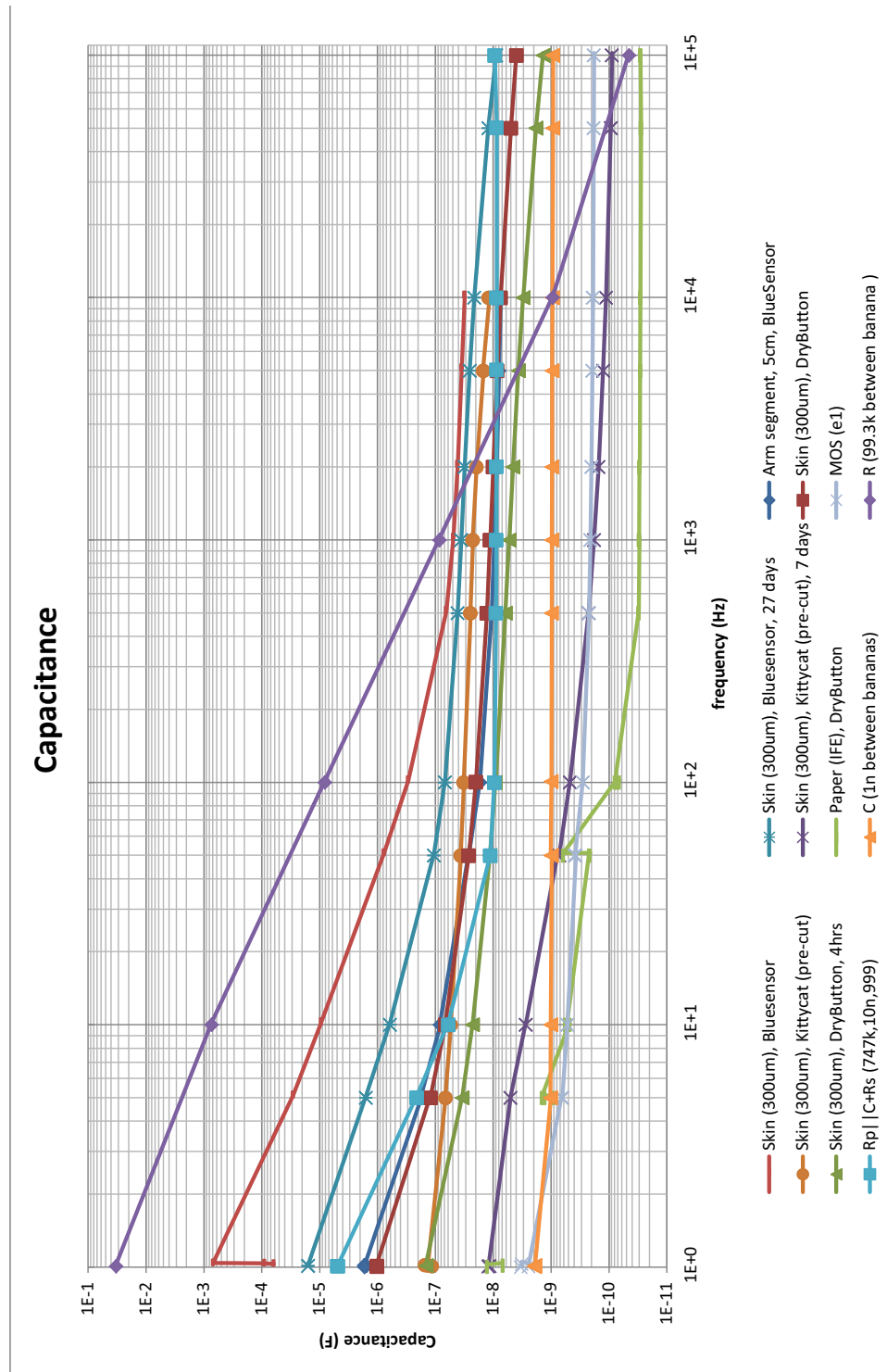
Figure B.3: Capacitance vs. frequency for measurements performed with MemCapMeter.

Appendix C

MATLAB Code

```matlab
% ALL.m
% Kristian Storås (Storaas)
% University of Oslo, January 2012
% Last edit: 30.07.12
%─────────────────────────────
% Simulates measurements over some simple electrical ...
    ekvivalent models
% of tissue. This consists of resistance Rp and capacative ...
    component in
% parallell, in series with resistance Rs. This is done with ideal
% capacitor C, Constant Phase Element CPE and a simple ...
    memcapacitive model
% Cmem as the capacitive element. In addition it is all done ...
    with the
% capacitor model C.
%
% Plots Impedance vs. Frequency, Reactance vs. Resistance ...
    (Wessel diagram)
% and Phase Shift vs. Frequency.
% Applies a voltage, calculates current through circuit and ...
    integrates to
% get charge. Plots Charge vs. Voltage for 6 different ...
    frequencies (1, 10,
% 100, 1k, 10k and 100k Hz). Also plots Electrode Voltage and ...
    Current
% Sense Voltage vs. Time, and Capacitance vs. Voltage for one ...
    selected
% frequency (1 kHz).
%────────────────────────────────────────────────────────
clear all
close all


%────────────────────────────────────────────────────────
% Definition of parameters
%────────────────────────────────────────────────────────
dtr = 360/(2*pi);                    % Converts degrees to radians

F = [1e0 1e1 1e2 1e3 1e4 1e5];    % Frequenzy vector ...
    [10,..,100k] Hz
fs = 1e6;                            % Sample frequency = 1MS/s
```

```matlab
Rp = 7.47e5;                        % Parallell resistance = 747 kOhm
C = 10e-9;                          % Capacitor = 10 nF
Xc = -1i./(2*pi*F*C);              % Reactance = Impedance of ...
    the capacitor
Xcpe = (cos(70*2*pi/360) - 1i*sin(70*2*pi/360))./(2*pi*F*C);
                    % Impedance of Constant Phase Element ...
                        (phase = 70 deg)
Rs = 999;                           % Series resistance = 999 Ohm

Z1 = (1./Xc + 1/Rp).^-1 + Rs;      % Total impedance, Rp||C + Rs
Z2 = (1./Xcpe + 1/Rp).^-1 + Rs;    % Total impedance, Rp||CPE + Rs
Z3 = -1i./(2*pi*F*1e-9);           % Total impedance, C

%-------------------------------------------------------------------
% Bode diagram and Wessel diagram
%-------------------------------------------------------------------
% Plot impedance modulus (|Z|) against frequency
figure()
subplot(2,1,1)
loglog(F,abs(Z1),F,abs(Z2),F,abs(Z3))
xlabel('Frequency (Hz)'), ylabel('|Z| (Ohm)')
legend('Rp||C + Rs','Rp||CPE + Rs','C')

% Plot impedance phase (theta) versus frequency
subplot(2,1,2)
semilogx(F,angle(Z1)*dtr,F,angle(Z2)*dtr,F,angle(Z3)*dtr)
xlabel('Frequency (Hz)'), ylabel('Phaseshift (Degrees)')

% Plot imaginary part (X) of impedance against real part (R)
figure()
plot(real(Z1),-imag(Z1),real(Z2),-imag(Z2),real(Z2),-imag(Z3))
xlabel('R Resistance (Ohm)'), ylabel('-X Reactance (Ohm)')
legend('Rp||C + Rs','Rp||CPE + Rs','C')
%---------------
%---------------


%-------------------------------------------------------------------
% Plot Charge vs. Voltage for 6 different frequencies for ...
    Rp||C + Rs
%-------------------------------------------------------------------
figure()
%---------------
ind = 1;
f = F(ind);                         % Frequency (hz)
t = linspace(0,1/f,fs/f);          % Time vector, 0-2 (s)
dt = t(2);                          % Step size (s)

V = 0.5*sin(2*pi*f*t);             % Applied voltage (V)
I1 = 0.5*sin(2*pi*f*t-angle(Z1(ind)))/abs(Z1(ind));
                                    % Resulting current (A)
Q1 = cumtrapz(I1)*dt;              % Charge = integral of ...
    current (C)

% Plotting charge vs voltage
subplot(3,2,ind)
plot(V,Q1)
xlabel('Voltage (V)'), ylabel('Charge (C)')


%---------------
```

```matlab
ind = 2;
f = F(ind);                      % Frequency (hz)
t = linspace(0,1/f,fs/f);        % Time vector, 0—2 (s)
dt = t(2);                       % Step size (s)

V = 0.5*sin(2*pi*f*t);           % Applied voltage (V)
I1 = 0.5*sin(2*pi*f*t—angle(Z1(ind)))/abs(Z1(ind));
                                 % Resulting current (A)
Q1 = cumtrapz(I1)*dt;            % Charge = integral of ...
   current (C)

% Plotting charge vs voltage
subplot(3,2,ind)
plot(V,Q1)
xlabel('Voltage (V)'), ylabel('Charge (C)')
title('Charge vs. Voltage — Rp||C + Rs')

%——————————
ind = 3;
f = F(ind);                      % Frequency (hz)
t = linspace(0,1/f,fs/f);        % Time vector, 0—2 (s)
dt = t(2);                       % Step size (s)

V = 0.5*sin(2*pi*f*t);           % Applied voltage (V)
I1 = 0.5*sin(2*pi*f*t—angle(Z1(ind)))/abs(Z1(ind));
                                 % Resulting current (A)
Q1 = cumtrapz(I1)*dt;            % Charge = integral of ...
   current (C)

% Plotting charge vs voltage
subplot(3,2,ind)
plot(V,Q1)
xlabel('Voltage (V)'), ylabel('Charge (C)')

%——————————
ind = 4;
f = F(ind);                      % Frequency (hz)
t = linspace(0,1/f,fs/f);        % Time vector, 0—2 (s)
dt = t(2);                       % Step size (s)

V = 0.5*sin(2*pi*f*t);           % Applied voltage (V)
I1 = 0.5*sin(2*pi*f*t—angle(Z1(ind)))/abs(Z1(ind));
                                 % Resulting current (A)
Q1 = cumtrapz(I1)*dt;            % Charge = integral of ...
   current (C)

% Plotting charge vs voltage
subplot(3,2,ind)
plot(V,Q1)
xlabel('Voltage (V)'), ylabel('Charge (C)')

%——————————
ind = 5;
f = F(ind);                      % Frequency (hz)
t = linspace(0,1/f,fs/f);        % Time vector, 0—2 (s)
dt = t(2);                       % Step size (s)

V = 0.5*sin(2*pi*f*t);           % Applied voltage (V)
I1 = 0.5*sin(2*pi*f*t—angle(Z1(ind)))/abs(Z1(ind));
```

```matlab
                                        % Resulting current (A)
Q1 = cumtrapz(I1)*dt;                   % Charge = integral of ...
    current (C)

% Plotting charge vs voltage
subplot(3,2,ind)
plot(V,Q1)
xlabel('Voltage (V)'), ylabel('Charge (C)')


%————————
ind = 6;
f = F(ind);                             % Frequency (hz)
t = linspace(0,1/f,fs/f);              % Time vector, 0—2 (s)
dt = t(2);                              % Step size (s)

V = 0.5*sin(2*pi*f*t);                  % Applied voltage (V)
I1 = 0.5*sin(2*pi*f*t—angle(Z1(ind)))/abs(Z1(ind));
                                        % Resulting current (A)
Q1 = cumtrapz(I1)*dt;                   % Charge = integral of ...
    current (C)

% Plotting charge vs voltage
subplot(3,2,ind)
plot(V,Q1)
xlabel('Voltage (V)'), ylabel('Charge (C)')
%————————
%————————


%————————————————————————————————————————————
% Plot Charge vs. Voltage for 6 different frequencies for ...
    Rp||CPE + Rs
%————————————————————————————————————————————
figure()
%————————
ind = 1;
f = F(ind);                             % Frequency (hz)
t = linspace(0,1/f,fs/f);              % Time vector, 0—2 (s)
dt = t(2);                              % Step size (s)

V = 0.5*sin(2*pi*f*t);                  % Applied voltage (V)
I2 = 0.5*sin(2*pi*f*t—angle(Z2(ind)))/abs(Z2(ind));
                                        % Resulting current (A)
Q2 = cumtrapz(I2)*dt;                   % Charge = integral of ...
    current (C)

% Plotting charge vs voltage
subplot(3,2,ind)
plot(V,Q2)
xlabel('Voltage (V)'), ylabel('Charge (C)')

%————————
ind = 2;
f = F(ind);                             % Frequency (hz)
t = linspace(0,1/f,fs/f);              % Time vector, 0—2 (s)
dt = t(2);                              % Step size (s)

V = 0.5*sin(2*pi*f*t);                  % Applied voltage (V)
I2 = 0.5*sin(2*pi*f*t—angle(Z2(ind)))/abs(Z2(ind));
                                        % Resulting current (A)
```

```matlab
Q2 = cumtrapz(I2)*dt;              % Charge = integral of ...
    current (C)

% Plotting charge vs voltage
subplot(3,2,ind)
plot(V,Q2)
xlabel('Voltage (V)'), ylabel('Charge (C)')
title('Charge vs. Voltage — Rp||CPE + Rs')

%—————————
ind = 3;
f = F(ind);                        % Frequency (hz)
t = linspace(0,1/f,fs/f);          % Time vector, 0—2 (s)
dt = t(2);                         % Step size (s)

V = 0.5*sin(2*pi*f*t);             % Applied voltage (V)
I2 = 0.5*sin(2*pi*f*t—angle(Z2(ind)))/abs(Z2(ind));
                                   % Resulting current (A)
Q2 = cumtrapz(I2)*dt;              % Charge = integral of ...
    current (C)

% Plotting charge vs voltage
subplot(3,2,ind)
plot(V,Q2)
xlabel('Voltage (V)'), ylabel('Charge (C)')

%—————————
ind = 4;
f = F(ind);                        % Frequency (hz)
t = linspace(0,1/f,fs/f);          % Time vector, 0—2 (s)
dt = t(2);                         % Step size (s)

V = 0.5*sin(2*pi*f*t);             % Applied voltage (V)
I2 = 0.5*sin(2*pi*f*t—angle(Z2(ind)))/abs(Z2(ind));
                                   % Resulting current (A)
Q2 = cumtrapz(I2)*dt;              % Charge = integral of ...
    current (C)

% Plotting charge vs voltage
subplot(3,2,ind)
plot(V,Q2)
xlabel('Voltage (V)'), ylabel('Charge (C)')

%—————————
ind = 5;
f = F(ind);                        % Frequency (hz)
t = linspace(0,1/f,fs/f);          % Time vector, 0—2 (s)
dt = t(2);                         % Step size (s)

V = 0.5*sin(2*pi*f*t);             % Applied voltage (V)
I2 = 0.5*sin(2*pi*f*t—angle(Z2(ind)))/abs(Z2(ind));
                                   % Resulting current (A)
Q2 = cumtrapz(I2)*dt;              % Charge = integral of ...
    current (C)

% Plotting charge vs voltage
subplot(3,2,ind)
plot(V,Q2)
xlabel('Voltage (V)'), ylabel('Charge (C)')
```

```matlab
%————————
ind = 6;
f = F(ind);                         % Frequency (hz)
t = linspace(0,1/f,fs/f);           % Time vector, 0—2 (s)
dt = t(2);                          % Step size (s)

V = 0.5*sin(2*pi*f*t);              % Applied voltage (V)
I2 = 0.5*sin(2*pi*f*t—angle(Z2(ind)))/abs(Z2(ind));
                                    % Resulting current (A)
Q2 = cumtrapz(I2)*dt;               % Charge = integral of ...
    current (C)

% Plotting charge vs voltage
subplot(3,2,ind)
plot(V,Q2)
xlabel('Voltage (V)'), ylabel('Charge (C)')
%————————
%————————


%————————————————————————————————————————————————
% Plot Charge vs. Voltage for 6 different frequencies for C
%————————————————————————————————————————————————
figure()
%————————
ind = 1;
f = F(ind);                         % Frequency (hz)
t = linspace(0,1/f,fs/f);           % Time vector, 0—2 (s)
dt = t(2);                          % Step size (s)

V = 0.5*sin(2*pi*f*t);              % Applied voltage (V)
I3 = 0.5*sin(2*pi*f*t—angle(Z3(ind)))/abs(Z3(ind));
                                    % Resulting current (A)
Q3 = cumtrapz(I3)*dt;               % Charge = integral of ...
    current (C)

% Plotting charge vs voltage
subplot(3,2,ind)
plot(V,Q3)
xlabel('Voltage (V)'), ylabel('Charge (C)')

%————————
ind = 2;
f = F(ind);                         % Frequency (hz)
t = linspace(0,1/f,fs/f);           % Time vector, 0—2 (s)
dt = t(2);                          % Step size (s)

V = 0.5*sin(2*pi*f*t);              % Applied voltage (V)
I3 = 0.5*sin(2*pi*f*t—angle(Z3(ind)))/abs(Z3(ind));
                                    % Resulting current (A)
Q3 = cumtrapz(I3)*dt;               % Charge = integral of ...
    current (C)

% Plotting charge vs voltage
subplot(3,2,ind)
plot(V,Q3)
xlabel('Voltage (V)'), ylabel('Charge (C)')
title('Charge vs. Voltage — C')
```

```matlab
%————————————
ind = 3;
f = F(ind);                     % Frequency (hz)
t = linspace(0,1/f,fs/f);       % Time vector, 0—2 (s)
dt = t(2);                      % Step size (s)

V = 0.5*sin(2*pi*f*t);          % Applied voltage (V)
I3 = 0.5*sin(2*pi*f*t—angle(Z3(ind)))/abs(Z3(ind));
                                % Resulting current (A)
Q3 = cumtrapz(I3)*dt;           % Charge = integral of ...
   current (C)

% Plotting charge vs voltage
subplot(3,2,ind)
plot(V,Q3)
xlabel('Voltage (V)'), ylabel('Charge (C)')

%————————————
ind = 4;
f = F(ind);                     % Frequency (hz)
t = linspace(0,1/f,fs/f);       % Time vector, 0—2 (s)
dt = t(2);                      % Step size (s)

V = 0.5*sin(2*pi*f*t);          % Applied voltage (V)
I3 = 0.5*sin(2*pi*f*t—angle(Z3(ind)))/abs(Z3(ind));
                                % Resulting current (A)
Q3 = cumtrapz(I3)*dt;           % Charge = integral of ...
   current (C)

% Plotting charge vs voltage
subplot(3,2,ind)
plot(V,Q3)
xlabel('Voltage (V)'), ylabel('Charge (C)')

%————————————
ind = 5;
f = F(ind);                     % Frequency (hz)
t = linspace(0,1/f,fs/f);       % Time vector, 0—2 (s)
dt = t(2);                      % Step size (s)

V = 0.5*sin(2*pi*f*t);          % Applied voltage (V)
I3 = 0.5*sin(2*pi*f*t—angle(Z3(ind)))/abs(Z3(ind));
                                % Resulting current (A)
Q3 = cumtrapz(I3)*dt;           % Charge = integral of ...
   current (C)

% Plotting charge vs voltage
subplot(3,2,ind)
plot(V,Q3)
xlabel('Voltage (V)'), ylabel('Charge (C)')

%————————————
ind = 6;
f = F(ind);                     % Frequency (hz)
t = linspace(0,1/f,fs/f);       % Time vector, 0—2 (s)
dt = t(2);                      % Step size (s)

V = 0.5*sin(2*pi*f*t);          % Applied voltage (V)
I3 = 0.5*sin(2*pi*f*t—angle(Z3(ind)))/abs(Z3(ind));
```

```matlab
                                    % Resulting current (A)
Q3 = cumtrapz(I3)*dt;               % Charge = integral of ...
    current (C)

% Plotting charge vs voltage
subplot(3,2,ind)
plot(V,Q3)
xlabel('Voltage (V)'), ylabel('Charge (C)')
%————————
%————————


%————————————————————————————————————————
% Plot Charge vs. Voltage for 6 different frequencies for ...
    Rp||Cmem + Rs
%————————————————————————————————————————
figure()
%————————
ind = 1;
f = F(ind);                         % Frequency (hz)
t = linspace(0,1/f,fs/f);           % Time vector, 0—2 (s)
dt = t(2);                          % Step size (s)

V = 0.5*sin(2*pi*f*t);              % Applied voltage (V)
Cmem = C*(1 + V);                   % Capacitance
x_t = -1i./(2*pi*f*Cmem);           % Reactance = Impedance of ...
    the capacitor
z_t = (1./x_t + 1/Rp).^-1 + Rs;     % Total impedance, Rp||C + Rs
I4 = (0.5*sin(2*pi*f*t-angle(z_t)))./abs(z_t);
                                    % Resulting current (A)
Q4 = cumtrapz(I4)*dt;               % Charge = integral of ...
    current (C)

% Plotting charge vs voltage
subplot(3,2,ind)
plot(V,Q4)
xlabel('Voltage (V)'), ylabel('Charge (C)')

%————————
ind = 2;
f = F(ind);                         % Frequency (hz)
t = linspace(0,1/f,fs/f);           % Time vector, 0—2 (s)
dt = t(2);                          % Step size (s)

V = 0.5*sin(2*pi*f*t);              % Applied voltage (V)
Cmem = C*(1 + V);                   % Capacitance
x_t = -1i./(2*pi*f*Cmem);           % Reactance = Impedance of ...
    the capacitor
z_t = (1./x_t + 1/Rp).^-1 + Rs;     % Total impedance, Rp||C + Rs
I4 = (0.5*sin(2*pi*f*t-angle(z_t)))./abs(z_t);
                                    % Resulting current (A)
Q4 = cumtrapz(I4)*dt;               % Charge = integral of ...
    current (C)

% Plotting charge vs voltage
subplot(3,2,ind)
plot(V,Q4)
xlabel('Voltage (V)'), ylabel('Charge (C)')
title('Charge vs. Voltage — Rp||Cmem + Rs')
```

```matlab
%————————————
ind = 3;
f = F(ind);                     % Frequency (hz)
t = linspace(0,1/f,fs/f);       % Time vector, 0—2 (s)
dt = t(2);                      % Step size (s)

V = 0.5*sin(2*pi*f*t);          % Applied voltage (V)
Cmem = C*(1 + V);               % Capacitance
x_t = −1i./(2*pi*f*Cmem);       % Reactance = Impedance of ...
    the capacitor
z_t = (1./x_t + 1/Rp).^−1 + Rs; % Total impedance, Rp||C + Rs
I4 = (0.5*sin(2*pi*f*t−angle(z_t)))./abs(z_t);
                                % Resulting current (A)
Q4 = cumtrapz(I4)*dt;           % Charge = integral of ...
    current (C)

% Plotting charge vs voltage
subplot(3,2,ind)
plot(V,Q4)
xlabel('Voltage (V)'), ylabel('Charge (C)')

%————————————
ind = 4;
ff = F(ind);                    % Frequency (hz)
t = linspace(0,1/f,fs/f);       % Time vector, 0—2 (s)
dt = t(2);                      % Step size (s)

V = 0.5*sin(2*pi*f*t);          % Applied voltage (V)
Cmem = C*(1 + V);               % Capacitance
x_t = −1i./(2*pi*f*Cmem);       % Reactance = Impedance of ...
    the capacitor
z_t = (1./x_t + 1/Rp).^−1 + Rs ; % Total impedance, Rp||C + Rs
I4 = (0.5*sin(2*pi*f*t−angle(z_t)))./abs(z_t);
                                % Resulting current (A)
Q4 = cumtrapz(I4)*dt;           % Charge = integral of ...
    current (C)

% Plotting charge vs voltage
subplot(3,2,ind)
plot(V,Q4)
xlabel('Voltage (V)'), ylabel('Charge (C)')

%————————————
ind = 5;
f = F(ind);                     % Frequency (hz)
t = linspace(0,1/f,fs/f);       % Time vector, 0—2 (s)
dt = t(2);                      % Step size (s)

V = 0.5*sin(2*pi*f*t);          % Applied voltage (V)
Cmem = C*(1 + V);               % Capacitance
x_t = −1i./(2*pi*f*Cmem);       % Reactance = Impedance of ...
    the capacitor
z_t = (1./x_t + 1/Rp).^−1 + Rs; % Total impedance, Rp||C + Rs
I4 = (0.5*sin(2*pi*f*t−angle(z_t)))./abs(z_t);
                                % Resulting current (A)
Q4 = cumtrapz(I4)*dt;           % Charge = integral of ...
    current (C)

% Plotting charge vs voltage
```

```matlab
subplot(3,2,ind)
plot(V,Q4)
xlabel('Voltage (V)'), ylabel('Charge (C)')

%———————————
ind = 6;
f = F(ind);                         % Frequency (hz)
t = linspace(0,1/f,fs/f);           % Time vector, 0—2 (s)
dt = t(2);                          % Step size (s)

V = 0.5*sin(2*pi*f*t);              % Applied voltage (V)
Cmem = C*(1 + V);                   % Capacitance
x_t = —1i./(2*pi*f*Cmem);          % Reactance = Impedance of ...
    the capacitor
z_t = (1./x_t + 1/Rp).^—1 + Rs;    % Total impedance, Rp||C + Rs
I4 = (0.5*sin(2*pi*f*t—angle(z_t)))./abs(z_t);
                                    % Resulting current (A)
Q4 = cumtrapz(I4)*dt;               % Charge = integral of ...
    current (C)

% Plotting charge vs voltage
subplot(3,2,ind)
plot(V,Q4)
xlabel('Voltage (V)'), ylabel('Charge (C)')
%———————————
%———————————


%—————————————————————————————————————————————————————
% Plot Raw Signals (V and V_I) vs. Time for the four models
%—————————————————————————————————————————————————————
ind = 4;
f = F(ind);                         % Frequency (hz)
t = linspace(0,2/f,fs/f);           % Time vector, 0—2 (s)
Rf = 1e5;                           % Front End Gain

V = 0.5*sin(2*pi*f*t);              % Applied voltage (V)

% Resulting current (A)
I1 = 0.5*sin(2*pi*f*t—angle(Z1(ind)))/abs(Z1(ind));
I2 = 0.5*sin(2*pi*f*t—angle(Z2(ind)))/abs(Z2(ind));
I3 = 0.5*sin(2*pi*f*t—angle(Z3(ind)))/abs(Z3(ind));
Cmem = C*(1 + V);                   % Capacitance
x_t = —1i./(2*pi*f*Cmem);          % Reactance = Impedance of ...
    the capacitor
z_t = (1./x_t + 1/Rp).^—1 + Rs;    % Total impedance, Rp||C + Rs
I4 = (0.5*sin(2*pi*f*t—angle(z_t)))./abs(z_t);

% Plot Voltage and Current for Rp||C + Rs
figure()
plot(t,V,'b',t,I1*Rf*(—1),'r')
xlabel('Time (s)'), ylabel('Amplitude (V)')
legend('V','V\_I')
title('DAQ Raw signals — All channels — Rp||C + Rs')

% Plot Voltage and Current for Rp||CPE + Rs
figure()
plot(t,V,'b',t,I2*Rf*(—1),'r')
xlabel('Time (s)'), ylabel('Amplitude (V)')
legend('V','V\_I')
```

```matlab
title('DAQ Raw signals — All channels — Rp||CPE + Rs')

% Plot Voltage and Current for Rp||Cmem + Rs
figure()
plot(t,V,'b',t,I3*Rf*(−1),'r')
xlabel('Time (s)'), ylabel('Amplitude (V)')
legend('V','V\_I')
title('DAQ Raw signals — All channels — C')

% Plot Voltage and Current for C
figure()
plot(t,V,'b',t,I4*Rf*(−1),'r')
xlabel('Time (s)'), ylabel('Amplitude (V)')
legend('V','V\_I')
title('DAQ Raw signals — All channels — Rp||Cmem + Rs')
%——————————
%——————————


%———————————————————————————————————————
% Calculate Capacitance for 1 kz and plot Capacitance vs. ...
    Voltage for
% the four models.
%———————————————————————————————————————
ind = 4;
f = F(ind);                     % Frequency (hz)
t = linspace(0,1/f,fs/f);       % Time vector, 0—2 (s)
dt = t(2);                      % Step size (s)

V = 0.5*sin(2*pi*f*t);          % Applied voltage (V)

% Resulting current (A)
I1 = 0.5*sin(2*pi*f*t−angle(Z1(ind)))/abs(Z1(ind));
I2 = 0.5*sin(2*pi*f*t−angle(Z2(ind)))/abs(Z2(ind));
I3 = 0.5*sin(2*pi*f*t−angle(Z3(ind)))/abs(Z3(ind));
Cmem = C*(1 + V);               % Capacitance
x_t = −1i./(2*pi*f*Cmem);       % Reactance = Impedance of ...
    the capacitor
z_t = (1./x_t + 1/Rp).^−1 + Rs; % Total impedance, Rp||C + Rs
I4 = (0.5*sin(2*pi*f*t−angle(z_t)))./abs(z_t);

% Charge = integral of current (C)
Q1 = cumtrapz(I1)*dt;
Q2 = cumtrapz(I2)*dt;
Q3 = cumtrapz(I3)*dt;
Q4 = cumtrapz(I4)*dt;

% Calculate capacitance for the three models for 1 kz
% (Doing it the long way, to do it the same way as in ...
    MemCapMeter.vi)
Xcal1 = (max(V)/max(I1))*sin(angle(Z1(ind)));
Xcal2 = (max(V)/max(I2))*sin(angle(Z2(ind)));
Xcal3 = (max(V)/max(I3))*sin(angle(Z3(ind)));
Xcal4 = (max(V)/max(I4))*sin(max(angle(z_t)));
C1 = −1./(2*pi*f*Xcal1)
C2 = −1./(2*pi*f*Xcal2)
C3 = −1./(2*pi*f*Xcal3)
C4 = −1./(2*pi*f*Xcal4)
```

```matlab
% Plot Capacitance vs. Voltage for Rp||C + Rs
figure()
subplot(1,2,1)
plot(V,Q1./V)
xlabel('Voltage (V)'), ylabel('Capacitance (F)')
subplot(1,2,2)
plot(V,Q1./V)
axis([-0.5 0.5 0*C1 2*C1])
xlabel('Voltage (V)'), ylabel('Capacitance (F)')
title('Capacitance vs. Voltage - Rp||C + Rs')

% Plot Capacitance vs. Voltage for Rp||CPE + Rs
figure()
subplot(1,2,1)
plot(V,Q2./V)
xlabel('Voltage (V)'), ylabel('Capacitance (F)')
subplot(1,2,2)
plot(V,Q2./V)
axis([-0.5 0.5 0*C2 2*C2])
xlabel('Voltage (V)'), ylabel('Capacitance (F)')
title('Capacitance vs. Voltage - Rp||CPE + Rs')

% Plot Capacitance vs. Voltage for  Rp||Cmem + Rs
figure()
subplot(1,2,1)
plot(V,Q3./V)
xlabel('Voltage (V)'), ylabel('Capacitance (F)')
subplot(1,2,2)
plot(V,Q3./V)
axis([-0.5 0.5 0*C3 2*C3])
xlabel('Voltage (V)'), ylabel('Capacitance (F)')
title('Capacitance vs. Voltage - C')

% Plot Capacitance vs. Voltage for C
figure()
subplot(1,2,1)
plot(V,Q4./V)
xlabel('Voltage (V)'), ylabel('Capacitance (F)')
subplot(1,2,2)
plot(V,Q4./V)
axis([-0.5 0.5 0*C4 2*C4])
xlabel('Voltage (V)'), ylabel('Capacitance (F)')
title('Capacitance vs. Voltage - Rp||Cmem + Rs')
%---------------------------------------------------------
%---------------------------------------------------------

%---------------------------------------------------------
% Changes to simulate current limit resistor effect on C-V curves
%---------------------------------------------------------
Rcl = 1e3;
Z2 = Rcl + (1./Xc + 1/Rp).^-1 + Rs;  % Total impedance

Vcl = I2*Rcl;                        % Current limit resistor ...
    voltage
V = V - Vcl;                         % Rp||CPE + Rs model voltage

% Plot Capacitance vs. Voltage for Rp||CPE + Rs
figure()
subplot(1,2,1)
```

```matlab
plot(V,Q2./V)
xlabel('Voltage (V)'), ylabel('Capacitance (F)')
subplot(1,2,2)
plot(V,Q2./V)
axis([-0.5 0.5 0*C2 2*C2])
xlabel('Voltage (V)'), ylabel('Capacitance (F)')
title('Capacitance vs. Voltage — Rcl + Rp||C + Rs')
%——————————
%——————————


%————————————————————————————————————————————————————
% Changes to simulate 50 Hz noise and DC offset effect on q—V ...
    curves
%————————————————————————————————————————————————————


V = 0.5*sin(2*pi*f*t);          % Applied voltage (V)
x_t = -1i/(2*pi*f*C);           % Reactance = Impedance of ...
    the capacitor
z_t = (1/x_t + 1/Rp)^-1 + Rs;   % Total impedance, Rp||C + Rs
I1 = (0.5*sin(2*pi*f*t—angle(z_t)))./abs(z_t);
                                % Resulting current (A)
Q1 = cumtrapz(I1)*dt;           % Charge = integral of ...
    current (C)

% Plotting charge vs voltage
figure()
subplot(1,2,1)
plot(V,Q1,'b:')
axis([-0.6 0.6 -6e-9 +6e-9])
hold on
%————————————————————————


V = 0.5*sin(2*pi*f*t)+0.2*sin(2*pi*100*t); % Applied voltage (V)
x_t = -1i/(2*pi*f*C);           % Reactance = Impedance of ...
    the capacitor
z_t = (1/x_t + 1/Rp)^-1 + Rs;   % Total impedance, Rp||C + Rs
I1 = (0.5*sin(2*pi*f*t—angle(z_t)))./abs(z_t);
                                % Resulting current (A)
Q1 = cumtrapz(I1)*dt;           % Charge = integral of ...
    current (C)

% Plotting charge vs voltage
plot(V,Q1,'r—')
hold off
xlabel('Voltage (V)'), ylabel('Charge (C)')
legend('Normal','50 Hz noise')
%————————————————————————


V = 0.5*sin(2*pi*f*t);          % Applied voltage (V)
x_t = -1i/(2*pi*f*C);           % Reactance = Impedance of ...
    the capacitor
z_t = (1/x_t + 1/Rp)^-1 + Rs;   % Total impedance, Rp||C + Rs
I1 = (0.5*sin(2*pi*f*t—angle(z_t)))./abs(z_t);
                                % Resulting current (A)
Q1 = cumtrapz(I1)*dt;           % Charge = integral of ...
    current (C)

% Plotting charge vs voltage
subplot(1,2,2)
```

```matlab
plot(V,Q1,'b:')
axis([-0.6 0.6 -6e-9 +6e-9])
hold on
%────────────────────────


V = 20e-3+0.5*sin(2*pi*f*t);    % Applied voltage (V)
x_t = -1i/(2*pi*f*C);           % Reactance = Impedance of the ...
    capacitor
z_t = (1/x_t + 1/Rp)^-1 + Rs;   % Total impedance, Rp||C + Rs

% Big series resistance and capacitor
I1 = (20e-3+0.5*sin(2*pi*f*t-angle(z_t)))./abs(z_t);
    % Resulting current (A)
Q1 = cumtrapz(I1)*dt;           % Charge = integral of current (C)

% Plotting charge vs voltage
plot(V,Q1,'r-')
title('Charge vs. Voltage with and without noise for Rp||C + Rs')
xlabel('Voltage (V)'), ylabel('Charge (C)')
legend('Normal','DC offset')
hold off
%─────────────
%─────────────


%─────────────────────────────────────────────────────
% Calculation of capacitance for $R_p||C + R_s$ model
%─────────────────────────────────────────────────────
F = logspace(0,5,1000);            % Frequency vector, 1-100k Hz
Z1 = ((2*pi*F*C)./(-1i) + 1/Rp).^-1 + Rs;
                                   % Total impedance, Rp||C + Rs

% Plot circuit capacitance versus frequency
figure()
[AX,H1,H2] = ...
    plotyy(F,angle(Z1)*dtr,F,-1./(2*pi*F.*imag(Z1)),'semilogx','loglog');
xlabel('Frequency (Hz)')
set(get(AX(1),'Ylabel'),'String','Phase (Degrees)')
set(get(AX(2),'Ylabel'),'String','Capacitance (F)')
set(H1,'LineStyle','--')
legend('Phase','Capacitance')
title('Phase and Capacitance plot for Rp||C + Rs')
%─────────────
%─────────────
```